Master's thesis

NTNU
Norwegian University of Science and Technology
Faculty of Natural Sciences
Department of Biology

Dina Tevik Rogstad

Effects of Textile Microfibres on the Marine Microalgae *Isochrysis galbana* (T-ISO)

Master's thesis in Environmental Toxicology and Chemistry
Supervisor: Martin Wagner
Co-supervisor: Iurgi Imanol Salaverria-Zabalegui
May 2019

NTNU
Norwegian University of
Science and Technology

Dina Tevik Rogstad

Effects of Textile Microfibres on the Marine Microalgae *Isochrysis galbana* (T-ISO)

Master's thesis in Environmental Toxicology and Chemistry
Supervisor: Martin Wagner
Co-supervisor: Iurgi Imanol Salaverria-Zabalegui
May 2019

Norwegian University of Science and Technology
Faculty of Natural Sciences
Department of Biology

NTNU
Kunnskap for en bedre verden

Acknowledgements

This master thesis was written at the Department of Biology, Norwegian University of Science and Technology (NTNU) Trondheim 2019, and was financed through the Research Council of Norway project MICROFIBRE under the grant agreement no. 26840.

I would like to thank Associate Professor Martin Wagner and Researcher Iurgi Salaverria-Zabalegui, my supervisors at the Department of Biology (NTNU), for their guidance, encouragement and constructive feedback during the development of my work. My thanks are also extended to Senior Engineer Tora Bardal for helping me with the instruments at Sealab and to Dag Altin for advising me about algae cultivation.

Furthermore, I would like to express my deep gratitude to Senior Researcher Matilde Skogen Chauton at SINTEF and Professor Christiane Funk at Umeå University (UMU), for giving me the opportunity to develop parts of my work at the lab facilities of the Chemical Biological Centre (KBC) at UMU through the NordAqua exchange programme. Without you, I would have never met all the fantastic people at KBC. I would also like to show my appreciation to Zivan Gojkovic, for making me believe in myself; Amit, for his patience and kindness; André, for his positive engagement (and for developing my Portuguese); Andras Gorzsas, for helping me with the FTIR analyses; Jonathan for making my time outside university joyful; and of course the rest of you at KBC for making my stay in Umeå unforgettable.

Joachim and Martin, your aid during the last days of my writing was most cherished, and I much appreciate your help in finalising this thesis.

Lastly, I would like to thank my family and friends for supporting me, and my love, Emil, for his motivation and interest in my work throughout this whole process.

Trondheim, May 2019,

Dina Tevik Rogstad

Abstract

Textile microfibres (MFs) are of increasing concern in marine ecosystems, as large numbers of MF debris enter the ocean annually via waste and wastewater. Despite the persistence and bioavailability of MFs to marine organisms, few studies have investigated their sub-lethal impacts on microalgae or discussed the potential bottom-up consequences in marine ecosystems. For this reason, the current study aimed at investigating the effects of three common MFs (polyester, polyamide and wool) on growth, photosynthetic activity and biochemical composition in the marine microalgae *Isochrysis galbana* (clone T-ISO). MF sizes of 60 and 3000 µm at concentrations of 0.0422-4.22 µg/mL, and MF leachates (4.22 µg/mL) were used. The experiments indicated reduced population sizes by exposure to 60 µm and 3000 µm MFs, with a tendency towards polymer- and size-related effects. High levels of MFs induced significant effects on growth, and PES leachates significantly increased end biomass. MF leachates did not affect photosynthetic efficiency; nonetheless, the relative carbohydrate content tended to shift from glucose-like towards cellulose-like compounds. These results indicate some metabolic effects in *I. galbana* exposed to environmentally relevant levels of MFs, suggesting that marine food webs in proximity to wastewater outlets and heavily MF-polluted areas could be susceptible to impacts.

Keywords:
Microplastics, microfibres, marine microalgae, fibre toxicity

Sammendrag

Tekstilmikrofibre (MF) er i økende grad en bekymring i marine økosystemer, ettersom store mengder av MF ender i havet hvert år via avfall og avløpsvann. Til tross for høy persistens og biotilgjengeligheten av MF i marine organismer, har få studier undersøkt deres negative virkninger på mikroalger, eller diskutert potensielle bunn-opp-konsekvenser i marine økosystemer. På bakgrunn av dette, var målet med denne studien å undersøke effektene av tre vanlige MF (polyester, polyamid og ull) på vekst, fotosyntetisk aktivitet og biokjemisk sammensetning i den marine mikroalgen *Isochrysis galbana* (klone T-ISO). Lengder på 60 og 3000 μm i konsentrasjoner på 0,0422-4,22 μg/mL og MF-sigevann (4,22 μg/mL) ble anvendt. Reduserte populasjonsstørrelser ble funnet fra eksponering til 60 og 3000 μm MF, med en tendens til polymer- og størrelsesrelaterte effekter. Høye nivåer av MF induserte signifikante effekter på vekst, og PES-sigevann økte sluttbiomassen signifikant. Eksponering til sigevann fra MF påvirket ikke fotosyntetisk effektivitet, men forflyttet det relative karbohydratinnholdet fra glukose-lignende til cellulose-lignende forbindelser. Disse resultatene indikerer at det er noen metabolske effekter på *I. galbana* eksponert for miljørelaterte nivåer av MF, og utelukker dermed ikke muligheten for effekter videre opp i næringsnettet, i kystvann nær avløpsavløp og i tungt MF-forurensede områder.

Table of Contents

Abbreviations

μ	Growth rate of microalga
μ_{ASG}	Average specific growth rate of microalga
ANOVA	Analysis of variance
ATR	Attenuated total reflectance
BPA	Bisphenol-*a*
Chl-*a*	Chlorophyll-*a*
Chl*a*F	Chlorophyll-*a* fluorescence
CO_2	Carbon dioxide
CONW	Conwy-enriched seawater culture medium
DW	Dry weight
EC_{50}	Effect concentration on 50% of the population
F_0	Base-level fluorescence in dark adapted cells; F_0' in light-adapted cells
FTIR	Fourier-transform infrared spectroscopy
F_v/F_m	Photochemical efficiency in a dark-adapted cell state. Variable fluorescence (F_v), maximum fluorescence (F_m)
IQR	Interquartile range of a dataset, from Q1 to Q3 (25^{th}-75^{th} percentile)
MF	Microfibre
MP	Microplastic
MPF	Microplastic fibres
N	Nitrogen
NP	4-Nonylphenol
NR	Nile Red (9-(diethylamino)-5H-benzo[*a*]phenoxazin-5-one)
O_2	Oxygen
OD	Optical density; light attenuation and scattering at a specific wavelength
P	Phosphorus
PA	Polyamide or nylon 66
Pb	Lead
PE	Polyethylene
PES	Polyester
PS	Polystyrene
PSII	Photosystem II
QY	Quantum yield of PSII. Also known as photochemical efficiency of photosystem II (F_v/F_m)
rpm	Revolutions per minute
Sb	Antimony
SD	Standard deviation of a dataset
SE	Standard error of a dataset
TCS	Triclosan
Ti	Titanium
ZnSe	Zinc selenide

1. Introduction

1.1. Plastics

Since the key breakthrough of plastic polymers in the mid-twentieth century, production and consumption have increased exponentially, due to low costs and the manifold application ranges (Plastics Europe, 2017). Plastic polymers are versatile and can, in principle, be made with any desirable property through polymerisation of various monomers and chemical additives (*e.g.*, plasticisers, dyes, flame retardants etc.) to meet specific application demands[1] (Andrady, 2017; Chen and Patel, 2012; Plastics Europe, 2017). The annual global production of plastic materials increased from 1.5 to 348 million tonnes between 1950 and 2017 (Geyer et al., 2017; Plastics Europe, 2017) and today, the production of these surpass most other man-made materials (Geyer et al., 2017). The development of plastics has been considered beneficial to society, enabling more flexibility in daily activities. However, one of the primary assets of plastics, namely their durability, is also among the properties promoting their accumulation in most environmental compartments. The low degradability originates from the underlying production process, where unsustainable petrochemicals are applied as the dominant raw material for production of monomer constituents (Barnes et al., 2009; PlasticsEurope, 2018). Because of high production and consumption rates, a dominant portion of plastics end up in landfills and environmental compartments, due to product and waste mismanagement (Barnes et al., 2009). Once entering the environment, plastics fragment and spread as debris of multiple shapes and sizes, and has been detected in air, soil, sediments, household dust and in oceans (Barnes et al., 2009; Dris et al., 2015, 2017; Horton et al., 2017; Thompson et al., 2004). Some studies estimate that more than 269 000 tonnes of plastic debris floats in the ocean surface today (Cózar et al., 2014; Eriksen et al., 2014; Eunomia, 2016). As plastics distribute globally, environmental factors such as UV-radiation, temperature, pH, salinity, mechanical stress and biotic interaction provoke fragmentation; furthermore, creating mesoplastics (5000-50 000 μm), microplastics (1-5000 μm) and eventually nanoplastics (1-100 nm) (Andrady, 2011; Barnes et al., 2009; Cole et al., 2011; Hartmann et al., 2019). Consequently, as the average size of the plastics decreases, the global abundance and distribution increases perpetually with most eventually ending up in marine environments (Bergmann et al., 2015; Browne, 2015; Jambeck et al., 2015).

[1] https://www.plasticseurope.org/en/about-plastics/what-are-plastics

1.2. Microplastics in the marine environment

Microplastics (MPs) are of increasing concern in the context of ecotoxicology and ecosystem health, due to increasing numbers of studies reporting their presence in fresh- and saltwater environments (Andrady, 2011; Eerkes-Medrano et al., 2015; Horton et al., 2017; Woodall et al., 2014), foodstuffs (Liebezeit and Liebezeit, 2014, 2013), airborne particles (Dris et al., 2017, 2015; GESAMP, 2016) among other. The dominating factors determining environmental fate, and potential interactions of MPs with biota, are their size range and abundance in multiple clines of the water column (Vroom et al., 2017). Furthermore, the size and shape of MPs relate to their original source, intrinsic properties (*e.g.*, polymer composition and additives), and the degree of fragmentation because of previously mentioned environmental factors (Lambert et al., 2017).

The ocean is thought to act as a final sink to MPs, both due to the vast area and depth, and the numerous entry routes from populated areas via rivers and marine traffic. Because MPs can distribute throughout the water column, the concern is that organisms dwelling near the water surface (epipelagic) and on the bottom (benthic) are at risk for exposure. The buoyancy of MPs and risk of interaction with marine biota in the water column is determined by water turbulence and mixing, biofouling, and by innate mass density, charge, size and shape of the MPs (GESAMP, 2016; Syberg et al., 2015). For instance, the mass density of the most common (virgin) plastic polymers: polystyrene (PS, 0.96-1.05 g/cm^{-3}) and polyethylene (PE, 0.91-0.94 g/cm^{-3}), are lower than the average mass of seawater (1.02-1.03 g/cm^{-3}) (Andrady, 2011; Ellen MacArthur Foundation, 2017; Wang et al., 2018). Hence, PS and PE would theoretically be positively buoyant in the ocean, potentially interacting more with epipelagic organisms such as phyto-, zooplankton and other plankton species. Conversely, the denser polymers polyamide (PA, 1.15 g/cm^{-3}) and polyester (PES, 1.40 g/cm^{-3}) - commonly deriving from fishing gear and apparel fibres - could eventually interact more with benthic organisms such as mussels, crabs and marine worms.

To date, ingestion of different MPs has been demonstrated in species of zooplankton (Cole et al., 2013; Desforges et al., 2015; Lyakurwa, 2017; Setälä et al., 2014), mussels (Browne et al., 2008), fish (Kühn et al., 2018; Lusher et al., 2013; Rochman et al., 2015), seabirds (van Franeker et al., 2011), and more. As ingestion is thought to be the primary route of exposure, the relatively small dimensions of MPs increase their potential for ingestion by a broad range

of species. Nonetheless, the risk and hazard upon ingestion depends on the abundance and bioavailability of MPs to exposed organisms. Currently, there is a knowledge gap related to both environmental concentrations and potential harmful effects of MP exposure. Laboratory studies on MP toxicity usually exceed what is so far recognised as environmentally relevant concentrations, still, few studies report consistent data on adverse effects (Lenz et al., 2016; Phuong et al., 2016).

1.2.1. Microplastic fibres from textiles

Ecotoxicological studies on MPs have so far primarily focused on pristine, spherical beads (Anbumani and Kakkar, 2018; Henry et al., 2018; Lambert et al., 2017); however, empirical studies suggest that microplastic fibres (MPFs) represent the dominating portion of marine plastic litter (Boucher and Friot, 2017; Browne et al., 2011; Wright et al., 2013). Consequently, the awareness and concern for impacts by MFs are now on the rise because of the ever-increasing global demand for textiles (Ellen MacArthur Foundation, 2017). In fact, a dominant share of the global textile market comprises synthetic fibres (Figure 1.1) such as PES, PA and acrylic, where annual textile consumptions are approximately 50-70 million tonnes (~7-9 kg *per capita*) (Boucher and Friot, 2017; Carr, 2017; Ellen MacArthur Foundation, 2017; FAO/ICAC, 2013). Moreover, 12% of textile fibres are estimated to be lost during production and distribution, meaning that approximately 0.19 million tonnes of MPFs shed and release into oceans annually (Eunomia, 2016). Furthermore, Browne *et al.* (2011) reported that roughly 85% of global shoreline MP pollution derived from synthetic textiles, and it has been estimated that 20-35% of MPs in the marine environment are fibres from synthetic clothing (Boucher and Friot, 2017; Eunomia, 2016). When considering that MPFs comprise up to 35% of primary MPs - not resulting from fragmentation of larger plastics - in the ocean (Boucher and Friot, 2017; Henry et al., 2018), more focus should be directed towards this group of marine pollutants. Additionally, the Ellen MacArthur Foundation estimates that the textile markets' demand and supply will likely triple from today's amount by 2050, due to emerging markets such as Asia and Africa (Ellen MacArthur Foundation, 2017).

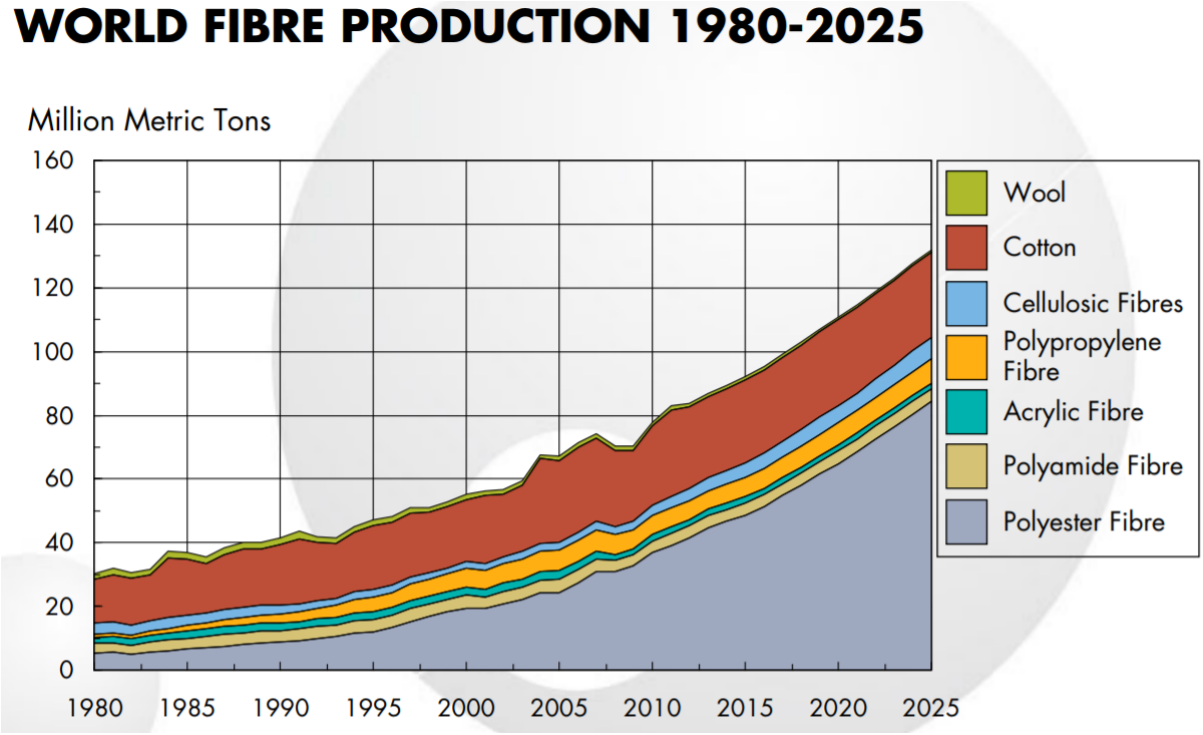

Figure 1.1: Global fibre production, categorised by fibre type. Source: Tecnon OrbiChem[2]

Some experimental studies have quantified the fibre shedding through washing of synthetic textiles, and have also investigating factors affecting the abundance in washing machine effluents (Browne et al., 2011; Hartline et al., 2016; Napper and Thompson, 2016). Others aimed to determine regional concentrations of MFs in ocean surface waters, as exemplified in Table 1.1 (Gago et al., 2018). This table - adapted from Table 1 in Gago *et al.* (2018) - summarises a few of the reported MF concentrations at different sampling locations in the Northern Hemisphere. What this review by Gago *et al.* indicates, is that surface water concentrations are relatively low, particularly compared to wastewater effluents and ocean sediments. Large spatial and temporal variations in MPF densities across geographical regions have also been found. Additional questions arising in relation to MPFs are then: do environmentally relevant concentrations pose any hazard to marine epipelagic organisms, and will the impact depend upon chemical or physical characteristics or both? So far, the answers to these questions are challenging to obtain, because of the industrial secrecy around chemical additives and the previously mentioned lack of toxicological studies (Ellen MacArthur Foundation, 2017; Henry et al., 2018).

[2] Yang Qin (2014), *Global Fibres Overview*; Tecnon OrbiChem. Synthetic Fibres Raw Materials Committee Meeting at APIC 2014 Pattaya, 16 May 2014

Table 1.1: Summary table of studies detecting microfibres (MFs) in ocean surface waters.

Location	Date	MFs/m^3	References
Southern coast of Korea	2012	450 ± 410	Song et al., 2014
Swedish west coast	2007	50-2400	Norén, 2007
Scotland and Iceland	1960-2000	0.01-0.045	Thompson et al., 2004
Baltic Sea	2013	0.45 ± 0	Magnusson and Norén, 2014
Gulf of Finland	2013	0.01-0.65	Setälä et al., 2016
North Pacific Gyre	2007	0.001-0.003	Mendoza and Jones, 2015

1.2.2. Ecological impacts of microplastic fibres

The impacts of MPF pollution on the environment are currently inadequately understood, despite evidence of entanglement and ingestion among aquatic organisms (Bergmann et al., 2015; Dave and Aspegren, 2010). Like MPs, impacts of MPFs are thought to be through physical or chemical pathways (Henry et al., 2018), *i.e.*, their shape (ability to twist and entangle) and potential for leaching or adsorbing compounds. Among the relatively few studies in which MPFs have been investigated, species like *Daphnia magna* have are reported to ingest and become entangled in the fibres (Dave and Aspegren, 2010; Jemec et al., 2016), ingestion by crabs (Watts et al., 2015), fish (Kühn et al., 2018; Lusher et al., 2013; Rochman et al., 2015) and birds (Zhao et al., 2016). The shape of MPFs also give them large surface areas with great adsorption potential for other hydrophobic compounds. In turn, they may act as vectors of harmful organic compounds to organisms exposed to, and ingesting the fibres (Koelmans et al., 2016; Mato et al., 2001; Ogata et al., 2009). Additionally, compounds that are applied during production of plastic fibres may be retained in the finished textiles and leach out during weathering and ingestion (Dave and Aspegren, 2010; Ellen MacArthur Foundation, 2017). The variable compositions and content of additives, and low transparency across the industry, makes it challenging to project the true scale of release into and impacts on ecosystems during the washing or discarding of textiles.

1.3. Microalgae

Roughly half of the global net primary production occurs in aquatic ecosystems, wherein phytoplankton, or microalgae, are the dominant producer (Barbosa, 2009). These prokaryotic organisms possess unique photochemical machinery, converting solar energy into energy-rich

biomass through photosynthetic processes, requiring only water, carbon dioxide (CO_2) and micronutrients. Because of their autotrophy, ability to recycle inorganic nutrients (*i.e.*, carbon, nitrogen and phosphorus) and ability to produce oxygen (O_2), they are of paramount importance in the global energy and nutrient flow. Microalgae have also gained scientific interest, due to their potential as a source of high-value nutrients, feed in agri- and aquaculture, bioremediators of wastewater, and for acting as well-established indicators of ecosystem health (Carpenter and Smith, 1972; Siegel and Franz, 2010; Sukenik and Wahnon, 1991; Tredici, 2010). As they constitute the primary trophic level, any impact on microalgae can cause ramifications throughout entire food webs.

1.3.1. Relevance and use in ecotoxicology

Microalgae have a long history of use in ecological and toxicological assessments of waterbodies, as their sensitivity towards environmental alterations make them good indicators for presence and toxicity of environmental pollutants (Eullaffroy and Vernet, 2003; Stevenson, 2014). For instance, the standard alga growth inhibition guideline (OECD, 2006) is widely used for initial hazard assessments, quantifying growth rates and growth inhibition for treated and non-treated individuals. It is based on an exponentially growing alga population (Figure 1.2), and usually lasts for 72 to 96 h. It does not consider the carrying capacity (*i.e.*, maximum cell density) of the population, after reaching a stationary growth phase. Furthermore, sub-lethal toxicity of compounds can be investigated through physiological parameters associated with photosynthesis. Such sub-lethal assays often involve chlorophyll-*a* fluorescence (Chl*a*F) of plants and algae, because it is considered to be an early indicator of stress-induced damage to the photosynthetic apparatus (Agati et al., 1993; Maxwell and Johnson, 2000; Pérez et al., 2009). Under optimal conditions, captured light energy is primarily dissipated via chemical conversion, whereas smaller proportions are dissipated as thermal heat and fluorescence. As Chl*a*F, photochemistry and thermal dissipation are in balance, stressful conditions tend to increase the fluorescence, reflecting changes in the photosynthetic capacity (Agati et al., 1993; Suggett et al., 2011). Simple and non-invasive methods of assessing algal toxicity by Chl*a*F can be achieved by measuring base-level fluorescence in dark (F_0) or light (F_0') adapted states. Ideally, these would then be followed by more reliable fluorescence kinetics and quantification of photochemical efficiency of photosystem II (PSII; QY or F_v/F_m).

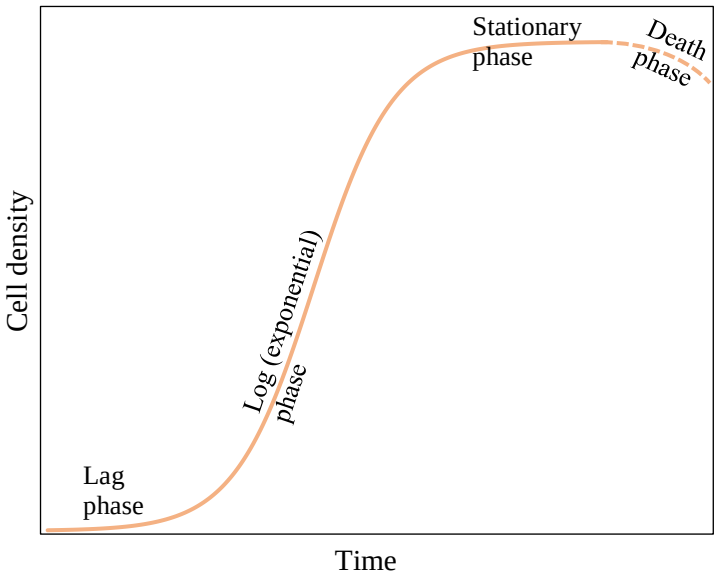

Figure 1.2: Growth kinetics of a microalgal population.

Photosynthetic parameters alone tend to correlate poorly with growth rates and should ideally be monitored in combination with physiological parameters such as membrane or whole-cell biochemical structures. Due to the unique metabolic flexibility of microalgae, environmental conditions (*i.e.*, temperature, nutrients, light, salinity) and biotic factors (*e.g.*, growth rate) influence their biochemical composition, thus, reflecting the physiological state (Cordoba-Matson et al., 2013; Durmaz et al., 2008; Murdock and Wetzel, 2009; Renaud et al., 1995; Sukenik and Wahnon, 1991). Growth rates are defined by intrinsic macromolecular pools, implying that physiological status (*i.e.*, carbon allocation strategies) can be monitored based non alterations in carbohydrate, lipid and protein content (Renaud et al., 1995; Wagner et al., 2013). Conventional techniques for identifying macromolecular composition of microalgae include extraction and colorimetric tests, requiring large amounts of available biomass material. Vibrational spectroscopy, on the other hand, requires less material and is widely used for studying macromolecular composition of biological materials such as phytoplankton. For instance, Fourier-transform infrared (FTIR) spectroscopy detect specific vibrational bands of chemical bonds as they absorb IR light (Murdock and Wetzel, 2009; Wagner et al., 2013). These absorption bands - or peaks - reflect the specific energy levels resulting from bending and stretching vibrations, where absorption intensity depends on the dipole moment of the respective bond. Accordingly, general behavioural patterns of each molecular bond can be explained according to the principle of Beer-Lambert's absorption law (Griffiths and de Haseth, 2007). In algal research, the dominating proportion of relevant macromolecular information lies

within the wavelength regions of 2800-3000 cm^{-1} and 900-1800 cm^{-1} , although, FTIR-spectra are specific to both physiological state and taxon (Duygu et al., 2012; Wagner et al., 2013). More specifically, the spectral wavebands and peaks representing carbohydrates, proteins and lipids in algal biomass, are listed in Table 1.2. Multiple studies quantify relative carbohydrate and lipid content by normalising the respective peak intensities to specific protein peaks (*i.e.*, amide I or amide II) (Murdock and Wetzel, 2009; Wagner et al., 2013), as environmental stressors have negligible short-term effects on protein content.

Table 1.2: Tentative spectral interpretations of microalgal FTIR spectra.

Band	Wavenumber range [cm^{-1}]	Main peak [cm^{-1}]	Typical band assignments*	Type of vibration
I	970-1135	1035	Carbohydrate[a] stretching and phosphodiester stretching	*ν*(C-O-C), *ν*(>P=O)
II	1140-1170	1147 or 1164	Carbohydrate[b] polysaccharides stretching	*ν*(C-O-C)
III	1485-1580	1543	Protein amide II bending (deformation) and stretching	*δ*(N-H), *ν*(C-N)
IV	1585-1710	1645	Protein amide I stretching	*ν*(C=O)
V	1720-1769	1745	Cellulose and fatty acids stretching (esters)	*ν*(C=O)

*Band assignments based on Table 2 from Duygu et al. (2012)

[a] Glucose- or glycogen-like

[b] Cellulose-like

1.3.2. Effects of MFs on microalgae

To this date, there are no laboratory studies assessing the impacts of MFs on primary producers such as microalgae, although, studies on MPs have reported growth inhibition, reduced Chl-*a* content and photosynthetic activity at low (ppm) concentrations (Anbumani and Kakkar, 2018; Prata et al., 2018). As reviewed by Prata *et al.* (2019), the impacts of MFs are contradictory, as some observe reduction of Chl-*a* content (Besseling et al., 2014; Zhang et al., 2017), photosynthetic activity (Mao et al., 2018; Zhang et al., 2017) and growth (biomass) (Sjollema et al., 2016; Zhang et al., 2017). Others observe no effects on the same parameters: Chl-*a* content (Long et al., 2017), photosynthetic activity (Sjollema et al., 2016; Zhang et al., 2017) and growth (Long et al., 2017; Prata et al., 2018). This suggests that MPs have inconsistent impacts on measured physiological parameters and across species. As a dominant portion of MPs in marine environments are textile MFs, more research regarding their toxicological impacts on microalgae is needed. This is important, due to their role as indicators of ecosystem health and because marine ecosystems are regarded as the terminal sink of MPs and MFs.

As a representative for marine microalgae in this project, the prymnesiophyte *Isochrysis galbana* (clone *Tisochrysis lutea* (T-ISO)) was selected, based on its inclusion in crustacean and bivalve diets in aquaculture (Drillet et al., 2011; Starr et al., 1999), its internationally acceptance as a bioassay species (Garrido et al., 2019; Tato et al., 2018) and its predominance in marine phytoplankton communities (Long et al., 2017). The alga itself is a small, golden-brown flagellate with an equivalent spherical diameter (ESD) of 4-6 µm and a high content of polyunsaturated fatty acids (PUFAs). The latter makes it a valuable source of fatty acids in marine ecosystems and a trophic marker in epipelagic environments (Dalsgaard et al., 2003). Impacts on growth, primary production or biochemical composition of *I. galbana* and other marine microalgae could, therefore, ramify throughout marine food webs, effectively affecting whole ecosystems.

1.4. Aims and hypotheses

This thesis was a part of the MICROFIBRE project, funded by the Research Council of Norway (grant agreement no. 26840), which assesses the environmental impacts of microplastic fibres from textiles, among others. Within this context, the present work aimed to assess the sub-lethal impacts of the most prevalent MPFs PES and PA on the marine microalgae *I. galbana* (T-ISO), by evaluating different responses during chronic exposure to these MPFs. Furthermore, untreated wool MFs were used as a representative for non-synthetic fibres. The main aims of this project were:

1) Investigating the effects of MFs on growth of *I. galbana* during chronic exposure, addressing alterations in growth patterns including growth rates (lag and log phase) and cumulative cell production.
2) Investigating the effects of MFs on photosynthetic activity in *I. galbana* during chronic exposure, using Chl*a*F per microalgal cell and cumulative Chl*a*F as a proxy.
3) Address impacts of MF leachates on photochemical efficiency and biochemical composition; the latter by using an FTIR-derived approach.

Based on the aims of the study, the following hypotheses were made:

- MFs exert different modes of impact depending on polymer type (*i.e.*, synthetic or non-synthetic), concentration and size (length).
- MF leachates alone exhibit lower effects than suspended MFs of 60 and 3000 µm lengths.

2. Materials and Methods

The experiments in this project were performed at two different facilities: NTNU Sealab in Trondheim (December 2018/January 2019) and Kjemisk-Biologisk Center at Umeå University (February-March 2019). Each subsection is described in a chronological order and, therefore, the location of each experiment is not specified further.

2.1. Materials and preparations

2.1.1. *I. galbana* parent culture

A parent culture of *I. galbana* (clone T-ISO) was obtained from Altin's BioTrix and prepared in a 5-L borosilicate glass flask, in seawater enriched with Conwy medium (CONW; Appendix A, Table A2). Seawater, obtained from the Trondheim fjord, was sand-filtered (0.22 µm) before use. The culture was inoculated in a 24 h light cycle under stable conditions (21 ± 0.5°C, 87 ± 5.7 µmol photons m^{-2} s^{-1}), irradiated by cool-white fluorescent lights (Philips TL-D 18W/840), and aerated with an aquarium pump (ELITE 800, Rolf C. Hagen Inc.). Near-exponential growth was maintained by re-inoculation every 3 w, keeping an initial cell concentration of 1-1.1x10^4 cells/mL. This parent culture was further used in all experiments.

2.1.2. Microfibre cutting

The plastic fibre materials PES and PA were selected to comprise the most commercially produced and environmentally relevant polymers, frequently identified in marine samples (Browne et al., 2011; Gago et al., 2018). Additionally, untreated sheep's wool was selected as a non-synthetic material, as reference for any effects of the synthetic polymers. Short (60 µm) and long (3000 µm) fibres were cut from PES, PA and wool, to identify possible effects of the MF length and/or polymer composition and were selected to represent the lower and higher parts of the MP size scale. More specifically, 60 µm was selected because of its "fibrous" appearance, having an aspect ratio (length-to-width) of three or greater (Appendix A2, Table A3-A4), whereas MFs of 3000 µm and longer, are frequently found in aquatic samples (Gago et al., 2018).

All MFs were prepared from spools of white, polyfilament yarns according to the protocol developed by Cole (2016) because it generated MFs of consistent sizes, compared to grinding or milling. A cryogenic microtome (HM 500 M Microtome Cryostat, Microm Gmbh, Germany)

was used to cut the 60 µm MFs at -20 °C, but owing to size limitations of the instrument, the 3000 µm MFs were cut manually with a scalpel. After cutting, the MFs were suspended in distilled H_2O, then vacuum filtrated and dried (40°C, 20-30 h) before storage in sealed glass vials. Size distribution and consistency of the cut MFs was analysed by microscopic examination (Nikon Eclipse E200, Nikon Instruments Inc., USA) and imaging (Nikon DS-5Mc, Nikon Instruments Inc., USA), followed by image analysis (ImageJ, US NIH). Imaging analysis included measurements of lengths and widths and subsequent statistical analysis of the data to determine normal distribution and group differences (see section 2.4.5 for further details).

2.1.3. Microfibre stock suspensions

Stock suspensions of each MF type (PES, PA, wool) and size (60 and 3000 µm) were prepared by weighing, using an analytical microbalance (XP2U, Mettler Toledo), and suspending the MFs in CONW in separate 500-mL borosilicate flasks with PTFE cap linings (VWR International LLC, Germany). The stocks were then stored for approximately 1 and 2 mo (dim/normal room light intensity, 21°C) until the exposure experiments were initiated (3000 and 60 µm MFs, respectively). Each of the six stocks were made into a concentration of 4.22 µg MFs/mL CONW, corresponding to the highest exposure concentration of the experiment (Appendix A, Table A5).

2.1.4. Microfibre leachates

Leachates of PES, PA and wool MFs were prepared, in order to quantify and qualify the composition of chemicals leaching from the fibres into the CONW medium. Firstly, each of the three yarns (PES, PA, wool) were cut (1-3 mm) with sterile scissors, weighted into 40-mL clear glass vials (VOA vial w/PTFE lined caps, VWR International LLC, Germany) and suspended in CONW medium made from autoclaved, artificial seawater into concentrations of 4.22 µg/mL (Appendix A1, Table A6). All leachate samples were made in duplicate. The vials were then sealed (screw caps, parafilm), covered (aluminium foil) and incubated (20.8°C, 120 rpm) in an incubation shaker (Innova® 43, New Brunswick™ Scientific Co. Ltd., USA). After 7 d (162 h), the leachates were sterile filtered (Filtropur S, 0.20 µm, Sarstedt, Germany) and transferred into i) separate 40-mL glass vials for exposure experiments or ii) 4-mL glass vials (Kimax®, DWK Life Sciences LLC, USA) for chemical analysis. The latter were stored sterile in hydrochloric acid (HCl, 5 µL, 15%). Artificial seawater was used due to lack of access to natural seawater at the lab facilities of KBC in Umeå.

2.2. Method development

Before starting the exposure experiments, a method for cultivation, sampling and analyses was tested and validated to ensure low influence from protocols on the analyses of physiological parameters (*i.e.*, cell number, growth rate, Chl*a*F). Additionally, instrument analysis parameters such as for Chl*a*F measurements, were adjusted to the *I. galbana* culture used here.

2.2.1. Pilot cultivation

A pilot cultivation of *I. galbana* was performed in 40-mL glass vials placed on a rotating plankton wheel cultivation system (Appendix A, Figure A1). This was done in order to identify and evaluate i) specific growth patterns, ii) a subsampling method (Lyakurwa, 2017), and iii) to determine an optimal initial cell density of *I. galbana*.

Initially, four groups representing different culture densities (2000, 4000, 6000 and 8000 cells/mL) were prepared in quadruplicates, into 40-mL glass vials sealed with screw caps and PTFE cap liners. Each density was made by diluting the parent culture with CONW, and the glass vials with cap liners were used to promote suspension of MFs in the medium, reducing surface adhesion. All replicates were then incubated for 12 d in the plankton wheel under constant conditions (21°C, 87 ± 5.7 µmol photons m^{-2} s^{-1} continuous light, 0.80 revolutions per minute, rpm). Irradiances were measured from within the centre of the vials (ULM-500, Heinz Walz GmbH, Germany) in upright (parallel) and horizontal (perpendicular) positions, relative to the light source (Appendix A, Figure A1). Daily monitoring (24 ± 4 h) included subsampling of 10 mL (2x5 mL), pH measurements (WTW™ ProfiLine™ pH 3210, Germany), and determination of cell density using an electronic particle counter (section 2.4.1) The sampling and culture volume were consistent throughout the experiment, and all samples were promptly replenished with fresh CONW.

2.2.2. Other methods

After the pilot cultivation, species-specific instrument parameters for analysing Chl*a*F in the algal cultures were determined (section 2.4.2 and Appendix B). Additionally, exposure groups with MFs required filtration before cell counting and ChlaF analysis, in order not to block the particle counter's aperture. Therefore, to assess whether filtration of algal cultures i) retained algae on the filters or ii) impacted the Chl*a*F measurements, a filtration procedure was tested

and analysed (Appendix B). To semi-quantitatively determine *in vivo* lipid content of *I. galbana*, a chromophore-staining method was also developed and tested (Appendix B). However, due to issues preparing the standard curves of the fluorescence intensity as a function of chromophore concentration, this method was not further developed or applied in the final exposure experiments.

2.3. Exposure

2.3.1. Microfibres: 60 and 3000 µm

Two exposure experiments á 13 d were performed, each consisting *of I. galbana* cultures with one of three MF types (PES, PA or wool), in a series of three MF concentrations (low, 0.0422; medium, 0.422; high, 4.22 µg/mL) (Appendix A, Table A4 and Figure A1). The exposure to 60 µm and 3000 µm MFs were run at separate time intervals, due to physical constrictions of the plankton wheel (maximum capacity of 48 40-mL vials). In total, each experiment comprised 33 samples, whereof six were triplicates of algae and CONW controls, without MFs. The concentration series was based on a project previously conducted with spherical MP particles (PS, 10 µm) in concentrations of 75, 750 and 7500 MPs/mL (Lyakurwa, 2017).

All cultures were prepared as described in section 2.2.1 with identical cultivation conditions. Based on the method development, an initial cell density of 10 000 cells/mL was selected. The medium and low MF concentrations were made by diluting the MF stocks 1:10 and 1:100, respectively. Algal and CONW controls were prepared in the same way as the exposed cultures, only replacing the MF suspensions with pure CONW. Each sample was distributed on the plankton wheel as shown in Figure A1 (Appendix A), and the sampling and Chl*a*F analysis performed as described in section 2.2.1 and 2.4.2. Samples of 8 mL were taken from each vial one and two d before the end of the experiments, and was filtered (1.2 µm GF/C Whatman), packed separately in aluminium foil and stored at -80℃ for further FTIR spectroscopy and pigment analyses.

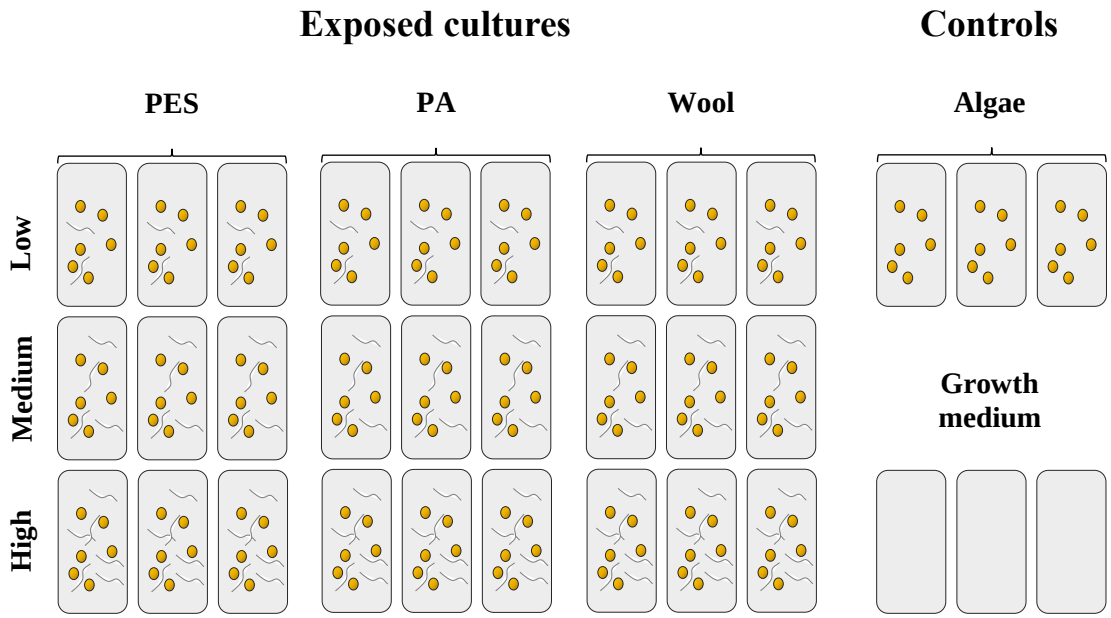

Figure 2.1: Illustration of the experimental setup. Separate cultures of *I. galbana* were incubated in triplicates in 40-ml glass vials with MFs (PES, PA or wool), in a series of three MF concentrations (low, 0.0422 µg/mL; medium, 0.422 µg/mL; high 4.22 µg/mL). *I. galbana* cultures without MFs, and pure CONW served as experimental controls. The setup was run once and separately with 3000 µm and 60 µm MFs. PES, polyester; PA, polyamide. For detailed plankton wheel setup, see Appendix A, Figure A1.

2.3.2. Microfibre leachates

To assess whether any of the observed effects on *I. galbana* from the 60 µm and 3000 µm MFs exposure experiments (section 2.3.1) were due to chemical impacts alone or combined with physical impacts, a second exposure was performed using the MF leachates prepared in section 2.1.4. Sterile leachates of each fibre type (PES, PA, wool) from the 40-mL vials were diluted into three separate cultures of *I. galbana* (375 mL) in 500-mL borosilicate bottles. All cultures originated from one common culture diluted to 31 500 cells/mL (1800 mL), ensuring similar population densities in all samples. The final leachate concentration corresponded to the highest from section 2.3.1. The algae-leachate cultures were then equally distributed into three sterile inoculum flasks (TC flask T175 ^{W}/vent cap, Sarstedt, Germany), and incubated (20.8°C, 120 rpm, 41 ± 9 µmol photons m^{-2} s^{-1} continuous cool-white light) in an incubation shaker (Innova® 43) for 7 d. All preparations and samplings were performed sterile. Daily (24 ± 2 h), 7 mL of culture was sampled for analysis of i) pH, ii) optical density (OD at λ=530, 680 and 750 nm), iii) photochemical quantum yield (QY, F_v/F_m) and iv) cell density, as described in section 2.4.1 and 2.4.3. After the final sampling and analyses on day 7, the dry weight dry weight biomass was determined for all samples (section 2.4.3)

2.4. Analytical procedures

2.4.1. Cell concentration, growth rate and growth curves

The population density of *I. galbana* (cells/mL) was measured with an electronic particle counter (Multisizer 3™ Coulter Counter®, Beckman Coulter Inc., Germany) equipped with a 100 µm aperture, based on the Coulter principle (Graham, 2003). The cultures were diluted with filtered seawater (FSW) into 20-mL plastic cups (Coulter Counter® cups, Deltalab, Barcelona, Spain) before measurements, optimising the precision by keeping cell densities within 4000-30 000 cells/mL. Based on theoretical equivalent spherical diameters (ESD) of *I. galbana* (Harris et al., 2000; Parke, 1949; Rey et al., 2001; Starr et al., 1999) and by imaging analysis, each cell was identified as signals within the size range of 2.5-7 µm.

The daily (μ_{SG}) and average specific growth rate (μ_{ASG}) were determined from cell counts and calculated according to the OECD guideline 201 (OECD, 2006) as the logarithmic increase in cell number (cells/mL):

$$\mu_{i-j} \frac{ln\, X_j - ln\, X_i}{t_j - t_i}$$

where μ_{i-j} is the average specific growth rate from time *i* to *j*; X_i is the biomass at time *i*, and X_j is the biomass at time *j*. µ was determined for all exposure groups. The percentage of growth rate inhibition (*Ir*) in each replicate was calculated relatively to the mean of the controls:

$$Ir\ (\%) = \frac{Y_c - Y_t}{Y_c} \times 100\%$$

Where Y_c is the mean μ_{ASG} of the control; Y_t is the μ_{ASG} of individual replicates of MF-exposed *I. galbana*. The exponential growth rates and maximum culture densities were estimated in SigmaPlot 14.0 (Systat Software Inc., San Jose, CA, USA) from sigmoid regression curves fitted to the data using the following equation:

$$f = min + \frac{max - min}{1 + 10^{(logEC50 - x) \times hillslope}}$$

Where *min* and *max* are the initial and maximal cell densities (cells/mL), respectively; $logEC_{50}$ is the day at which 50% of the maximum population density is reached; *x* is the time (days) and *hillslope* represents the exponential growth rate. All curves shared the common parameter *min*; 10 000 (60 µm) and 11 000 (3000 µm).

The area under the curve (AUC) was used as a proxy for algal biomass across the growth period and approximations were calculated using the Riemann Sum formula for definite integrals:

$$\int_a^b f(x)dx = \lim_{x\to\infty} \sum_{i=0.06}^{n} f(x_i) \times \frac{(b-a)}{n}$$

Where *a* and *b* are separate timepoints of an interval *i* (d) and *n* is the total number of intervals. The definite integrals were calculated and summarised for each 0.06 interval, within the time periods 0-13 and 0-7 d.

2.4.2. Spectrofluorometric analyses

As an indication of physiological state of the cultures, *in vivo* Chl*a*F was analysed for samples exposed to fibres. Initially, to determine the correct measurement parameters for *I. galbana*, approximately 12 mL was sampled from the parent culture and diluted into six 2-mL aliquots (50 000 cells/mL, 10x10 mm PS cuvettes). Then, each sample was scanned with a spectrofluorimeter (Varian Cary Eclipse, Agilent Technologies, Inc., USA), assessing suitable excitation (ex.) and emission (em.) wavelengths for peak Chl*a*F (Appendix B, Table B1 and Figure B3). Furthermore, Chl*a*F per cell was calculated by dividing the Chl*a*F fluorescence value (measured) by the cell number (cells/mL) of the corresponding sample from that day.

2.4.3. OD, QY and dry weight biomass

As a means of semi-quantitatively deducing algal cell densities, Chl-*a* and carotenoid pigments, OD spectra were measured spectrophotometrically (T90+ UV/VIS Spectrometer, PG Instruments Ltd, UK) at room temperature. Wavelengths of 750 nm, 680 nm and 530 nm were used to detect non-specific particles (*i.e.*, cells), Chl-*a* from PSII and carotenoids, respectively. QY, representing the maximum photosynthetic efficiency of PSII in dark-adapted conditions, was measured with a portable fluorimeter (AquaPen-C 100, Photon Systems Instruments, Czech Republic), after 20 min of dark-incubation.

Algal dry weight (DW) biomass was determined at the end of the leachate experiment (section 2.3.2) by vacuum filtrating 4 mL (in duplicate) from each sample (0.2 µm GF/A Whatman), dried (70℃, 24 h) and stored in a desiccator (2 h) before weighing (XS205, Mettler Toledo). Algal DW (g/L) was then calculated by differential weight using the following equation:

$$DW = \frac{W_j - W_i}{x} \times 1000$$

where W (g) represents the weight before (W_i) and after (W_j) filtration, and x (mL) is the filtrated culture volume.

2.4.4. FTIR spectroscopy

To obtain the semiquantitative distribution of molecular components such as lipids, proteins and carbohydrates in the exposed and non-exposed algae, samples were analysed by attenuated total reflectance (ATR) fourier-transform infrared (FTIR) spectroscopy (Vertex 70/80V platinum ATR, Bruker Optik GmbH, Germany) under vacuum. After termination of the experiment, remaining samples were centrifuged (4000 rpm, 15°C, 20 min; Eppendorf 5810R, Eppendorf GmbH, Germany), and the resulting pellet lyophilized overnight (-40°C, Hetosicc CD 52-1, Heto, Denmark). The spectra were then recorded for the lyophilized pellets in the range of 400-4000 cm^{-1} at 2 cm^{-1} spectral resolution, using an empty sample chamber (the diamond) as a background. FTIR absorbance data were recorded and visualized using the OPUS software (Bruker Optics, Ettlingen, Germany) (Appendix C, Figure C5). For further analysis, the spectra were exported to and processed in MATLAB using an open-source MATLAB script (Vibrational Spectroscopy Core Facility, Umeå University). The spectra were cut to obtain a fingerprint region within 840-1770 cm^{-1}; baseline corrected using asymmetric least squares (λ=10 000 000, p=0.001) and smoothed by Savitzky-Golay filtering (polynomial 1st order, frame=3). This spectral pre-treatment was done to correct for differences in peak intensities between low and high wave frequencies. To minimise the fluctuations in peak absorption resulting from inhomogeneous amount of biomass placed on the ZnSe crystal, amide I (1645 cm^{-1}) peak was used as an internal reference for normalisation of carbohydrate and lipid content (Mecozzi et al., 2007; Meng et al., 2014).

2.4.5. Statistical analyses

For simple calculations, visualisation and sorting of raw data, Microsoft Excel (Windows Office 2016) was used, whereas the statistical and graphical software IBM SPSS Statistics (version 25.0. for Windows, IBM Corp., Armonk, NY, USA), GraphPad Prism (version 8 for Windows, GraphPad software, San Diego, CA, USA) and SigmaPlot 14.0, were selected for statistical analyses of the data.

Following the MF cutting protocol, the consistency in size distribution of the MFs were validated statistically by comparing lengths, widths and aspect ratios against each other. This was done in IBM SPSS 25.0 by performing a one-way analysis of variance (ANOVA; α=0.05). Individual differences between samples were identified using the Tukey's pairwise multiple comparisons post hoc analysis (α=0.05). All ANOVAs were performed after testing for normality (Shapiro-Wilk test and Q-Q plots; p<0.05) as this is required of the analysis. Since the ANOVA test is robust against non-normalized data (*i.e.*, Type I errors are not profoundly increased; Blanca et al., 2017), this test was also used when assumptions of normality could not be ascertained. Similarly, ANOVA was used to identify differences in the aimed endpoints in the exposure studies. When a significant difference was found between treatments, each treatment was compared to the control using Dunnet's post hoc analysis (SigmaPlot 14.0). Here, Dunnet's analysis was considered superior to Tukey's, because the analysis considers fewer test groups, risking fewer false positive (significant) results.

To determine whether the Chl*a*F was positively correlated to the increasing cell density (cells/mL), both a linear Pearson's correlation (Excel) and a monotonic Spearman's rho correlation (GraphPad Prism 8) was calculated. Chl-*a* content increase monotonically with increasing cell densities and alter in response to environmental factors. Therefore, it was interesting to test whether there would be any differences in the correlation between Chl*a*F and cell density, as a function of MF concentration. The probability level was set at p<0.05 for both tests.

3. Results

3.1. Method development

3.1.1. Plankton wheel pilot cultivation and subsampling

Average specific growth rates (μ_{ASG}) from the pilot cultivation of *I. galbana* are presented as numbers of cell divisions per day, for a total of 12 d, in Figure 3.1; additional information can be found in Appendix B. In lag phase, the group of 6000 cells/mL grew significantly more rapid than 2000 cells/mL, as indicated by a one-way ANOVA; $F_{3,12}$=5.0, p=0.017. However, in log phase (day 3-6) the group of 2000 cells/mL had a higher growth rate than the group of 6000 cells/mL and significantly higher than the group of 8000 cells/mL; $F_{3,12}$=5.38, p=0.014. Despite the differences in μ_{ASG} of lag and log phase, the final cell densities on day 12 were non-significantly different between groups; $F_{3,12}$=3.0, p=0.075. However, populations of *I. galbana* with low initial cell density appeared to have higher maximum population densities at termination on day 21 (Appendix B, Figure B2). The daily specific growth (μ_{SG}) between day 4-5 and 5-6 were not accounted for, due to missing cell counts on day 5. Based on the growth curves presented in Appendix B (Figure B2) all cultures had similar growth patterns in the plankton wheel cultivation system, as the parent culture in a 5-L round-flask.

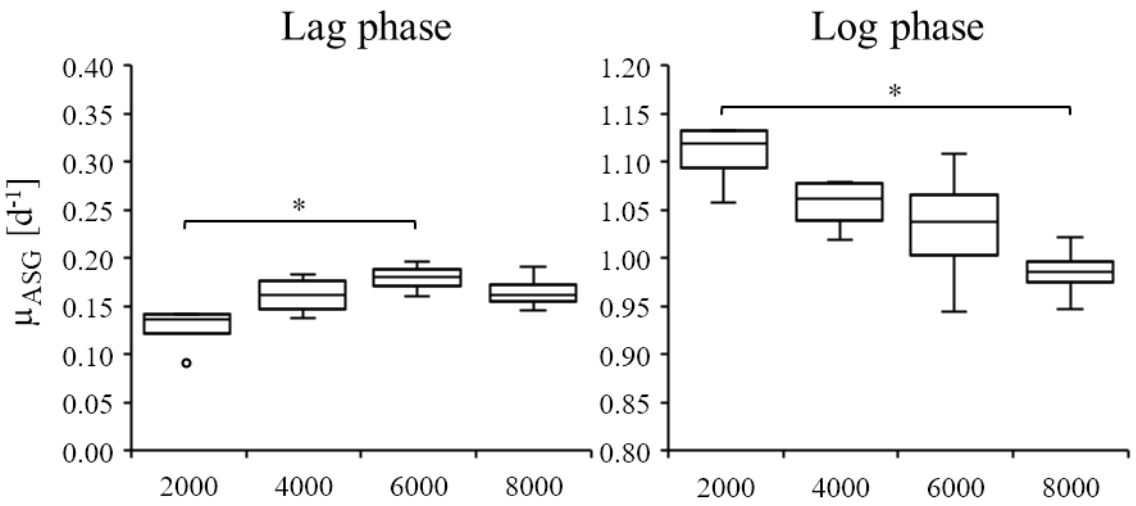

Figure 3.1: Average specific growth rates (μ_{ASG}) of *I. galbana* in lag and log phase during pilot cultivation. Boxes represent the interquartile range (IQR) of the data including the median (mid-line), 25th and 75th percentiles (n=4); whiskers represent the minimum and maximum values (± 1.5*IQR); dot represents suspected outliers. Numbers 2000-8000 represent initial cell densities (cells/mL) at inoculation. Asterisks indicate significances between groups (one-way ANOVA); * p<0.05.

3.2. Effects of microfibres on growth

3.2.1. Lag phase

The μ_{ASG} of lag phase (day 0-4) for *I. galbana* exposed to 60 and 3000 µm MFs are presented in Figure 3.2, with related information presented in Appendix C. In this experiment, exposure to 60 µm MFs resulted in a concentration-dependent increase in μ_{ASG}, with highly significant differences between the control and *I. galbana* exposed to PES H, PA H, Wool H and Wool M; $F_{9,20}$=10.7, p<0.0001. Treatments of PES and PA at medium and low, and wool at low concentrations did not increase the μ_{ASG} significantly (p>0.05). Exposure to 3000 µm MFs resulted in a weaker concentration-dependent increase in μ_{ASG} relative to the control, where all means were close to the control; thus, non-significantly different from the control; $F_{9,20}$=1.8, p=0.14.

Exposure of *I. galbana* to 7-d MF leachates (corresponding to 4.22 µg/mL) of PES, PA and wool increased the mean μ_{ASG} of all treatments relative to the control during lag phase (day 0-5; Figure 3.3A). However, the differences in μ_{ASG} between controls and exposed groups were non-significant; $F_{3,8}$=3.4, p=0.075.

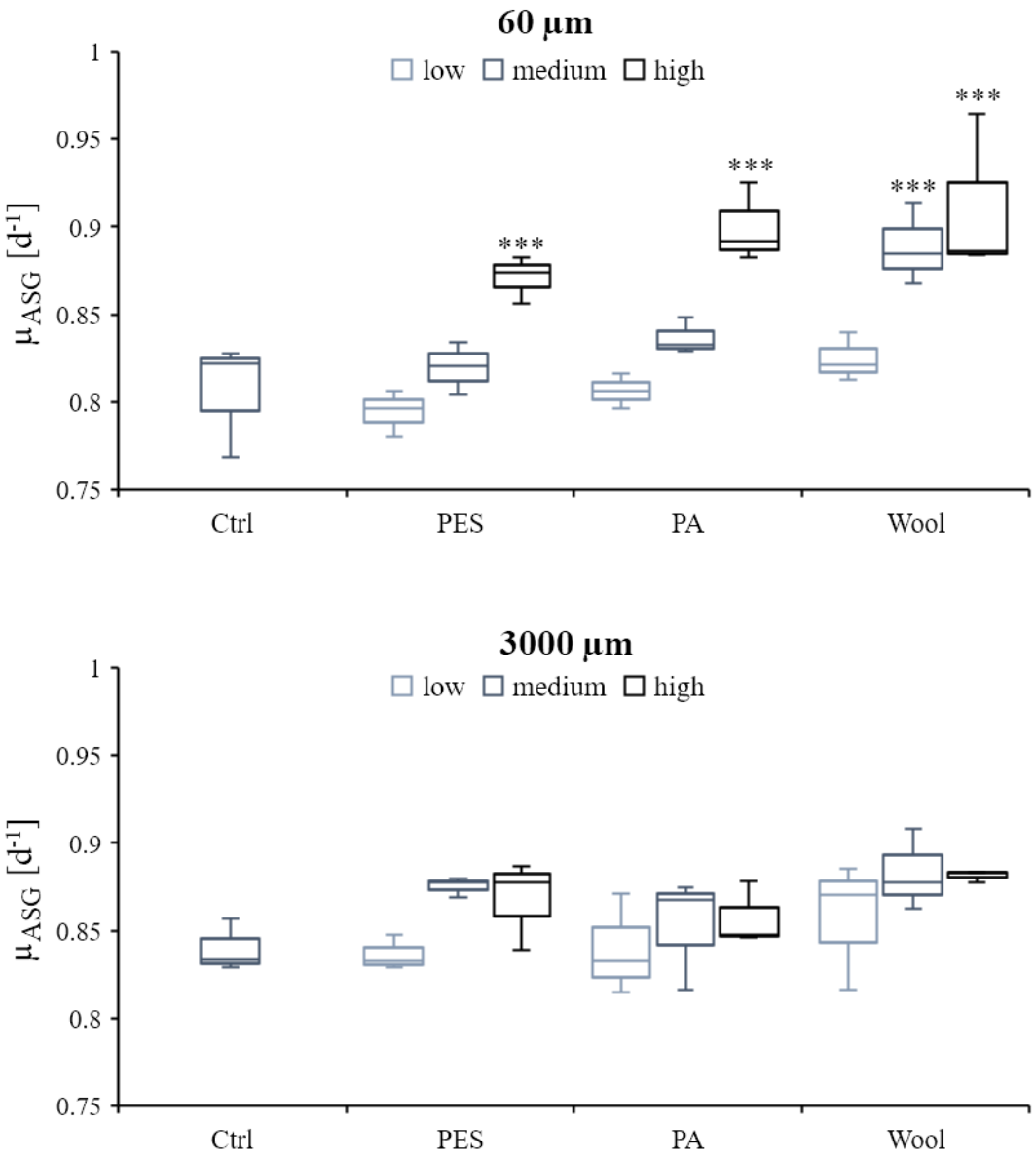

Figure 3.2: Average specific growth rates (μ_{ASG}) of *I. galbana* in lag phase, during exposure to 60 µm and 3000 µm PES (polyester), PA (polyamide) and wool microfibres at low (L, 0.0422 µg/mL); medium (M, 0.422 µg/mL) and high (H, 4.22µg/mL) concentrations. Boxes represent the IQR of the data including the median (mid-line), 25th and 75th percentiles (n=3); whiskers represent the minimum and maximum values (± 1.5*IQR). Asterisks indicate significance from control (one-way ANOVA); * p<0.05, ***p<0.001. Ctrl, non-exposed control.

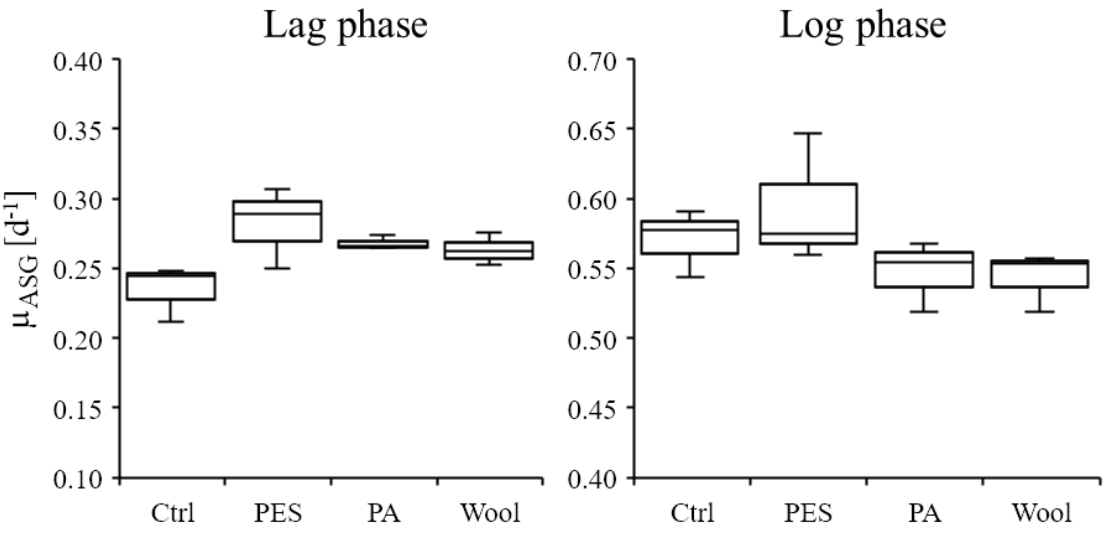

Figure 3.3: Average specific growth rate (μ_{ASG}, n=3) of *I. galbana* in lag and log phase, during exposure to MF leachates of polyester (PES), polyamide (PA) and wool corresponding to 4.22 µg/mL. Boxes represent the IQR of the data including the median (mid-line), 25th and 75th percentiles (n=3); whiskers represent the minimum and maximum values (± 1.5*IQR). Ctrl, non-exposed control.

3.2.2. Log phase

Exposure to 60 µm MFs did not result in a similar concentration-related response of μ_{ASG} in the exponential growth phase (day 4-7), as that indicated in lag phase (Figure 3.4). Among the 60 µm MFs, PES M was the only exposure resulting in a significant increase of μ_{ASG} relative to the control; $F_{9,20}$=5.6, p=0.04. Exposure to 3000 µm MFs resulted in an overall reduction of μ_{ASG} in log phase, compared to the control; however, a concentration-dependent decrease was not prominent, as observed for 60 µm MFs. In this experiment, Wool H and Wool M were the only treatments significantly reducing the μ_{ASG} relative to the control; $F_{9,20}$=2.6, p<0.036. Like 60 µm MFs exposure, Wool L resulted in greater within-samples variation of μ_{ASG}.

Exposure of *I. galbana* to MF leachates of PA and wool reduced the mean μ_{ASG} relative to the control (Figure 3.3), but only by 4-5%. PES leachates, on the other hand, resulted in a weakly increased mean μ_{ASG}, albeit non-significantly; $F_{3,8}$=1.74, p=0.24.

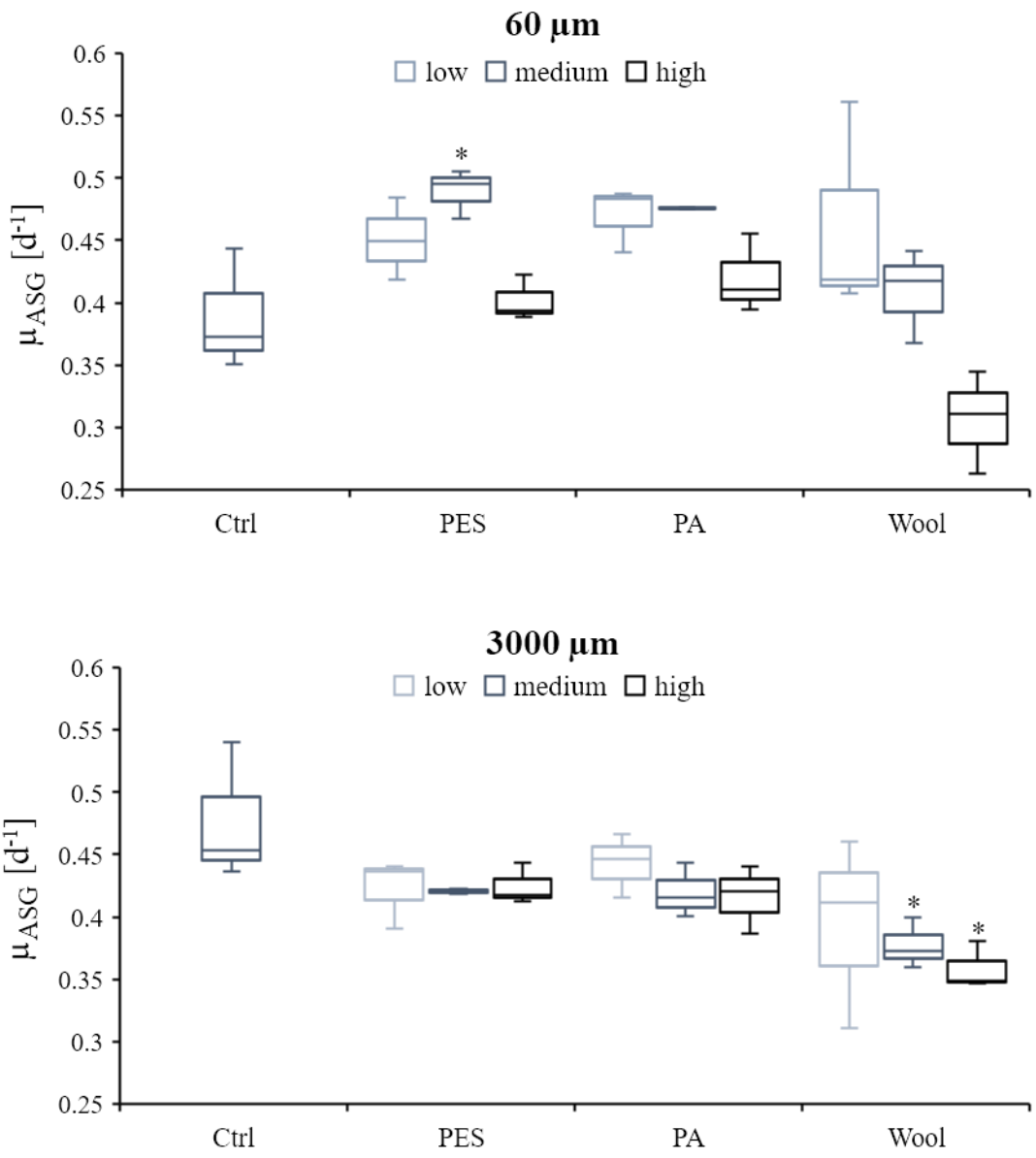

Figure 3.4: Average specific growth rates (µASG) of I. galbana in log phase, during exposure to 60 µm and 3000 µm PES (polyester), PA (polyamide) and wool microfibres at low (L, 0.0422 µg/mL); medium (M, 0.422 µg/mL) and high (H, 4.22µg/mL) concentrations. Boxes represent the IQR of the data including the median (mid-line), 25th and 75th percentiles (n=3); whiskers represent the minimum and maximum values (± 1.5*IQR). Asterisks indicate significance from control (one-way ANOVA); * $p<0.05$. Ctrl, non-exposed control.

3.2.3. Cumulative cell production

The total cell production, calculated from the sigmoid growth regressions (Appendix C, Figure C3), are presented as AUCs in Figure 3.5. Additional information can be found in Appendix C. Overall, 13 d exposure to 60 µm PES L and Wool H reduced the mean cumulative biomass production by 8.8% and 12.3% relative to the control (11 650 000 cells/mL), respectively. In contrast, Wool M and PA M increased the total produced biomass by 5.2% and 3.9%, respectively. Exposure to 3000 µm MFs caused an overall reduction in total produced biomass from 3.4% (PES M) to 11.1% (Wool H) relative to the control (12 300 000 cells/mL). Generally, wool reduced the total biomass production the most among the MF polymers, although the differences were marginal. No statistical analyses were performed on these data, as relative alterations of 10% were considered ecologically significant (Sjollema et al., 2016).

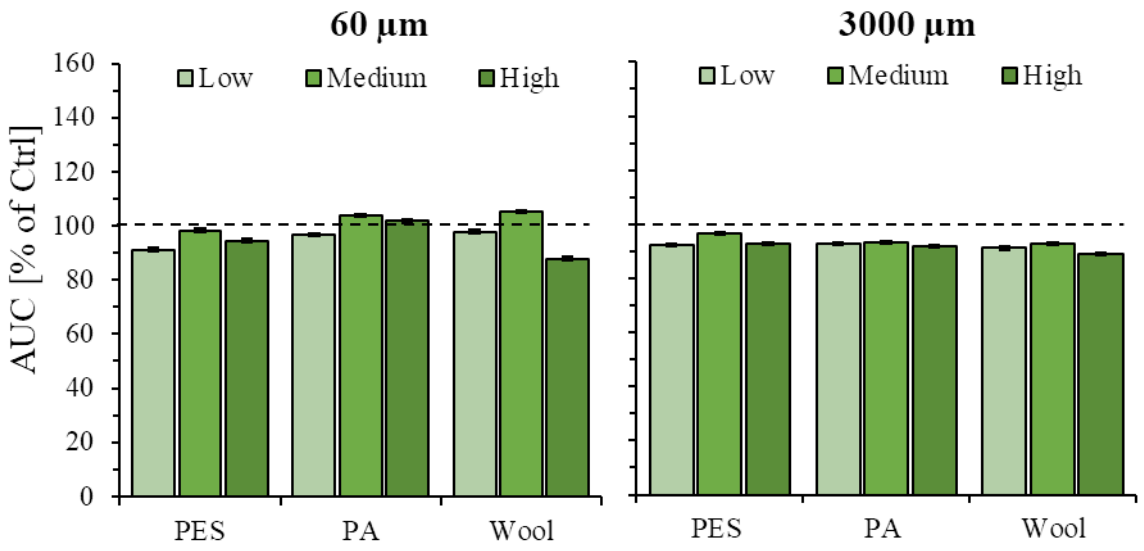

Figure 3.5: Cumulative cell production after 13 d exposure of *I. galbana* to 60 and 3000 µm MFs of polyester (PES), polyamide (PA) and wool, at low (0.0422 µg/mL); medium (0.422 µg/mL) and high (4.22 µg/mL) concentrations. Bars represents mean area under the sigmoid regression curves (AUC) ± standard error (SE) of the regression estimates (*n*=3). Ctrl, control.

At the end of log phase (day 7), 60 µm MFs altered the total cell production in a concentration-dependent manner (Figure 3.6), where PES H, PA H and Wool H stimulated the mean production significantly by 21.6-37.1% of the control (2 100 000 cells/mL). Similarly, exposure to medium levels of PES, PA and wool significantly increased the mean cumulative cell production by up to 33.1% (Wool M). In contrast, low concentrations had no significant effect on total cell production. During exposure to 3000 µm MFs, none of the concentrations or polymer types had significant effects on the total cell productions relative to the control (2 800 000 cells/mL).

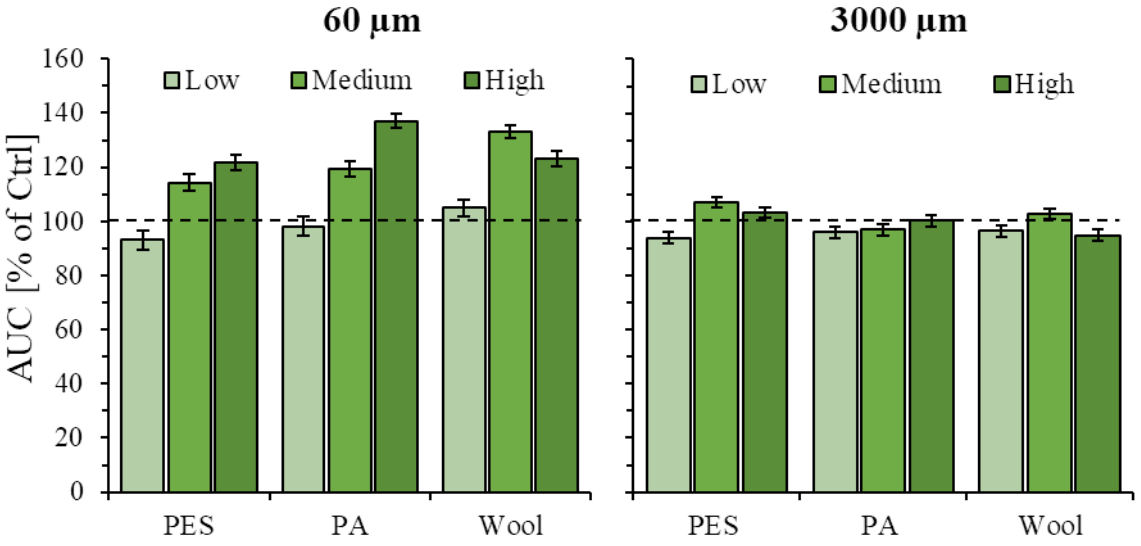

Figure 3.6: Cumulative cell production after 7 d exposure of *I. galbana* to 60 and 3000 µm MFs of polyester (PES), polyamide (PA) and wool at low (0.0422 µg/mL); medium (0.422 µg/mL) and high (4.22 µg/mL) concentrations. Bars represents mean area under the sigmoid regression curves (AUC) ± standard error (SE) of the regression estimates (*n*=3). Ctrl, control.

7-d exposure of *I. galbana* to MF leachates resulted in a polymer-dependent increase in total cell production, like that previously observed with 60 µm MFs (Figure 3.7). PES was the only polymer with a stimulatory effect on mean cumulative cell production, producing 11.3% more than the control (6 000 000 cells/mL), with PA and wool having a mean production of 4.3% and -0.3% relative to the control, respectively.

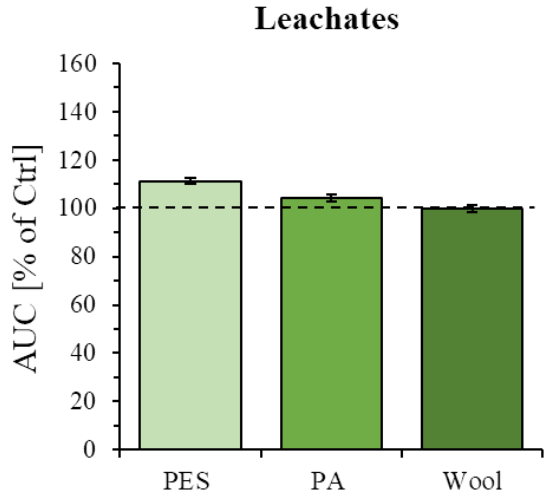

Figure 3.7: Cumulative cell production from 7 d exposure of *I. galbana* to MF leachates of polyester (PES), polyamide (PA) and wool (4.22 µg/mL). Bars represents mean area under the sigmoid regression curves (AUC) ± standard error (SE) of the regression estimates (n=3). Ctrl, control.

3.2.4. Leachate effects on dry weight (DW) biomass

At the end of the MF leachate experiment (7 d) the total DW biomass was calculated, as illustrated in Figure 3.8. Similar to the cumulative biomass production in the previous section (3.2.3), the mean DW biomass of *I. galbana* exposed to PES was significantly higher than the control; $F_{3,20}$=3.2, p=0.047. Wool and PA leachates did not alter biomass production significantly from the control.

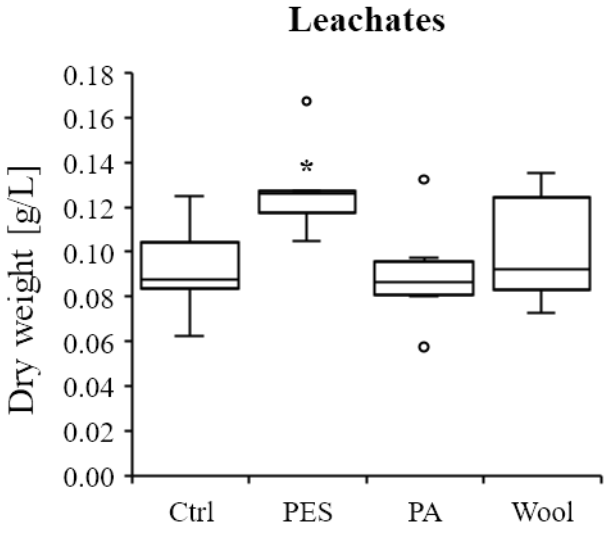

Figure 3.8: Total DW biomass (g/L) of *I. galbana* from 7 d exposure to MF leachates of polyester (PES), polyamide (PA) and wool (4.22 µg/mL). Boxes represent the IQR of the data including the median (mid-line), 25th and 75th percentiles (n=6); whiskers represent the minimum and maximum values (±1.5*IQR); dots represent suspected outliers. Asterisk indicate significant difference from the control (one-way ANOVA); *p<0.05). Ctrl, non-exposed control; DW, dry weight.

3.3. Effects on photosynthetic activity (Chl*a*F)

3.3.1. Chl*a*F per cell over time

The daily Chl-*a* fluorescence (Chl*a*F) per microalgal cell during exposure to 60 and 3000 µm MFs are illustrated in Figure 3.9. Calculations were based on daily Chl*a*F measurements and corresponding cell numbers. Individual daily means (± SD) are presented in Appendix C (Figure C4 and Table C3-C4). Overall, the Chl*a*F had a peak in mid-lag phase (day 2); decreased towards the end of log phase (day 7); stabilised throughout stationary growth phase, and increased towards death phase (day 12-13), for all treatments. Exposure of *I. galbana* to 60 µm MFs of PES, PA and Wool resulted in a concentration-dependent decrease in mean Chl*a*F per cell during lag phase (day 0-4), relative to the mean of the control. On the onset of log phase (day 3), exposure to PES H and PA H resulted in a significant reduction in Chl*a*F per cell; $F_{20,9}$=3.9, p=0.016. In contrast, medium and low concentrations of PES, PA and Wool altered Chl*a*F non-significantly on a per cell basis (p>0.08). Exposure to 3000 µm MFs resulted in larger within-treatments variations of Chl*a*F per cell in lag phase (day 0-2), compared to 60 µm exposure. Furthermore, 3000 µm Wool H was the only polymer type and concentration causing significant reductions in Chl*a*F, compared to the control (day 4); $F_{9,20}$=4.1, p=0.002.

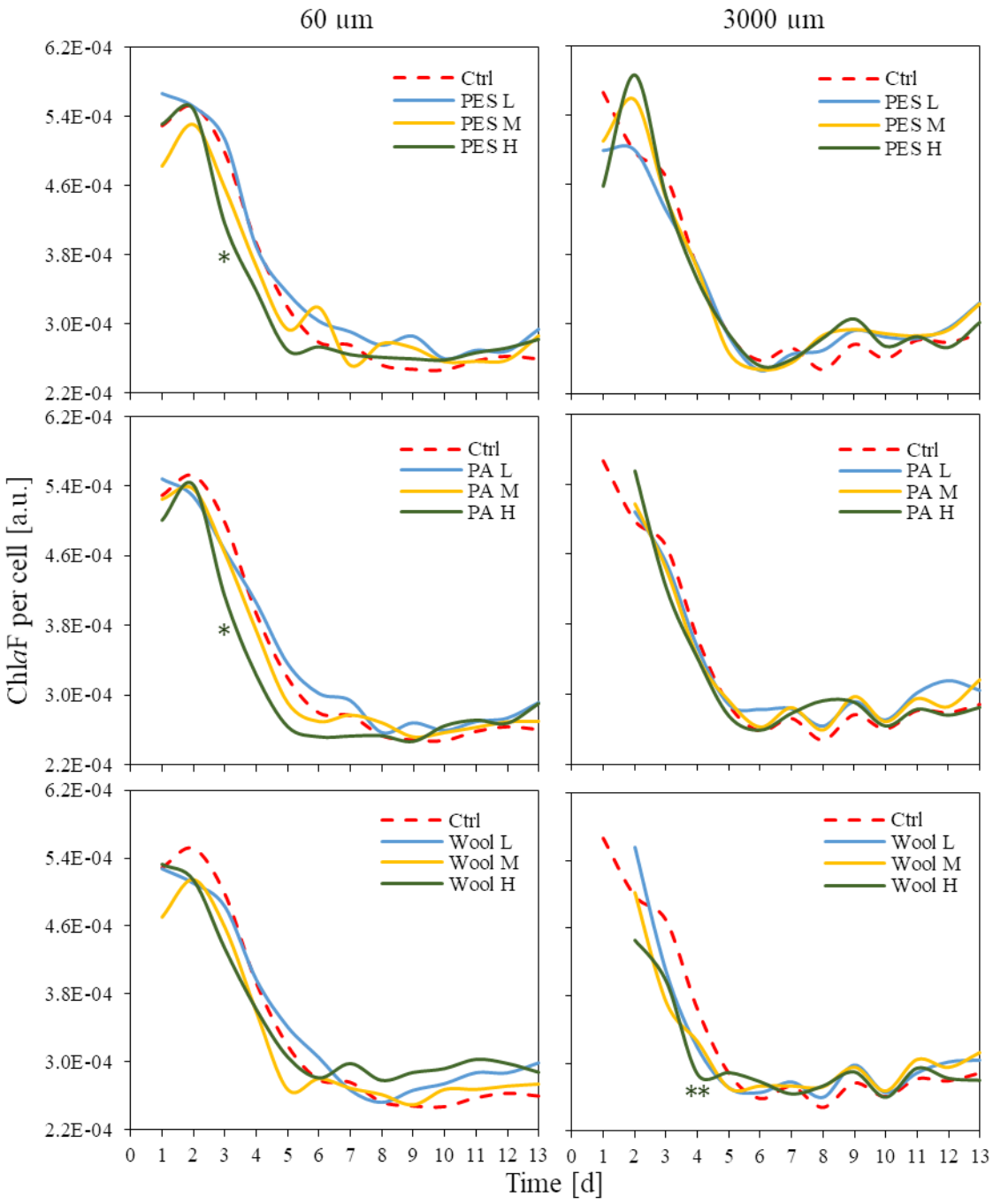

Figure 3.9: Chlorophyll-*a* fluorescence (Chl*a*F) per *I. galbana* cell over time, during exposure to 60 and 3000 µm MFs of polyester (PES), polyamide (PA) and wool, at low (L, 0.0422 µg/mL); medium (M, 0.422 µg/mL) and high (H, 4.22 µg/mL) concentrations. Asterisk indicate significant difference from the control (one-way ANOVA); *p<0.05, **p<0.01). Ctrl, non-exposed control; a.u., arbitrary unit.

3.3.3. Cumulative ChlaF per microalgal cell

The mean cumulative Chl*a*F per microalgal cell is presented as percentages of the control mean (± SD) for *I. galbana* exposed to MFs in Figure 3.10. The AUCs were calculated from day 1-13 for 60 µm, and day 2-13 for 3000 µm, due to sampling issues on day 1 in the latter. Exposure to 60 µm MFs resulted in a concentration-dependent decrease of Chl*a*F per cell, relative to the control; albeit, none of the alterations were significant; $F_{9,20}$=3.33, p=0.21. Exposure to 3000 µm MFs PES at low, medium and high concentrations resulted in increased Chl*a*F per cell, whereas PA and wool reduced the fluorescence at all concentrations. None of the 3000 µm fibres caused any significant alterations in Chl*a*F per cell relative to the control; $F_{9,19}$=1.96, p=0.103.

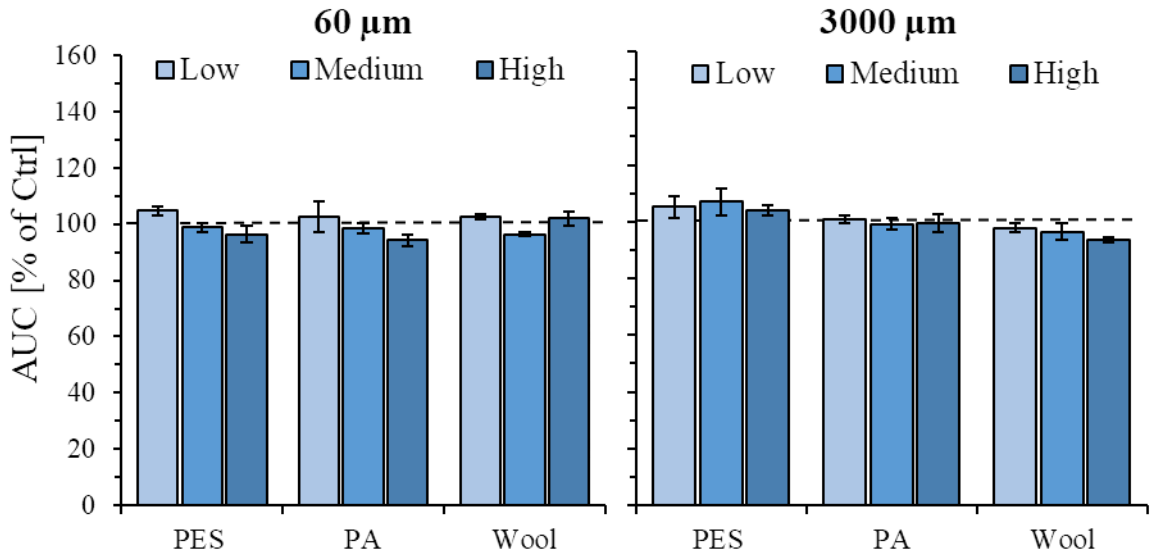

Figure 3.10: Cumulative Chl*a*F per microalgal cell for *I. galbana* exposed to 60 and 3000 µm MFs of polyester (PES), polyamide (PA) and wool, at low (0.0422 µg/mL); medium (0.422 µg/mL) and high (4.22 µg/mL) concentrations for 13 d. Bars present mean percentages of the control (± SD, n=3), where AUC calculations are based on raw data, not regression curves. AUC; area under the curve; Ctrl, non-exposed control.

3.3.5. Quantum yield during leachate exposures

For *I. galbana* exposed to MF leachates, the daily photochemical efficiencies of photosystem II (QY or F_v/F_m) (Figure 3.11) were calculated daily for 7 d. There were no differences between the control and exposed treatments for any of the days. However, the increase rate of QY from day 0-4 (lag) for control was significantly different from that of PES, PA and Wool; $F_{3,8}$=105.4, p<0.0001. In contrast, no statistical difference in the increased rate of QY was found between treatments in log phase (day 5-7); $F_{3,8}$=4.26, p>0.05.

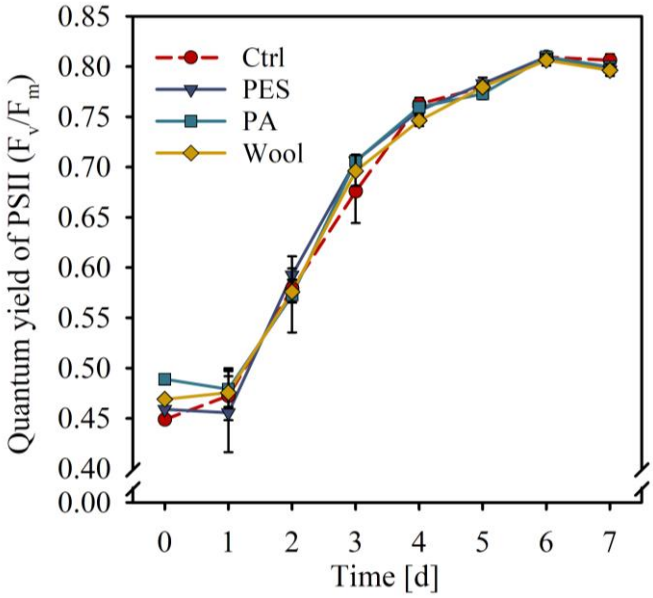

Figure 3.11: Quantum yield of photosystem II (PSII; F_v/F_m) for treatments of *I. galbana* non-exposed (Ctrl) and exposed to polyester (PES), polyamide (PA) and wool MF leachates (4.22 µg/L).

3.4. Effects on molecular composition

Mean absorbance spectra (n=3) from the ATR-FTIR analysis of leachate-exposed *I. galbana* are presented in Figure 3.12. From these spectra, identification and relative quantification of the dominating functional groups (carbohydrates and lipids) are presented as single-peak intensity ratios, following normalisation to protein (amide I; Table 3.1). *I. galbana* exposed to MF leachates had a non-significant decrease in glucose-like carbohydrate absorbance-peak intensity at 1035 cm^{-1}, relative to the control; $F_{3,7}$=4.2, p=0.055. PES and PA appeared to decrease the relative carbohydrate content more than wool. The relative amount of polysaccharide carbohydrates (CC, 1140-1170 cm^{-1}) differed largely (albeit, non-significantly) between treatments, where exposed treatments had peak-shifts towards lower frequencies (1144-1148 cm^{-1}) relative to the control (1163-1165 cm^{-1}), indicating structural changes.

Furthermore, the relative CC content (CC:P) at 1148 cm^{-1} was higher for treatments exposed to PES, PA and wool, than for the control; although, non-significantly here, also; $F_{3,7}$=2.9, p=0.11. PES, PA and wool leachates caused slight reductions of the amide II peak intensity (1543 cm^{-1}) relative to the control, as well as increasing the relative lipid content (L:P) non-significantly; due to large standard deviations within each treatment; $F_{3,7}$=0.52, p=0.68.

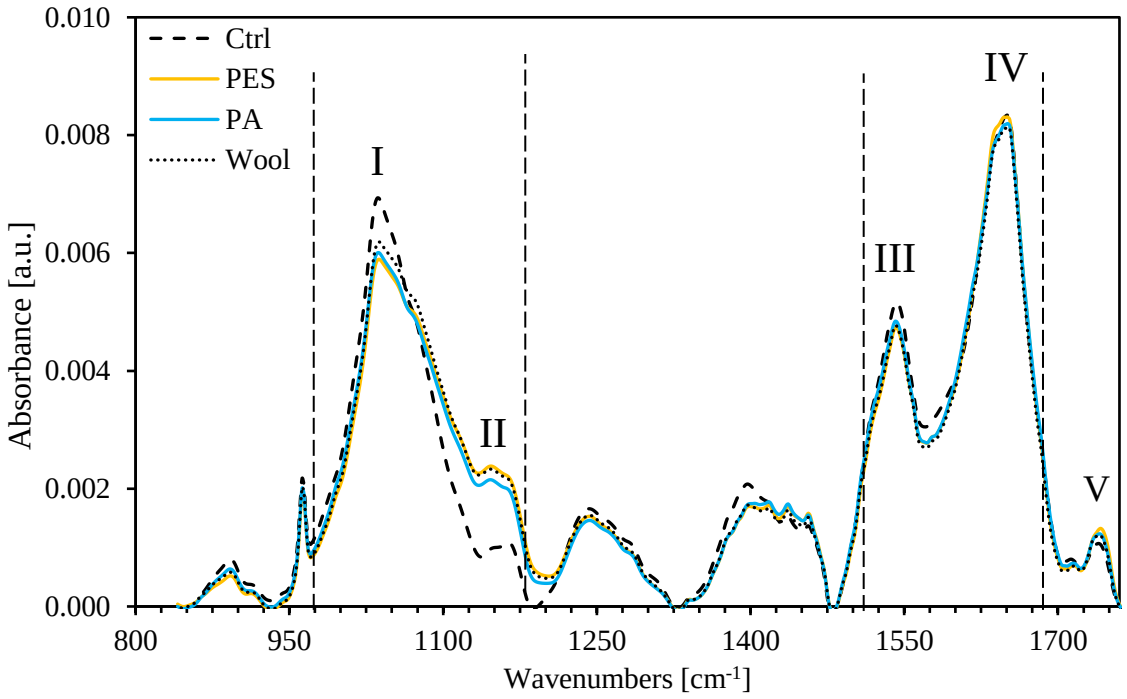

Figure 3.12: Mean attenuated total reflectance fourier-transform infrared (ATR-FTIR) absorbance spectra of *I. galbana* exposed for 7 d to MF leachates of polyester (PES), polyamide (PA) and wool at 4.22 µg/mL (n=3; Ctrl n=2). Bands separated with dotted lines represent the dominating functional groups: carbohydrates (I & II), proteins (III) and (IV), and lipids (V). The roman number assignments are given in Table 2.2.4; individual spectra are given in Appendix C, Figure C6 and Table C3.

Table 3.1: Relative content of carbohydrates (C) and lipids (L), based on single-peak intensities normalised to amide I protein. C:P and L:P represent the relative carbohydrate and lipid content, respectively. Values represent mean (± SD) per treatment (n=3).

	Carbohydrates[a] (1035 cm^{-1})	**Carbohydrates[b] (1148 cm^{-1})**	**Lipids (1745 cm^{-1})**
Ctrl[c]	0.85 ± 0.043	0.12 ± 0.031	0.11 ± 0.037
PES	0.74 ± 0.035	0.26 ± 0.021	0.14 ± 0.012
PA	0.76 ± 0.005	0.31 ± 0.076	0.13 ± 0.007
Wool	0.77 ± 0.012	0.29 ± 0.075	0.13 ± 0.005

[a] glucose and glycogen-like
[b] cellulose-like
[c] n=2

4. Discussion

This study aimed at investigating the chronic effects of textile MFs on *I. galbana* (T-ISO), by assessing physiological parameters such as growth, photosynthetic activity and biochemical composition. Physicochemical properties of the MFs such as polymer type, size and concentration were evaluated in relation to these physiological responses and the experiments were divided into three, due to physical constrictions of the experimental setup: i) exposure to 60 µm MFs, ii) exposure to 3000 µm MFs and iii) exposure to MF leachates. The latter was performed in Umeå, Sweden, which explains why measured parameters of growth and photosynthesis were different from that of the 60 µm and 3000 µm MF experiments. The results of the exposure studies are discussed according to the initial aims and hypotheses: effects on growth followed by photosynthetic activity and biochemical composition. Lastly, the ecological relevance of the findings in relation to populations of *I. galbana* and marine ecosystems are discussed, followed by a methodological evaluation and research prospects.

4.1. Effects of microfibres on growth

Algae represent the baseline available energy at any given time in an ecosystem, building the foundation of most aquatic food webs (von Dassow and Montresor, 2011). Furthermore, microalgae function as indicators of ecosystem health, due to their role as drivers of geochemical cycling, primary production and seasonal variations in biodiversity (Barbosa, 2009). Related to microplastic research, few studies have evaluated the chronic impacts of MPs on population growth of microalgae; particularly MPFs (Prata et al., 2018).

4.1.1. Growth rates

In the present study, the initial growth rates (lag phase) of *I. galbana* was found to be stimulated in a concentration-dependent manner upon treatment with 60 µm MFs. In fact, the early growth of *I. galbana* treated with high concentrations of 60 µm PES, PA and wool was significantly greater than the non-exposed control. The same was found for Wool M, with stimulatory effects relative to the control being in the order of Wool H (12%)>PA H (11%)>Wool M (10%)>PES H (7%). This concentration-related trend was not as prominent for 3000 µm MFs, and none of the treatments resulted in significantly increased growth rates, compared to the control. An explanation for this could relate to the number of suspended fibres that was present in each of the 60 µm and 3000 µm exposures, as the polymers' densities and sizes affected the overall

fibre numbers (Appendix A, Table A4). Treatments with 60 µm MFs had approximately 50 times higher number of MFs/mL than did 3000 µm MF treatments. Additionally, the 3000 µm synthetics (PES and PA) tended to entangle more than wool, decreasing the effective suspended fibre density. By this reasoning, the results might indicate that the number of fibres in suspension, rather than the individual MF sizes, were impacting algae the most (Jemec et al., 2016). Alternatively, any chemically related effects could be masked in the case of fibre entanglement, as the effective surface-to-volume area (thus, leaching potential) would be reduced. Most environmental MPs are hypothesised to cause both physical and chemical impacts (Teuten et al., 2009) but the results from the present study cannot conclude with either. Regarding the relevance of the exposure concentrations, the lowest exposure concentrations corresponded to 2-3 fibres/mL (60 µm) and 0.04-0.06 fibres/mL (3000 µm), which roughly resemble environmentally relevant concentrations (Table 1.1; Gago et al., 2018). Particularly, when taking into account that the MF smaller than 300 µm are not readily detected in marine surface waters upon using conventional sampling methods such as plankton nets and trawling (Dris et al., 2015; Eriksen et al., 2014). As the MF leachates relate to high levels of MFs (*i.e.*, 4.22 µg/mL), they were expected to stimulate lag phase growth in *I. galbana*, like that of 60 µm and 3000 µm MFs. Indeed, this was observed, where μ_{ASG} was increased by >10% by PES, PA and wool (Figure 3.3); albeit, non-significantly. In contrast to 60 and 3000 µm MFs, PES leachate stimulated growth the most; not wool, as previously seen.

The impacts of MFs in log phase differed from the lag phase, where high concentrations of 60 and 3000 µm MFs generally stimulated growth or had no effect, respectively. Among the MF exposures, wool impacted μ_{ASG} most prominently but non-significantly with 60 µm MFs. On the other hand, 60 µm PES M stimulated μ_{ASG} significantly, relative to the control, and had a μ_{ASG} that was 37.5% higher than Wool H. 60 µm wool had no consistent concentration-dependent increase or decrease (Figure 3.4). These inconsistent effects might be a result of differences in additive leaching potentials between synthetic MFs and wool. Wool had stronger (significant, in the case of 60 µm MFs) effects on growth at both high and medium concentrations than PES and PA. Similar findings were indicated in freshwater *D. magna* by Dave and Aspegren (2010), where textile fibres of wool and cotton were found to be more acutely toxic than synthetics after 48 h exposure. Nonetheless, the initial growth stimulation by 60 µm MF treatments of *I. galbana* contrasts with the observed 48-h immobilisation of *D. magna*. Although the present study did not investigate the additive profiles of the treatment MFs, the same textile yarns were analysed for additives by FTIR in a parallel study (Sait,

unpublished MSc thesis). In her study, Sait found elements such as Titanium (Ti) and antimony (Sb) and bisphenol-a (BPA) in the MFs; similar findings of BPA were also observed in dyed MPFs from marine litter samples by Gauquie (2015). In Sait's study, untreated wool MFs contained higher amounts of BPA and elements than MFs of PES, PA and polyacrylic. This could likely be linked to the relatively high polarity of BPA ($\log K_{ow}$=3.4), as it might have a greater sorption potential to polar compounds such as cotton. Consequently, leaching into ambient water (*e.g.*, laundry waters, wastewater, marine water) could be a more prominent risk for wool (Saini et al., 2016). Assuming BPA is released from the MFs, this could indicate that treatment with wool MFs posed a greater potential for chemical impacts on *I. galbana* in this study, compared to the MPFs.

Like the initial growth stimulation observed here, two studies investigating BPA toxicity in the microalgae *Chlorella pyrenoidosa* found hormetic responses from BPA at low concentrations. Growth was stimulated by 19.4 % after 72 h (0.1 mg/L; Duan et al., 2019) and by >25% and >125% after 48 h and 96 h of exposure (1.6 mg/L; Li et al., 2017), respectively. A third study evaluated the toxicological risk of BPA, triclosan (TCS) and 4-nonylphenol (NP) - all common phenolic compounds of environmental concern, from plastics and wastewater - on *I. galbana*. In this study, the "no observed effect" and "lowest observed effect concentrations" (NOEC and LOEC, respectively) for BPA were found to be 0.5 and 1 mg/L, respectively; even though none of the compounds gave hormetic responses. In addition to BPA, TCS and NP, various chemical additives throughout the textile industry are considered agents of ecotoxicological risk; for instance chlorinated solvents, elements (Sb, lead (Pb), cadmium (Cd)), biocides (pentachlorophenol on wool) and plasticisers (BPA) (Verma, 2008). In toxicological experiments, the time, length and intensity of exposure affects subsequent biological responses (Verma, 2008); thus, increased toxic responses usually correlate with increasing exposure time. In the present study, the inhibiting effects of MF treatments were generally more prominent during initial growth (Figure 3.2) than exponential (Figure 3.3), potentially indicating a slightly time-dependent response also.

The 3000 µm MF treatment resulted in both a concentration and a polymer-related growth inhibition in initial growth, relative to the control; although, only Wool L and Wool M were significantly different. None of the leachate treatments had any significant effects on exponential μ_{ASG}. Nonetheless, a slightly polymer-related effect was found (Figure 3.7). Between experiments, the μ_{ASG} were not comparable (*i.e.*, 60 µm, 3000 µm and leachates)

because they were performed at different times, and with distinct population generations of *I. galbana*. Although the growth of the parent culture was healthy before the onset of each experiment, variations in time- and population-specific factors such as cell size and growth stage of the population majority, could likely have affected overall growth rates between experiments. Also, the low μ_{ASG} of *I. galbana* populations from the leachate study could have been due to the low initial pH of the culture medium (pH=6.5), as a pH within 7.0-8.0 is considered optimal for *I. galbana* (Abu-Rezq et al., 1999; Pérez, 1994). A probable cause of this low pH was a reduced buffering capacity of the artificial seawater in use, compared to the seawater from the Trondheim fjord.

4.1.2. Cumulative cell production

Algal biomass production responds in a monotonic manner to toxic stressors, and temporal and spatial variabilities in light, temperature and substratum, making it a good indicator of environmental stressors (Stevenson, 2014). In the present study, however, dry weight biomass was not measured after exposure to 60 and 3000 µm MFs, due to small sample volumes (40 mL) and daily sub-sampling volumes (10 mL). Instead, the cumulative cell production was calculated from the area under the sigmoidal regression curves (Figure 3.5-3.7 and Figure C3 in Appendix C). Importantly, dry weight biomass is not accurately reflected by cumulative cell numbers, as individual cell volumes and molecular composition per cell can vary significantly. Based on the inaccuracy of the data, SDs were not included and statistical tests were not performed between treatment groups; instead alterations <10% from the control were considered ecologically negligible because variations in algal densities occur naturally (Sjollema et al., 2016). 60 and 3000 µm Wool H were the only exposures which significantly reduced the cumulative cell production relative to the control, after 13 d exposure (Figure 3.5-6). In contrast, 7 d exposure to medium and high concentrations of 60 µm MFs all significantly stimulated cumulative cell production; whereas 3000 µm MFs had no significant effect on cell production. Upon 7 d exposure to MF leachates (Figure 3.7), PES was the only treatment with strong stimulating effects on cell production (11.3%), which was also seen from the growth curves (Appendix D). Comparisons between exposures to 60 and 3000 µm MFs and MF leachate at day 7 indicated no trends in polymer-dependent effects, as only cell production during exposure to PES leachates were distinctly different from the others.

In a recent review on alga toxicity of spherical MPs and NPs (Prata et al., 2019), three of the studies exposing microalgae for more than five days observed altered population growths (Lagarde et al., 2016; Lyakurwa, 2017; Mao et al., 2018). In one of the studies, PS beads (10 µm) were found to significantly stimulate growth in *Rhodomonas baltica* at concentrations of 750 MPs/mL (0.464 µg/mL), and conversely inhibit growth at 7500 MPs/mL (4.64 µg/mL), with no apparent effects from 75 MPs/mL (0.0464 µg/mL). In contrast, Long *et al.* (2017) observed no growth inhibition in *I. galbana* (T-ISO) treated with 2 µm PS beads (0.00396 µg/mL) for 35 d. However, both authors observed progressive decreases in suspended MPs throughout the experiments, losing roughly 40.9% (Lyakurwa, 2017) and 75 ± 4% (day 14; Long et al., 2017) to glassware adhesion and hetero-aggregation. Their loss of MPs – and the loss of MPFs to entanglement in the present study - could ultimately have impacted the effective treatment concentrations of MPs and MPFs. If the majority of observed effects were due to physical impacts, the observed toxicity could have been impacted in all studies.

A MF exposure study on the freshwater crustacean *D. magna* by Jemec *et al.* (2016) found no effects on individual growth (*i.e.*, body size) after 48 h; neither by PES MFs (62-1400 µm at 12.5-100 µg/mL) nor their 48-h leachates (100 µg/mL). Furthermore, Dave and Aspegren (2010) reported a 48-h EC_{50} range from <1.6 to >63 mg/mL in *D. magna* upon treatment with synthetic fibres, and indicated stronger effects of wool fibres (EC_{50}=6.7-40 mg/mL). Similarly, the current study found more prominent effects on growth (μ_{ASG} and cumulative cell production) by high treatments of wool MFs, compared to synthetics. As ambient conditions such as temperature and pH, additive levels and composition of MFs affect the effective leaching rates (Dave and Aspegren, 2010), polymer leaching and degradation likely pose a greater risk upon ingestion by homeotherm organisms with acidic gut conditions, high enzyme activity and mechanical gut processing (Andrady, 2011; Teuten et al., 2009). The gut pH of daphniids ranges between 6-6.8 and 6.6-7.2 in the midgut and posterior gut, respectively (Ebert, 2005) and could be one explanation for why Lithner *et al.* found no acute toxicity (*i.e.*, immobilisation) in *D. magna* exposed to PES leachates (Lithner et al., 2009). Also, the risk of chemical impacts from MPFs in microalgae and daphniids are likely dependent on passive diffusion of non-polar contaminants (Teuten et al., 2009), rather than ingestion. Contrarily, Bhattacharya *et al.* (2010) and Zhang *et al.* (2017) suggested that high levels of spherical NPs (0.08-0.58 µg/mL) and MPs (0-50 µg/mL) exerted physical toxicity through cell surface adsorption; however, as the current study used MFs >10 and >500 times larger than the average

I. galbana cell, adsorption to and of MFs would unlikely cause the same physical effects as NPs.

4.2. Effects on photosynthetic activity (Chl*a*F)

Chl*a*F has proven a good, rapid and minimally invasive *in vivo* measurement of relative changes in Chl-*a* content in algal populations over time. Parameters such as QY (F_v/F_m, photochemical efficiency of PSII) and F_0 (minimum Chl*a*F from PSII) are frequently used as reliable indicators of photoinhibition and -acclimation. Chl*a*F is also widely applied as a proxy for algal biomass together with - or alternatively to - OD measured at wavelengths of 680 nm (light attenuation by Chl-*a*; Maxwell and Johnson, 2000). The current project investigated Chl*a*F (F_0', light-adapted state) during exposure to physical MFs and QY (F_v/F_m) and during exposure to MF leachates.

4.2.1. Chl*a*F per cell

In the present project, Chl*a*F and cells/mL were positively correlated (Pearson's and Spearman's rho correlation), indicating that the total amount of Chl-*a* in the populations was increasing with increasing population densities (Appendix C, Figure C1-2 and Table C1-2). However, the correlograms also indicated slightly higher Chl*a*F among exposed *I. galbana* than non-exposed. Based on these observations, Chl*a*F per cell was calculated and plotted to visualise the time-dependent variations between exposed and non-exposed treatments.

Exposure to the 60 µm MFs PES H and PA H were the only treatments that significantly reduced Chl*a*F per cell in lag phase (day 3), relative to the control. Compared with the growth rates in lag phase (Figure 3.2) high exposure concomitantly increased μ_{ASG} which, in turn, could indicate that cells were expending more of the absorbed light energy on photochemistry (*i.e.*, growth and reproduction) than to fluorescence emission. However, neither 60 µm Wool M nor Wool H MFs significantly reduced Chl*a*F per cell, despite both treatments significantly stimulating lag μ_{ASG}. During exposure to 3000 µm MFs, only Wool H significantly increased Chl*a*F per cell in early log phase (day 4). Additionally, Chl*a*F per cell appeared generally independent of concentration; coinciding well with the lag μ_{ASG} (Figure 3.2) where none of the exposed *I. galbana* had more rapid growth than control. Only high levels of MFs significantly reduced the Chl*a*F relative to the control, as was observed by Lyakurwa (2017) after 6 d

exposure of *R. baltica* to 10-µm PS beads (4.64 µg/mL), although Chl*a*F per cell was not investigated in his study. Similarly, low MF exposures had no significant effects on Chl*a*F in neither studies, as also observed by Long *et al.* (2017) after 35 d exposure of *I. galbana* (T-ISO) to 2-µm PS beads (0.004 µg/mL). Overall, the Chl*a*F per cell varied temporally but were, in general, inversely related to growth rate (non-restrictedly monotonic).

Chl*a*F is almost exclusively generated by the light-harvesting complexes of PSII at ambient temperatures (Hofstraat et al., 1994); thus, variations were likely results of altered energy allocations towards photochemistry. Alternatively, Chl*a*F reductions could be an effect of reduced light absorption per cell or per unit of Chl-*a* caused by i) self-shading effects in highly concentrated samples of algae, ii) shading by fibres, iii) reabsorption of Chl*a*F by suspended organic matter or antennae pigments or iv) reduced Chl-*a* content per cell (Agati et al., 1993; Arar and Collins, 1997). Shading by the larger fibres was unlikely, as fibre densities were low throughout the experiment. Alternatively, the effective light absorption per cell could have been reduced as the population grew denser; furthermore, increasing fluorescence reabsorption by surrounding cells and organic matter. The observed stimulation of Chl*a*F towards death phase could indicate an increase in [Chl-*a*] per cell, as population growth had stagnated; alternatively that cellular processes downstream from PSII (*e.g.*, carbon assimilation, respiration) were inhibited, or that proteins and membranes associated with photosynthesis were poorly functioning (Marwood et al., 2001).

4.2.2. Cumulative ChlaF per microalgal cell

The cumulative Chl*a*F per cell was calculated from 13 d exposure because of large daily variations, as an additional means of quantifying overall difference between exposed and non-exposed *I. galbana* (Figure 3.10). Calculations were made between day 2-13 for the 3000 µm exposure, due to sampling issues for PA and wool-treatment groups on day 1. None of the 60 µm MFs significantly reduced the cumulative Chl*a*F per cell, although a weak concentration-dependent response was observed for all except Wool H. The 3000 µm exposures had no significant effect on cumulative Chl*a*F relative to the control, either, even though a weakly polymer-dependent reduction was observed here.

High concentrations of MFs were hypothesized to increase total Chl*a*F in *I. galbana* as a stress-induced response but this was not observed in this study. Based on the daily Chl*a*F per cell

presented in Figure 3.9, Chl*a*F varied independently of growth patterns, possibly suggesting that [Chl-*a*] per cell and/or the light utilisation per cell varied daily. As previously discussed, Long *et al.* (2017) found no significant effects of 2-µm PS beads on Chl*a*F, suggesting negligible effects on [Chl-*a*] in exposed algae.

4.2.3. Photochemical quantum yield (QY)

From the leachate experiment, the daily QY (F_v/F_m) was not affected in *I. galbana* by any of the treatments (Figure 3.11), except for some minor differences in the two initial days (0-1). This could suggest that neither fluorescence nor photochemistry was significantly affected by MF leachates, knowing that changes in photosynthetic efficiency reflect changes in fluorescence and *vice versa* (Agati et al., 1993; Suggett et al., 2011). Alternatively, the sensitivity of *I. galbana* to leachate toxicity could have been reduced in this experiment, due to low initial pH conditions of the culture medium, as previously discussed.

In a recent study, Sjollema *et al.* (2016) found negligible effects on photosynthetic efficiency (QY) in *Dunaliella tertiolecta* from exposure to high levels of PS beads (72 h, 250 µg/mL, 6 µm), despite the light intensity in the culture being reduced up to 34% by the fibres. In contrast, a more recent study by Mao *et al.* (2018) reported a 9.6% reduction of QY in *C. pyrenoidosa* after 6 d exposure to 1.0 µm PS beads (100 µg/mL), suggesting a maximum depression of photosynthetic activity from lag to early log phase. Moreover, photosynthetic activity was stimulated from the end of log until stationary phase. Similarly, the present study observed significant depressions of Chl*a*F per cell in early log phase upon exposure to high levels of PES and PA (60 µm) and wool (3000 µm) (Figure 3.9); with an increase (non-significant) towards stationary phase by high levels of wool (60 µm).

4.3. Effects on molecular composition

FTIR spectroscopy is a convenient tool in physiological fingerprinting of phytoplankton communities, as it enables relative quantification of biochemical composition and comparisons between subcommunities (Stehfest et al., 2005; Wagner et al., 2013). The technique mirrors adaptational statuses of subcommunities and, therefore, facilitates comparison of physiological responses between populations grown under different conditions. As growth potential is primarily defined by patterns of energy allocation, high relative content of, for instance,

carbohydrates and lipids may indicate increases in growth and *vice versa* (Sukenik and Wahnon, 1991). Under natural light conditions, carbohydrates and lipids tend to accumulate upon nutrient limitation and other environmental stressors, because the assimilated carbon is not used for cell growth.

In the present study, the mean peak intensities of carbohydrates (C and CC), lipids (L) and protein (P, amide I) and the FTIR spectra were calculated from three replicates for all treatments of *I. galbana,* except for the control (*n*=2). This was due to a loss of a sample prior to analysis, resulting in large variations within treatment groups, as is visible from the individual spectra in Figure C6 (Appendix C). For this reason, the precision of the results was relatively low, potentially affecting the significance between treatments. Nonetheless, distinct reductions in relative carbohydrate content (C:P and CC:P) were found between the control and PES, PA and wool leachate treatments. The carbohydrate peaks (1035 and ~1148 cm^{-1}; associated with the C-O stretching and bending frequencies within glucose/glycogen and cellulose, respectively (Murdock and Wetzel, 2009)) were stoichiometrically shifted from energy storage (glucose-like carbohydrates) to cell integrity (cellulose-like) in exposed treatments, relative to the control. This could be seen from the decrease in the glucose-like peak and co-occurring increase in the cellulose-like peak absorption intensities. In the previously mentioned study by Mao *et al.* (2018) chronic exposure of PS beads resulted in cell wall thickening in *C. pyrenoidosa,* which could suggest that a similar response was observed in *I. galbana* in the present study. Alternatively, the reduced glucose storage content upon exposure to PES leachates, could be explained by the stimulated growth on day 7 (Figure 3.3 and Figure 3.7). However, similar biochemical shifts were also observed in *I. galbana* exposed to PA and wool leachates, despite low growth rates. The exposed treatments had growth rates and cumulative cell productions in the order of PES>PA>wool, and inverse relative glucose contents of PES<PA<wool. Albeit, a similar relationship could not be distinguished from the dry weight biomasses (Figure 3.8). The alterations in lipid content (L:P) were less distinct between treatments, being marginally elevated in exposed groups compared to the control.

Based on an FTIR study performed by Stehfest *et al.* (2005), this leachate experiment might have been too brief to induce any significant metabolic changes in *I. galbana* after only 7 d. Stehfest *et al.* investigated nutrient starvation in microalgae for 4 weeks and suggested that only long-term (>14 d) environmental stress was reflected in biochemical alterations. Similarly, the cell wall thickening observed by Mao *et al.* occurred after 13 d exposure to MPs (Mao et al.,

2018). Photosynthetic parameters such as pigmentation ([Chl-*a*]) and photosynthetic efficiency (QY) would be altered initially, as a more instant acclimatisation strategy.

A different study by Hu *et al.* (2017) used another approach by combining FTIR-based responses with standardised toxicity tests to address metal and herbicide toxicity in duckweed (*Lemna minor L.*). Their results indicated that biochemical alterations were associated with exposure to different compounds, and primarily attributable to structural changes of lipids, proteins, nucleic acids and carbohydrates. The herbicide acetochlor, which inhibits growth by blocking protein synthesis, was indeed associated with alterations of protein structure (amide I and amide II) and carbohydrates (glycogen, 1030 cm^{-1}). In contrast to Hu *et al.*, the present study did not perform any multivariate analyses, due to few samples and sample replicates. A principle components analysis (PCA) could, in this case, be helpful in characterising the differences within specific waveband regions between treatments of *I. galbana*; thus, indicate biochemical differences (Szymanska-Chargot and Zdunek, 2013).

4.4. Biological relevance of the results

4.4.1. Marine microalgae

Current studies on MP toxicity in microalgae is scarce; even more so on MPFs. As most laboratory studies observe limited effects of MPs on growth and photosynthetic parameters, this could suggest that current surface water concentrations have negligible impacts on aquatic primary producers (Prata et al., 2018; Wan et al., 2018). Nonetheless, few of these studies have focused on long-term exposure and none have so far assessed the impacts of MF leachates on biochemical structure of microalgal populations. MP is an ambiguous umbrella term (Lambert et al., 2017) including a vast variety of polymers, shapes and sizes; therefore, it is important to investigate the ecological impacts of separate classes of MPs and combinations of these.

The present study aimed at investigating individual effects of polymers, concentrations and sizes of MFs and MF leachates on the marine microalga *I. galbana*. The results indicated limited effects from PES, PA and wool on growth, photosynthetic activity and biochemical structure during multiple stages of growth. Moreover, the effects were inconsistent between experiments. From an ecological perspective, current environmental concentrations of MFs in ocean surface waters are likely of minor concern to larger populations of microalgae such as *I. galbana*. Effects on growth rate and photosynthesis was both stimulating and inhibiting at different stages

of growth, as has been previously observed with other species of microalgae (Mao et al., 2018). Furthermore, despite the concern for MFs often relating to MPFs, results from the 60 µm and 3000 µm exposures in this study could suggest that non-synthetic MFs such as wool has more prominent impacts than synthetics (Figure 3.2, 3.4 and Figure C3 (Appendix C)). In contrast, the leachate experiment indicated more prominent effect from PES leachates (Figure 3.7-8) only, without effects of PA and wool. This could imply that MFs leach non-significant amounts of chemicals into seawater, that are toxic to microalgae; alternatively, insufficient amounts to cause sub-lethal effects on growth and photosynthesis. In most marine waters, fibres would likely distribute and dilute within minutes to hours, due to factors such as physicochemical properties of the fibres and chemicals, wind and water currents, temperature and pH, among others. Combined, all factors affect individual leaching rates and the MFs' distribution geographically and in the water column.

The greatest risk for toxicological impacts of MFs would likely take place in severely polluted areas such as still waters in proximity to populated land and wastewater outlets (Browne et al., 2011; Dave and Aspegren, 2010; Henry et al., 2018). Here, severe pollution could have overall negative consequences for populations of microalgae, potentially reducing growth and photosynthesis. Furthermore, higher trophic organisms depending on microalgae as a primary source of energy could then be indirectly affected by nutrient depletion (Green et al., 2016; Sukenik and Wahnon, 1991; Tredici, 2010). Alternatively, growth-stimulating effects of MFs on algal populations could potentially generate an additional risk of algal blooms and local eutrophicating in coastal waters with unlimited access to nutrients from terrestrial run-off (Calvo-Flores et al., 2018; Ellen MacArthur Foundation, 2017).

Empirical findings suggest that environmental concentrations of MFs and, consequently, the risk for impacts on growth and photosynthesis in microalgae are limited. However, as the demand for textiles progressively increases globally (Ellen MacArthur Foundation, 2017; Henry et al., 2018) more MFs will eventually reach marine environments; potentially exacerbating today's risk of negative impacts on ecosystems and their inhabitants.

4.5. Methodological evaluation and future work

4.5.1. Pilot cultivation

A pilot cultivation experiment was run to assess the growth patterns of *I. galbana* on the plankton wheel setup (*i.e.*, length of lag and log phase and time of growth stagnation). Here, the culture growth did not stagnate before the termination of the experiment on day 12. Nonetheless, the daily µ (μ_{SG}) decreased towards day 12 indicated that all cultures were close to stagnation. Based on the growth rates and maximum cell densities on day 12 and 21, it was concluded that neither of the initial cell densities affected growth nor the final cell density significantly. Because the aim of this study was to assess chronic effects, the cell densities were also maintained below those used in the OECD 96-h growth inhibition test (OECD, 2006). Finally, 10 000 cells/mL was selected as initial cell concentration, to make sure the algae would be viable from initial stress throughout the study.

4.5.2. Study methodology and design

The present study aimed to assess the effects of MFs and MF leachates on the marine microalgae *I. galbana*, as this has not previously been investigated. Because similar studies of MFs toxicity in microalgae have not yet been published, method development was a major part of this project.

Regarding quantification of MFs throughout the exposure, the major issue was to determine the absolute quantity in suspension of each flask and vial. Unlike small MP beads which are identifiable by particle counters and flow cytometers (Long et al., 2017; Lyakurwa, 2017), the length and shape of the MFs caused a risk of blocking the apertures of such instruments. Furthermore, microscopy counting proved difficult, due to the low concentrations of MF; also, the synthetic MFs (*i.e.*, PES and PA) tended to entangle into larger fibre clusters. It is also important to point out that the leachates were initially prepared from 10 mg MFs/mL and were later diluted to 4.22 µg/mL. As the MF stocks were prepared 2 w and 2 mo in advance of the 60 µm and 3000 µm experiments, respectively, this might have affected the results. Methods to adequate count cells and analyse photosynthetic parameters and biochemical composition in *I. galbana* without interference from suspended MF was also addressed. A filtration trial indicated that the Chl*a*F measurements had lower sample variation once filtrated, compared to others with MFs in suspension present. Additionally, the filter mesh was small enough to retain MFs on it, while at the same time retaining negligible numbers of algae.

Parameters such as cell size distributions, ODs of carotenoids and Chl-*a* were additionally measured during this study but used primarily in the evaluation of cell viability. These additional parameters were opted out for the benefit of larger analyses such as FTIR, and for the ease of comparison between physical MF and leachate studies. Initially, the aim was to analyse multiple photosynthetic parameters of PSII, using an FRRf as described in Pérez *et al.* (2010); alternatively, comparing F_{680nm}/F_{735nm} ratios between exposed treatments, as the latter inform about interactions between PSII and PSI-bound Chl*a*F (Buonasera et al., 2011; Eullaffroy and Vernet, 2003). Advantages of such methods would be their favourable comparisons with standard algal growth inhibition tests, and the frequent use of F_{684nm}/F_{735nm} in plant/algal research to establish health states.

In general, FTIR spectroscopy is a promising method for toxicological assessments in phytoplankton, despite some apparent challenges such as 1) determining sample preparation for removing all excessive and interfering compounds and 2) acquiring suitable statistical methods for extracting biological information from the FTIR spectra. In the present study, samples were not washed before freeze-drying and remaining salt crystals might have provoked light scattering. Secondly, filtered and dried biomass from the 60 and 3000 µm MF exposure was too low to obtain any absorbance signal. Consequently, only the leachate-treated samples resulted in interpretable (but highly variable) FTIR spectra.

Tested methods that were not included in the end were 1) *in vivo* lipid staining and fluorescence analysis using Nile red; and 2) 72-h growth inhibition test in 96-well plates. The Nile red staining was aimed as a method of quantifying the lipid accumulation, as a metabolic parameter in *I. galbana*, and was developed on the basis of protocols by Chen *et al.* (2009) and Bertozzini *et al.* (2011). In practice, issues like poor water solubility of the test lipid (triolein) occurred in the algal cultures, generating inconsistent and non-linear fluorescence-concentration responses between replicates (Appendix B, Figure B4). A 72-h toxicity test was performed with an aim of assessing the EC_{50} of the MF leachates (Appendix B, Figure B6). The experiment was done in duplicate to ensure a stronger power of the results but failed because of a mix-up with the well plate classification; instead of using inadhesive culture plates for suspended cells, adhesive well plates facilitating cell adherence were given. Consequently, cell and pigment density data were spectrophotometrically inexplicable, due to the cells adhering to the plate bottom.

4.6. Recommendations for further research

Based on the present and previous ecotoxicology studies with MPs, more research is needed on the effects of MPs in marine ecosystems, with a greater emphasis on the impacts of various properties such as size, shape, polymers and additives. This is important to obtain more reliant ecotoxicological data of a greater spectrum of the MP species currently in use, such as MPFs. In the case of phytoplankton, toxicological parameters should include more than just growth inhibition and also investigate, for instance, cell volume, cell surface properties and membrane integrity, enzyme activity, photosynthetic efficiency and biochemical composition. As MPs appear to induce sub-lethal effects on marine organisms, such factors could be important to extrapolate ecosystem-level implications of MP pollution.

Furthermore, studies and reports (Dave and Aspegren, 2010; Ellen MacArthur Foundation, 2017) suggest that natural fibres might pose greater environmental impact than synthetics because of the manufacturing process releasing pesticides, natural biocides, oils and waxes, halogenated compounds, and bleaching and deterging agents from wool and cotton. Natural fibres also require more water and energy for processing and are believed to sorb organic compounds more readily than synthetics. However, benchmarking the occurrence and impacts of synthetic and natural fibres is challenging, due to low transparency and high inconsistency in the processing procedures within the industry (Ellen MacArthur Foundation, 2017). Nonetheless, more effort should be put into determining common chemical additives in textile fibres for consumption, and to assess the differences in impacts between polymer composites - polymeric matrices reinforced with (non-)polymeric reinforcement(s) – and pure (non-)synthetic textile fibres. As a means from the industry to enhance durability in textiles with less fibres shed, polyester polymers are commonly reinforced with cotton or wool (Browne et al., 2011; Carr, 2017; Hartmann et al., 2019; Napper and Thompson, 2016). These fibre composites shed less fibres and are not characterised as plastics; however, as synthetic polymers consitute the dominant ingredients, the ecotoxicological footprint might still be significant.

Despite the current lack of information on the ecotoxicology of MFs, it is well documented that most stages of the textile manufacturing process cause harmful impacts on aquatic and human life. Therefore, it is important for both producers and consumers to be aware of these harmful aspects of textile production and to act accordingly by consuming less and more consciously, until more is known about the socio-economic and ecological impacts of environmental textile

pollution. As indicated by Browne *et al.* (2011) the number of fibres being released per textile decreases with every wash; further suggesting that one solution to the pollution problem might be to reduce the overall textile consumption. Based on this and other studies investigating textile fibres' toxicity, it will be important to assess the ecological impacts of both natural and synthetic textile fibres on multiple trophic levels, in order to establish proper industrial regulations. In turn, this will assist the progress of developing more benign environments in term of ecological and human health.

6. Conclusions

Due to a current lack of knowledge on the toxicity of MFs in marine ecosystems, the present study aimed at investigating the impacts of PES, PA and wool MFs on the microalgae *I. galbana* (T-ISO). The results indicate that the overall population growth of *I. galbana* was reduced upon treatment with 60 and 3000 µm MFs, with weak effects related to polymer type and size. Responses such as specific growth rates, cumulative cell production and Chl*a*F per cell were weakly concentration-dependent, with high MFs treatments generally inducing stronger effects than medium and low. MF leachates had insignificant effects on photochemical efficiency; nonetheless reducing the relative content of glucose-like compounds and increasing relative content of polysaccharides. Moreover, leachates from PES MFs significantly increased the growth of *I. galbana*, as indicated by both cell numbers and dry weight biomass. Despite the lack of direct comparability between experiments, these results might indicate that there are some weak metabolic effects of MFs on *I. galbana*, albeit at concentrations above those found in open surface waters. Nonetheless, this study presents the importance of further investigating sub-lethal effects of MFs in marine phytoplankton.

References

Abu-Rezq, T.S., Al-Musallam, L., Al-Shimmari, J., Dias, P., 1999. Optimum production conditions for different high-quality marine algae. Hydrobiologia 403, 97–107. https://doi.org/https://doi.org/10.1023/A:1003725626504

Agati, G., Fusi, F., Mazzinghi, P., di Paola, M.L., 1993. A simple approach to the evaluation of the reabsorption of chlorophyll fluorescence spectra in intact leaves. J. Photochem. Photobiol. B Biol. 17, 163–171. https://doi.org/10.1016/1011-1344(93)80009-X

Anbumani, S., Kakkar, P., 2018. Ecotoxicological effects of microplastics on biota: a review. Environ. Sci. Pollut. Res. 1–24. https://doi.org/10.1007/s11356-018-1999-x

Andrady, A.L., 2017. The plastic in microplastics: A review. Mar. Pollut. Bull. 119, 12–22. https://doi.org/10.1016/J.MARPOLBUL.2017.01.082

Andrady, A.L., 2011. Microplastics in the marine environment. Mar. Pollut. Bull. 62, 1596–1605. https://doi.org/10.1016/J.MARPOLBUL.2011.05.030

Arar, E.J., Collins, G.B., 1997. Method 445.0 In Vitro Determination of Chlorophyll a and Pheophytin ain Marine and Freshwater Algae by Fluorescence. Washington DC.

Barbosa, A.B., 2009. Dynamics of living phytoplankton: Implications for paleoenvironmental reconstructions. IOP Conf. Ser. Earth Environ. Sci. 5, 012001. https://doi.org/10.1088/1755-1307/5/1/012001

Barnes, D.K.A., Galgani, F., Thompson, R.C., Barlaz, M., 2009. Accumulation and fragmentation of plastic debris in global environments. Philos. Trans. R. Soc. Lond. B. Biol. Sci. 364, 1985–98. https://doi.org/10.1098/rstb.2008.0205

Bergmann, M., Gutow, L., Klages, M., 2015. Marine Anthropogenic Litter. Springer International Publishing. https://doi.org/10.1007/978-3-319-16510-3

Bertozzini, E., Galluzzi, L., Penna, A., Magnani, M., 2011. Application of the standard addition method for the absolute quantification of neutral lipids in microalgae using Nile red. J. Microbiol. Methods 87, 17–23. https://doi.org/10.1016/j.mimet.2011.06.018

Besseling, E., Wang, B., Lürling, M., Koelmans, A.A., 2014. Nanoplastic Affects Growth of S. obliquus and Reproduction of D. magna. Environ. Sci. Technol. 48, 12336–12343. https://doi.org/10.1021/es503001d

Bhattacharya, P., Lin, S., Turner, J.P., Ke, P.C., 2010. Physical Adsorption of Charged Plastic Nanoparticles Affects Algal Photosynthesis. J. Phys. Chem. C 114, 16556–16561. https://doi.org/10.1021/jp1054759

Blanca, M.J., Alarcón, R., Arnau, J., Bendayan, R., 2017. Non-normal data: Is ANOVA still a valid option? Psicothema 29, 552–557. https://doi.org/10.7334/psicothema2016.383

Boucher, J., Friot, D., 2017. Primary Microplastics in the Oceans : a Global Evaluation of Sources. Gland, Switzerland. https://doi.org/https://doi.org/10.2305/IUCN.CH.2017.01.en

Browne, M.A., 2015. Sources and Pathways of Microplastics to Habitats, in: Marine Anthropogenic Litter. Springer International Publishing, Cham, pp. 229–244. https://doi.org/10.1007/978-3-319-16510-3_9

Browne, M.A., Crump, P., Niven, S.J., Teuten, E., Tonkin, A., Galloway, T., Thompson, R., 2011. Accumulation of Microplastic on Shorelines Woldwide: Sources and Sinks. Environ. Sci. Technol 45, 9175–9179. https://doi.org/10.1021/es201811s

Browne, M.A., Dissanayake, A., Galloway, T.S., Lowe, D.M., Thompson, R.C., 2008. Ingested Microscopic Plastic Translocates to the Circulatory System of the Mussel, Mytilus edulis (L.). Environ. Sci. Technol. 42, 5026–5031. https://doi.org/10.1021/es800249a

Buonasera, K., Lambreva, M., Rea, G., Touloupakis, E., Giardi, M.T., 2011. Technological applications of chlorophyll a fluorescence for the assessment of environmental pollutants. Anal. Bioanal. Chem. 401, 1139–1151. https://doi.org/10.1007/s00216-011-5166-1

Calvo-Flores, F.G., Isac-Garcia, J., Dobado, J.A., 2018. Emerging Pollutants: Origin, Structure and Properties, 1st ed. Wiley-VHC Verlag GmbH & Co, Weinheim. https://doi.org/10.2175/106143011X13075599870298

Carpenter, E.J., Smith, K.L.J., 1972. Plastics on the Sargasso Sea Surface. Science 175, 1240–1241. https://doi.org/10.1126/science.168.3928.246

Carr, S.A., 2017. Sources and dispersive modes of micro-fibers in the environment. Integr. Environ. Assess. Manag. 13, 466–469. https://doi.org/10.1002/ieam.1916

Chen, G.-Q., Patel, M.K., 2012. Plastics Derived from Biological Sources: Present and Future: A Technical and Environmental Review. Chem. Rev. 112, 2082–2099. https://doi.org/10.1021/cr200162d

Chen, W., Zhang, C., Song, L., Sommerfeld, M., Hu, Q., 2009. A high throughput Nile red method for quantitative measurement of neutral lipids in microalgae. J. Microbiol. Methods 77, 41–47. https://doi.org/10.1016/j.mimet.2009.01.001

Cole, M., 2016. A novel method for preparing microplastic fibers. Sci. Rep. 6, 34519. https://doi.org/10.1038/srep34519

Cole, M., Lindeque, P., Fileman, E., Halsband, C., Goodhead, R., Moger, J., Galloway, T.S., 2013. Microplastic Ingestion by Zooplankton. Environ. Sci. Technol. 47, 6646–6655. https://doi.org/10.1021/es400663f

Cole, M., Lindeque, P., Halsband, C., Galloway, T.S., 2011. Microplastics as contaminants in the marine environment: A review. Mar. Pollut. Bull. 62, 2588–2597. https://doi.org/10.1016/J.MARPOLBUL.2011.09.025

Cordoba-Matson, M. V, Arredondo-Vega, B.O., Carreon-Palau, L., 2013. Evaluation of growth, cell size and biomass of Isochrysis aff. galbana (T- ISO) with two LED regimes. All Results J. 4, 7–15.

Cózar, A., Echevarría, F., González-Gordillo, J.I., Irigoien, X., Ubeda, B., Hernández-León, S., Palma, A.T., Navarro, S., García-de-Lomas, J., Ruiz, A., Fernández-de-Puelles, M.L., Duarte, C.M., 2014. Plastic debris in the open ocean. Proc. Natl. Acad. Sci. U. S. A. 111, 10239–44. https://doi.org/10.1073/pnas.1314705111

Dalsgaard, J., St. John, M., Kattner, G., Müller-Navarra, D., Hagen, W., 2003. Fatty acid trophic markers in the pelagic marine environment. Adv. Mar. Biol. 46, 225–340. https://doi.org/10.1016/S0065-2881(03)46005-7

Dave, G., Aspegren, P., 2010. Comparative toxicity of leachates from 52 textiles to Daphnia magna. Ecotoxicol. Environ. Saf. 73, 1629–1632. https://doi.org/10.1016/J.ECOENV.2010.06.010

Desforges, J.-P.W., Galbraith, M., Ross, P.S., 2015. Ingestion of Microplastics by Zooplankton in the Northeast Pacific Ocean. Arch. Environ. Contam. Toxicol. 69, 320–330. https://doi.org/10.1007/s00244-015-0172-5

Drillet, G., Frouël, S., Sichlau, M.H., Jepsen, P.M., Højgaard, J.K., Joarder, A.K., Hansen, B.W., 2011. Status and recommendations on marine copepod cultivation for use as live feed. Aquaculture 315, 155–166. https://doi.org/10.1016/J.AQUACULTURE.2011.02.027

Dris, R., Gasperi, J., Mirande, C., Mandin, C., Guerrouache, M., Langlois, V., Tassin, B., 2017. A first overview of textile fibers, including microplastics, in indoor and outdoor environments. Environ. Pollut. 221, 453–458. https://doi.org/10.1016/j.envpol.2016.12.013

Dris, R., Gasperi, J., Rocher, V., Saad, M., Renault, N., Tassin, B., 2015. Microplastic contamination in an urban area: a case study in Greater Paris. Environ. Chem. 12, 592–599. https://doi.org/10.1071/EN14167

Duan, L., Chen, Q., Duan, S., Duan, L., Chen, Q., Duan, S., 2019. Transcriptional Analysis of Chlorella Pyrenoidosa Exposed to Bisphenol A. Int. J. Environ. Res. Public Health 16, 1374. https://doi.org/10.3390/ijerph16081374

Durmaz, Y., Donato, M., Monteiro, M., Gouveia, L., Nunes, M.L., Gama Pereira, T., Gokpınar, S., Bandarra, N.M., 2008. Effect of Temperature on Growth and Biochemical Composition (Sterols, α-tocopherol, Carotenoids, Fatty Acid Profiles) of the Microalga, Isoch rysis galbana. Isr. J. Aquac. 60, 190–197.

Duygu, D. (Yalcin), Udoh, A.U., Ozer, T. (Baykal), Akbulut, A., Erkaya, I. (Acikgoz), Yildiz, K., Guler, D., 2012. Fourier transform infrared (FTIR) spectroscopy for identification of Chlorella vulgaris Beijerinck 1890 and Scenedesmus obliquus (Turpin) Kützing 1833. African J. Biotechnol. 11, 3817–3824. https://doi.org/10.5897/AJB11.1863

Ebert, D., 2005. Introduction to Daphnia Biology, in: Ecology, Epidemiology, and Evolution of Parasitism in Daphnia [Internet]. National Center for Biotechnology Information (US), Bethesda (MD), USA.

Eerkes-Medrano, D., Thompson, R.C., Aldridge, D.C., 2015. Microplastics in freshwater systems: A review of the emerging threats, identification of knowledge gaps and prioritisation of research needs. Water Res. 75, 63–82. https://doi.org/10.1016/J.WATRES.2015.02.012

Ellen MacArthur Foundation, 2017. A new textiles economy: Redesigning fashion's future.

Eriksen, M., Lebreton, L.C.M., Carson, H.S., Thiel, M., Moore, C.J., Borerro, J.C., Galgani, F., Ryan, P.G., Reisser, J., 2014. Plastic Pollution in the World's Oceans: More than 5 Trillion Plastic Pieces Weighing over 250,000 Tons Afloat at Sea. PLoS One 9, e111913. https://doi.org/10.1371/journal.pone.0111913

Eullaffroy, P., Vernet, G., 2003. The F684/F735 chlorophyll fluorescence ratio: a potential tool for rapid detection and determination of herbicide phytotoxicity in algae. Water Res. 37, 1983–1990. https://doi.org/10.1016/S0043-1354(02)00621-8

Eunomia, 2016. Plastics in the Marine Environment, Eunomia Research & Consulting Ltd. Bristol, UK. https://doi.org/10.1002/0471721557.ch10

FAO/ICAC, 2013. World Apparel Fiber Consumption Survey. Washington.

Gago, J., Carretero, O., Filgueiras, A.V., Viñas, L., 2018. Synthetic microfibers in the marine environment: A review on their occurrence in seawater and sediments. Mar. Pollut. Bull. 127, 365–376. https://doi.org/10.1016/J.MARPOLBUL.2017.11.070

Garrido, S., Linares, M., Campillo, J.A., Albentosa, M., 2019. Effect of microplastics on the toxicity of chlorpyrifos to the microalgae Isochrysis galbana, clone t-ISO. Ecotoxicol. Environ. Saf. 173, 103–109. https://doi.org/10.1016/j.ecoenv.2019.02.020

Gauquie, J., Devriese, L., Robbens, J., De Witte, B., 2015. A qualitative screening and quantitative measurement of organic contaminants on different types of marine plastic debris. Chemosphere 138, 348–356. https://doi.org/10.1016/J.CHEMOSPHERE.2015.06.029

GESAMP, 2016. Sources, fate and effects of microplastics in the marine environment: part 2 of a global assessment.

Geyer, R., Jambeck, J.R., Law, K.L., 2017. Production, use, and fate of all plastics ever made. Sci. Adv. 3, 1–5. https://doi.org/10.1126/sciadv.1700782

Graham, M.D., 2003. The Coulter Principle: Foundation of an Industry. JALA J. Assoc. Lab. Autom. 8, 72–81. https://doi.org/10.1016/S1535-5535-03-00023-6

Green, D.S., Boots, B., Sigwart, J., Jiang, S., Rocha, C., 2016. Effects of conventional and biodegradable microplastics on a marine ecosystem engineer (Arenicola marina) and sediment nutrient cycling. Environ. Pollut. 208, 426–434. https://doi.org/10.1016/J.ENVPOL.2015.10.010

Griffiths, P.R., de Haseth, J.A., 2007. Fourier transform infrared spectrometry, 2nd ed. John Wiley & Sons, Inc., New Jersey.

Harris, R.P., Irigoien, X., Head, R.N., Rey, C., Hygum, B.H., Hansen, B.W., Niehoff, B., Meyer-Harms, B., Carlotti, F., 2000. Feeding, growth, and reproduction in the genus Calanus. ICES J. Mar. Sci. 57, 1708–1726. https://doi.org/10.1006/jmsc.2000.0959

Hartline, N.L., Bruce, N.J., Karba, S.N., Ruff, E.O., Sonar, S.U., Holden, P.A., 2016. Microfiber Masses Recovered from Conventional Machine Washing of New or Aged Garments. Environ. Sci. Technol. 50. https://doi.org/10.1021/acs.est.6b03045

Hartmann, N., Hüffer, T., Thompson, R.C., Hassellöv, M., Verschoor, A., Daugaard, A.E., Rist, S., Karlsson, T.M., Brennholt, N., Cole, M., Herrling, M.P., Heß, M., Ivleva, N.P., Lusher, A.L., Wagner, M., 2019. Are we speaking the same language? Recommendations for a definition and categorization framework for plastic debris. Environ. Sci. Technol. acs.est.8b05297. https://doi.org/10.1021/acs.est.8b05297

Henry, B., Laitala, K., Klepp, I.G., 2018. Microplastic pollution from textiles : A literature review. Oslo, Norway.

Hofstraat, J.W., Peeters, J.C.H., Snel, J.F.H., Geel, C., 1994. Simple determination of photosynthetic efficiency and photoinhibition of Dunaliella tertiolecta by saturating pulse fluorescence measurements. Mar. Ecol. Prog. Ser. 103, 187–196. https://doi.org/10.2307/24842238

Horton, A.A., Walton, A., Spurgeon, D.J., Lahive, E., Svendsen, C., 2017. Microplastics in freshwater and terrestrial environments: Evaluating the current understanding to identify the knowledge gaps and future research priorities. Sci. Total Environ. 586, 127–141. https://doi.org/10.1016/j.scitotenv.2017.01.190

Hu, L.-X., Ying, G.-G., Chen, X.-W., Huang, G.-Y., Liu, Y.-S., Jiang, Y.-X., Pan, C.-G., Tian, F., Martinz, F.L., 2017. Fourier-transform infrared spectroscopy as a novel approach to providing effect-based endpoints in Duckweed toxiciy testing. Environ. Toxicol. Chem. 36, 346–353. https://doi.org/10.1002/etc.3534

Jambeck, J., Geyer, R., Wilcox, C., Siegler, T.R., Perryman, M., Andrady, A., Narayan, R., Lavender, K., 2015. Plastic waste inputs from land into the ocean. Mar. Pollut. 347, 768–771. https://doi.org/10.1126/science.1260352

Jemec, A., Horvat, P., Kunej, U., Bele, M., Kr Zan, A., 2016. Uptake and effects of microplastic textile fibers on freshwater crustacean Daphnia magna *. Environ. Pollut. 219, 201–209. https://doi.org/10.1016/j.envpol.2016.10.037

Koelmans, A.A., Bakir, A., Burton, G.A., Janssen, C.R., 2016. Microplastic as a Vector for Chemicals in the Aquatic Environment: Critical Review and Model-Supported Reinterpretation of Empirical Studies. Environ. Sci. Technol. https://doi.org/10.1021/acs.est.5b06069

Kühn, S., Schaafsma, F.L., van Werven, B., Flores, H., Bergmann, M., Egelkraut-Holtus, M., Tekman, M.B., van Franeker, J.A., 2018. Plastic ingestion by juvenile polar cod (Boreogadus saida) in the Arctic Ocean. Polar Biol. 41. https://doi.org/10.1007/s00300-018-2283-8

Lagarde, F., Olivier, O., Zanella, M., Daniel, P., Hiard, S., Caruso, A., 2016. Microplastic interactions with freshwater microalgae: Hetero-aggregation and changes in plastic density appear strongly dependent on polymer type. Environ. Pollut. 215. https://doi.org/10.1016/j.envpol.2016.05.006

Lambert, S., Scherer, C., Wagner, M., 2017. Ecotoxicity testing of microplastics: Considering the heterogeneity of physicochemical properties. Integr. Environ. Assess. Manag. 13, 470–475. https://doi.org/10.1002/ieam.1901

Lenz, R., Enders, K., Nielsen, T.G., 2016. Microplastic exposure studies should be environmentally realistic. PNAS 113, E4121–E4122. https://doi.org/10.1073/pnas.1606615113

Li, D., Bi, R., Chen, H., Mu, L., Zhang, L., Chen, Q., Xie, H., Luo, Y., Xie, L., 2017. The acute toxicity of bisphenol A and lignin-derived bisphenol in algae, daphnids, and Japanese medaka. Environ. Sci. Pollut. Res. 24, 23872–23879. https://doi.org/10.1007/s11356-017-0018-y

Liebezeit, G., Liebezeit, E., 2014. Synthetic particles as contaminants in German beers. Food Addit. Contam. Part A 31, 1574–1578. https://doi.org/10.1080/19440049.2014.945099

Liebezeit, G., Liebezeit, E., 2013. Non-pollen particulates in honey and sugar. Food Addit. Contam. Part A 30, 2136–2140. https://doi.org/10.1080/19440049.2013.843025

Lithner, D., Damberg, J., Dave, G., Larsson, Å., 2009. Leachates from plastic consumer products – Screening for toxicity with Daphnia magna. Chemosphere 74, 1195–1200. https://doi.org/10.1016/J.CHEMOSPHERE.2008.11.022

Long, M., Paul-Pont, I., Hégaret, H., Moriceau, B., Lambert, C., Huvet, A., Soudant, P., 2017. Interactions between polystyrene microplastics and marine phytoplankton lead to species-specific hetero-aggregation. Environ. Pollut. 228, 454–463. https://doi.org/10.1016/J.ENVPOL.2017.05.047

Lusher, A.L., Mchugh, M., Thompson, R.C., 2013. Occurrence of microplastics in the gastrointestinal tract of pelagic and demersal fish from the English Channel. Mar. Pollut. Bull. 67, 94–99. https://doi.org/10.1016/j.marpolbul.2012.11.028

Lyakurwa, D.J., 2017. Uptake and effects of microplastic particles in selected marine microalgae species ; Oxyrrhis marina and Rhodomonas baltica 1–51.

Magnusson, K., Norén, F., 2014. Screening of microplastic particles in and down-stream a wastewater treatment plant. Stockholm.

Mao, Y., Ai, H., Chen, Y., Zhang, Z., Zeng, P., Kang, L., Li, W., Gu, W., He, Q., Li, H., 2018. Phytoplankton response to polystyrene microplastics: Perspective from an entire growth period. Chemosphere 208, 59–68. https://doi.org/10.1016/J.CHEMOSPHERE.2018.05.170

Marwood, C.A., Solomon, K.R., Greenberg, B.M., 2001. Chlorophyll fluorescence as a bioindicator of effects on growth in aquatic macrophytes from mixtures of polycyclic aromatic hydrocarbons. Environ. Toxicol. Chem. 20, 890–898. https://doi.org/10.1002/etc.5620200425

Mato, Y., Isobe, T., Takada, H., Kanehiro, H., Ohtake, C., Kaminuma, T., 2001. Plastic resin pellets as a transport medium for toxic chemicals in the marine environment. Environ. Sci. Technol. 35, 318–324. https://doi.org/10.1021/es0010498

Maxwell, K., Johnson, G.N., 2000. Chlorophyll fluorescence-a practical guide. J. Exp. Bot. 51, 659–668. https://doi.org/https://doi.org/10.1093/jexbot/51.345.659

Mecozzi, M., Pietroletti, M., Di Mento, R., 2007. Application of FTIR spectroscopy in ecotoxicological studies supported by multivariate analysis and 2D correlation spectroscopy. Vib. Spectrosc. 44, 228–235. https://doi.org/10.1016/J.VIBSPEC.2006.11.006

Mendoza, L.M.R., Jones, P.R., 2015. Characterisation of microplastics and toxic chemicals extracted from microplastic samples from the North Pacific Gyre. Environ. Chem. 12, 611. https://doi.org/10.1071/EN14236

Meng, Y., Yao, C., Xue, S., Yang, H., 2014. Application of Fourier transform infrared (FT-IR) spectroscopy in determination of microalgal compositions. Bioresour. Technol. 151, 347–354. https://doi.org/10.1016/J.BIORTECH.2013.10.064

Murdock, J.N., Wetzel, D.L., 2009. FT-IR Microspectroscopy Enhances Biological and Ecological Analysis of Algae. Appl. Spectrosc. Rev. 44, 335–361. https://doi.org/10.1080/05704920902907440

Napper, I.E., Thompson, R.C., 2016. Release of synthetic microplastic plastic fibres from domestic washing machines: Effects of fabric type and washing conditions. Mar. Pollut. Bull. 112, 39–45. https://doi.org/10.1016/j.marpolbul.2016.09.025

Norén, F., 2007. Small plastic particles in Coastal Swedish waters. Stockholm.

OECD, 2006. Test No. 201: Alga, Growth Inhibition Test, OECD Guidelines for the Testing of Chemicals, Section 2: Effects on Biotic Systems. OECD Publishing. https://doi.org/10.1787/9789264069923-en

Ogata, Y., Takada, H., Mizukawa, K., Hirai, H., Iwasa, S., Endo, S., Mato, Y., Saha, M., Okuda, K., Nakashima, A., Murakami, M., Zurcher, N., Booyatumanondo, R., Zakaria, M.P., Dung, L.Q., Gordon, M., Miguez, C., Suzuki, S., Moore, C., Karapanagioti, H.K., Weerts, S., McClurg, T., Burres, E., Smith, W., Velkenburg, M. Van, Lang, J.S., Lang, R.C., Laursen, D., Danner, B., Stewardson, N., Thompson, R.C., 2009. International Pellet Watch: Global monitoring of persistent organic pollutants (POPs) in coastal waters. 1. Initial phase data on PCBs, DDTs, and HCHs. Mar. Pollut. Bull. 58, 1437–1446. https://doi.org/10.1016/J.MARPOLBUL.2009.06.014

Parke, M., 1949. STUDIES ON MARINE FLAGELLATES. J. Mar. Biol. Assoc. United Kingdom 28, 255–288.

Pérez, J.A.S., 1994. n-3 Polyunsaturated fatty acid productivity of the marine microalga Isochrysis galbana. Growth conditions and phenotypic selection. J. Appl. Phycol. 6, 475–478. https://doi.org/https://doi.org/10.1007/BF02182401

Pérez, P., Beiras, R., Fernández, E., 2010. Monitoring copper toxicity in natural phytoplankton assemblages: application of Fast Repetition Rate fluorometry. Ecotoxicol. Environ. Saf. 73, 1292–1303. https://doi.org/10.1016/j.ecoenv.2010.06.008

Pérez, P., Fernández, E., Beiras, R., 2009. Toxicity of Benzalkonium Chloride on Monoalgal Cultures and Natural Assemblages of Marine Phytoplankton. Water. Air. Soil Pollut. 201, 319–330. https://doi.org/10.1007/s11270-008-9947-x

Phuong, N.N., Zalouk-Vergnoux, A., Poirier, L., Kamari, A., Châtel, A., Mouneyrac, C., Lagarde, F., 2016. Is there any consistency between the microplastics found in the field and those used in laboratory experiments? Environ. Pollut. 211, 111–123. https://doi.org/10.1016/J.ENVPOL.2015.12.035

Plastics Europe, 2017. Plastics – the Facts 2017.

PlasticsEurope, 2018. Plastics - the Facts 2017. An analysis of European plastics production, demand and waste data. Brussels, Belgium.

Prata, J.C., da Costa, J.P., Lopes, I., Duarte, A.C., Rocha-Santos, T., 2019. Effects of microplastics on microalgae populations: A critical review. Sci. Total Environ. 665, 400–405. https://doi.org/10.1016/J.SCITOTENV.2019.02.132

Prata, J.C., Lavorante, B.R.B.O., B.S.M. Montenegro, M. da C., Guilhermino, L., 2018. Influence of microplastics on the toxicity of the pharmaceuticals procainamide and doxycycline on the marine microalgae Tetraselmis chuii. Aquat. Toxicol. 197, 143–152. https://doi.org/10.1016/J.AQUATOX.2018.02.015

Renaud, S.M., Zhou, H.C., Parry, D.L., Thinh, L.-V., Woo, K.C., 1995. Effect of temperature on the growth, total lipid content and fatty acid composition of recently isolated tropical microalgae Isochrysis sp., Nitzschia closterium, Nitzschia paleacea, and commercial species Isochrysis sp. (clone T.ISO). J. Appl. Phycol. 7, 595–602. https://doi.org/https://doi.org/10.1007/BF00003948

Rey, C., Harris, R., Irigoien, X., Head, R., Carlotti, F., 2001. Influence of algal diet on growth and ingestion of Calanus helgolandicus nauplii. Mar. Ecol. Prog. Ser. 216, 151–165. https://doi.org/10.3354/meps216151

Rochman, C.M., Tahir, A., Williams, S.L., Baxa, D. V, Lam, R., Miller, J.T., Teh, F.-C., Werorilangi, S., Teh, S.J., 2015. Anthropogenic debris in seafood: Plastic debris and fibers from textiles in fish and bivalves sold for human consumption. Nat. Publ. Gr. 5, 1–10. https://doi.org/10.1038/srep14340

Saini, A., Thaysen, C., Jantunen, L., McQueen, R.H., Diamond, M.L., 2016. From Clothing to Laundry Water: Investigating the Fate of Phthalates, Brominated Flame Retardants, and Organophosphate Esters. Environ. Sci. Technol. 50, 9289–9297. https://doi.org/10.1021/acs.est.6b02038

Setälä, O., Fleming-Lehtinen, V., Lehtiniemi, M., 2014. Ingestion and transfer of microplastics in the planktonic food web. Environ. Pollut. 185, 77–83. https://doi.org/10.1016/J.ENVPOL.2013.10.013

Setälä, O., Magnusson, K., Lehtiniemi, M., Norén, F., 2016. Distribution and abundance of surface water microlitter in the Baltic Sea: A comparison of two sampling methods. Mar. Pollut. Bull. 110, 177–183. https://doi.org/10.1016/J.MARPOLBUL.2016.06.065

Siegel, D.A., Franz, B.A., 2010. Century of phytoplankton change. Nature 466, 569–571. https://doi.org/10.1038/466569a

Sjollema, S.B., Redondo-Hasselerharm, P., Leslie, H.A., Kraak, M.H.S., Vethaak, A.D., 2016. Do plastic particles affect microalgal photosynthesis and growth? Aquat. Toxicol. 170, 259–261. https://doi.org/10.1016/J.AQUATOX.2015.12.002

Song, Y.K., Hong, S.H., Jang, M., Kang, J.-H., Kwon, O.Y., Han, G.M., Shim, W.J., 2014. Large Accumulation of Micro-sized Synthetic Polymer Particles in the Sea Surface Microlayer. Environ. Sci. Technol. 48, 9014–9021. https://doi.org/10.1021/es501757s

Starr, M., Runge, J.A., Therriault, J., 1999. Effects of diatom diets on the reproduction of the planktonic copepod Calanus finmarchicus. SARSIA 84, 379–389.

Stehfest, K., Toepel, J., Wilhelm, C., 2005. The application of micro-FTIR spectroscopy to analyze nutrient stress-related changes in biomass composition of phytoplankton algae. Plant Physiol. Biochem. 43, 717–726. https://doi.org/10.1016/J.PLAPHY.2005.07.001

Stevenson, J., 2014. Ecological assessments with algae: a review and synthesis. J. Phycol. 50, 437–461. https://doi.org/10.1111/jpy.12189

Suggett, D.J., Prásil, O., Borowitzka, M.A., 2011. Chlorophyll a Fluorescence in Aquatic Sciences: Methods and Applications. Springer Dordrecht Heidelberg London New York, Dordrecht, Heidelberg, London, New York. https://doi.org/10.1007/978-90-481-9268-7

Sukenik, A., Wahnon, R., 1991. Biochemical quality of marine unicellular algae with special emphasis on lipid composition. I. Isochrysis galbana. Aquaculture 97, 61–72. https://doi.org/10.1016/0044-8486(91)90279-G

Syberg, K., Khan, F.R., Selck, H., Palmqvist, A., Banta, G.T., Daley, J., Sano, L., Duhaime, M.B., 2015. Microplastics: addressing ecological risk through lessons learned. Environ. Toxicol. Chem. 34, 945–953. https://doi.org/10.1002/etc.2914

Szymanska-Chargot, M., Zdunek, A., 2013. Use of FT-IR Spectra and PCA to the Bulk Characterization of Cell Wall Residues of Fruits and Vegetables Along a Fraction Process. Food Biophys. 8, 29–42. https://doi.org/10.1007/s11483-012-9279-7

Tato, T., Salgueiro-González, N., León, V.M., González, S., Beiras, R., 2018. Ecotoxicological evaluation of the risk posed by bisphenol A, triclosan, and 4-nonylphenol in coastal waters using early life stages of marine organisms (Isochrysis galbana, Mytilus galloprovincialis, Paracentrotus lividus, and Acartia clausi). Environ. Pollut. 232, 173–182. https://doi.org/10.1016/J.ENVPOL.2017.09.031

Teuten, E.L., Saquing, J.M., Knappe, D.R.U., Barlaz, M.A., Jonsson, S., Björn, A., Rowland, S.J., Thompson, R.C., Galloway, T.S., Yamashita, R., Ochi, D., Watanuki, Y., Moore, C., Viet, P.H., Tana, T.S., Prudente, M., Boonyatumanond, R., Zakaria, M.P., Akkhavong, K., Ogata, Y., Hirai, H., Iwasa, S., Mizukawa, K., Hagino, Y., Imamura, A., Saha, M., Takada, H., 2009. Transport and release of chemicals from plastics to the environment and to wildlife. Philos. Trans. R. Soc. B Biol. Sci. 364, 2027–2045. https://doi.org/10.1098/rstb.2008.0284

Thompson, R.C., Olsen, Y., Mitchell, R.P., Davis, A., Rowland, S.J., John, A.W.G., McGonigle, D., Russell, A.E., 2004. Lost at Sea: Where Is All the Plastic? Science (80-.). 304, 838–838. https://doi.org/10.1126/science.1094559

Tredici, M.R., 2010. Photobiology of microalgae mass cultures: understanding the tools for the next green revolution. Biofuels 1, 143–162. https://doi.org/https://doi.org/10.4155/bfs.09.10

van Franeker, J.A., Blaize, C., Danielsen, J., Fairclough, K., Gollan, J., Guse, N., Hansen, P.-L., Heubeck, M., Jensen, J.-K., Le Guillou, G., Olsen, B., Olsen, K.-O., Pedersen, J., Stienen, E.W.M., Turner, D.M., 2011. Monitoring plastic ingestion by the northern fulmar Fulmarus glacialis in the North Sea. Environ. Pollut. 159, 2609–2615. https://doi.org/10.1016/J.ENVPOL.2011.06.008

Verma, Y., 2008. Acute toxicity assessment of textile dyes and textile and dye industrial effluents using Daphnia magna bioassay. Toxicol. Ind. Health 24, 491–500. https://doi.org/10.1177/0748233708095769

von Dassow, P., Montresor, M., 2011. Unveiling the mysteries of phytoplankton life cycles: patterns and opportunities behind complexity. J. Plankton Res. 33, 3–12. https://doi.org/10.1093/plankt/fbq137

Vroom, R.J.E., Koelmans, A.A., Besseling, E., Halsband, C., 2017. Aging of microplastics promotes their ingestion by marine zooplankton. Environ. Pollut. 231, 987–996. https://doi.org/10.1016/j.envpol.2017.08.088

Wagner, H., Dunker, S., Liu, Z., Wilhelm, C., 2013. Subcommunity FTIR-spectroscopy to determine physiological cell states. Curr. Opin. Biotechnol. 24, 88–94. https://doi.org/10.1016/J.COPBIO.2012.09.008

Wan, J.-K., Chu, W.-L., Kok, Y.-Y., Lee, C.-S., 2018. Distribution of Microplastics and Nanoplastics in Aquatic Ecosystems and Their Impacts on Aquatic Organisms, with Emphasis on Microalgae, in: de Voogt, P. (Ed.), Reviews of Environmental Contamination and Toxicology. Springer, Cham, pp. 133–158. https://doi.org/10.1007/398

Wang, Z., Chen, M., Zhang, L., Wang, K., Yu, X., Zheng, Z., Zheng, R., 2018. Sorption behaviors of phenanthrene on the microplastics identified in a mariculture farm in Xiangshan Bay, southeastern China. Sci. Total Environ. 628–629, 1617–1626. https://doi.org/10.1016/j.scitotenv.2018.02.146

Watts, A.J.R., Urbina, M.A., Corr, S., Lewis, C., Galloway, T.S., 2015. Ingestion of Plastic Microfibers by the Crab Carcinus maenas and Its Effect on Food Consumption and Energy Balance. https://doi.org/10.1021/acs.est.5b04026

Woodall, L.C., Sanchez-Vidal, A., Canals, M., Paterson, G.L.J., Coppock, R., Sleight, V., Calafat, A., Rogers, A.D., Narayanaswamy, B.E., Thompson, R.C., 2014. The deep sea is a major sink for microplastic debris. R. Soc. Open Sci. 1, 140317–140317. https://doi.org/10.1098/rsos.140317

Wright, S.L., Thompson, R.C., Galloway, T.S., 2013. The physical impacts of microplastics on marine organisms: A review. Environ. Pollut. 178, 483–492. https://doi.org/10.1016/j.envpol.2013.02.031

Zhang, C., Chen, X., Wang, J., Tan, L., 2017. Toxic effects of microplastic on marine microalgae Skeletonema costatum: Interactions between microplastic and algae. Environ. Pollut. 220, 1282–1288. https://doi.org/10.1016/J.ENVPOL.2016.11.005

Zhao, S., Zhu, L., Li, D., 2016. Microscopic anthropogenic litter in terrestrial birds from Shanghai, China: Not only plastics but also natural fibers. Sci. Total Environ. 550, 1110–1115. https://doi.org/10.1016/J.SCITOTENV.2016.01.112

Appendix A

Materials, test species and exposure setup

Culture medium

The experiments performed in Trondheim (physical exposures), used filtered seawater from the Trondheim fjord as base of the cultivation medium. However, in Umeå artificial seawater was used as an alternative medium base (Table 1.1). The Conwy medium (CONW) was made by diluting the Conwy medium enrichment by 4‰ in either FSW or artificial seawater. For the artificial seawater, the pH needed to be re-adjusted to 7.8, as the Conwy enrichment is acidic.

Table A2: Recipe for the artificial seawater used in Umeå.

Reagent	Content per 1000 ml [g]	Final concentration [mM]
NaCl	26.29	450
KCl	0.74	10
$CaCl_2$	0.99	9
$MgCl_2•6H_2O$	6.09	30
$MgSO_4•7H_2O$	3.94	16

Table A3: Micronutrient content in the Conwy medium enrichment

Reagent	Content per 1000 ml [g]
$FeCl_3•6H_2O$	1.30
$MnCl_2•4H_2O$	0.36
H_3Bo_3	11.20
Na-EDTA	30.0
$NaH_2PO_4•H_2O$	20.0
$NaNO_3$	100.0
$ZnCl_2$	0.021
$CoCl_2•6H_2O$	0.20
$(NH_4)6Mo_7O_{24}•4H_2O$	0.90
$CuSO_4•5H_2O$	0.020
Thiamin HCl	0.10
Cyanocobalamin (B_{12})	0.005
Deionized water to 1000 ml	

MF cut descriptives, origin and properties

Table A3: Size descriptives of the cut microfibres (60 µm and 3000 µm)

	60 µm									3000 µm					
	Length			Width			Aspect ratio			Length			Width		
	PES	PA	Wool	PES	PA	Wool	PES	PA	Wool	PES	PA	Wool	PES	PA	Wool
Mean	61.4	58.1	61.4	16.0	18.0	19.7	3.93	3.27	3.28	2811.2	2824.3	3050.6	13.2	17.6	22.4
SD	10.2	29.0	20.1	2.5	2.2	4.5	0.81	1.58	1.29	265.0	217.1	1567.9	2.9	2.1	3.0
n	120	167	318.0	117	167	318	120	167	318	30.0	28.0	25.0	45.0	45.0	16.0
SE	0.9	2.2	1.1	0.2	0.2	0.3	0.07	0.12	0.07	48.4	41.0	313.6	0.4	0.3	0.7
Median	60.6	54.2	57.7	15.8	18.0	19.0	3.79	3.07	3.04	2794.2	2902.0	3089.2	13.2	17.4	23.0
Maks	114.9	393.2	268.0	22.0	25.3	43.9	6.44	20.22	14.87	3600.6	3117.5	9366.1	22.3	23.7	28.5
Min	34.8	36.8	26.6	11.3	6.2	9.3	1.97	1.70	1.07	2461.3	2120.6	444.3	7.9	13.5	16.9
Variance	104.93	840.81	404.92	6.31	4.67	20.35	0.66	2.50	1.67	70221.1	47115.5	2458454.9	8.3	4.3	8.7
				Below 3:1 [%] -->			10.8	47.3	48.4						

Table A4: Microfibre origins and properties (60 and 3000 µm)

Fibre type	Colour	Supplier	Width[a] [µm]	Density[b] (± SD)
PES	White (undyed)	Helly Hansen	15.8	1.359 ± 0.009
PA	White (yarn)	Pierre Robert Group	18.0	1.146 ± 0.006
Wool	Off-white (untreated)	Helly Hansen	19.0	1.312 ± 0.004

[a] median values calculated from 60 µm PES (n=117), PA (n=167) and wool (n=318)
[b] mean (n=2)

Polymer	Length [µm]	Density [g/cm^3]	Concentration [mg/mL] Low	Medium	high	Microfibres/mL Low	Medium	High	Fibres per vial (40 ml) Low	Medium	High
PES	60	1.385				3	28	283	113	1134	11337
	3000					0.06	1	6	2	23	227
PA	60	1.146	$4.22x10^{-5}$	$4.22x10^{-4}$	$4.22x10^{-3}$	3	27	267	107	1070	10699
	3000					0.05	1	5	2	21	214
Wool	60	1.312				2	21	209	83	834	8341
	3000					0.04	0	4	2	17	167

MF stock suspensions

Table A5: Mass-based concentrations of polyester (PES), polyamide (PA) and wool in the experimental stock suspensions. CONW, Conwy-enriched medium.

Fibre type	Length [µm]	Total mass [mg]	CONW [ml]	Final concentration [mg/ml]
PES	60	2.538	540	$4.23x10^{-3}$
	3000	2.526	540	$4.21x10^{-3}$
PA	60	2.532	540	$4.22x10^{-3}$
	3000	2.529	540	$4.22x10^{-3}$
Wool	60	2.527	540	$4.22x10^{-3}$
	3000	2.526	540	$4.21x10^{-3}$

Microfibre leachates

Table A6: Mass-based concentrations of the prepared MF leachates of polyester (PES), polyamide (PA) and wool. Values represent average values ± standard deviation (n=2).

	Added MFs [mg]	Added medium [ml]	Final concentrations [mg/ml]
PES	250.15 ± 0.16	24.61 ± 0.02	10.17 ± 0.00
PA	250.12 ± 0.13	24.66 ± 0.11	10.14 ± 0.05
Wool	235.79 ± 14.58	23.19 ± 1.46	10.17 ± 0.01

Exposure setup: plankton wheel (60 and 3000 µm MFs)

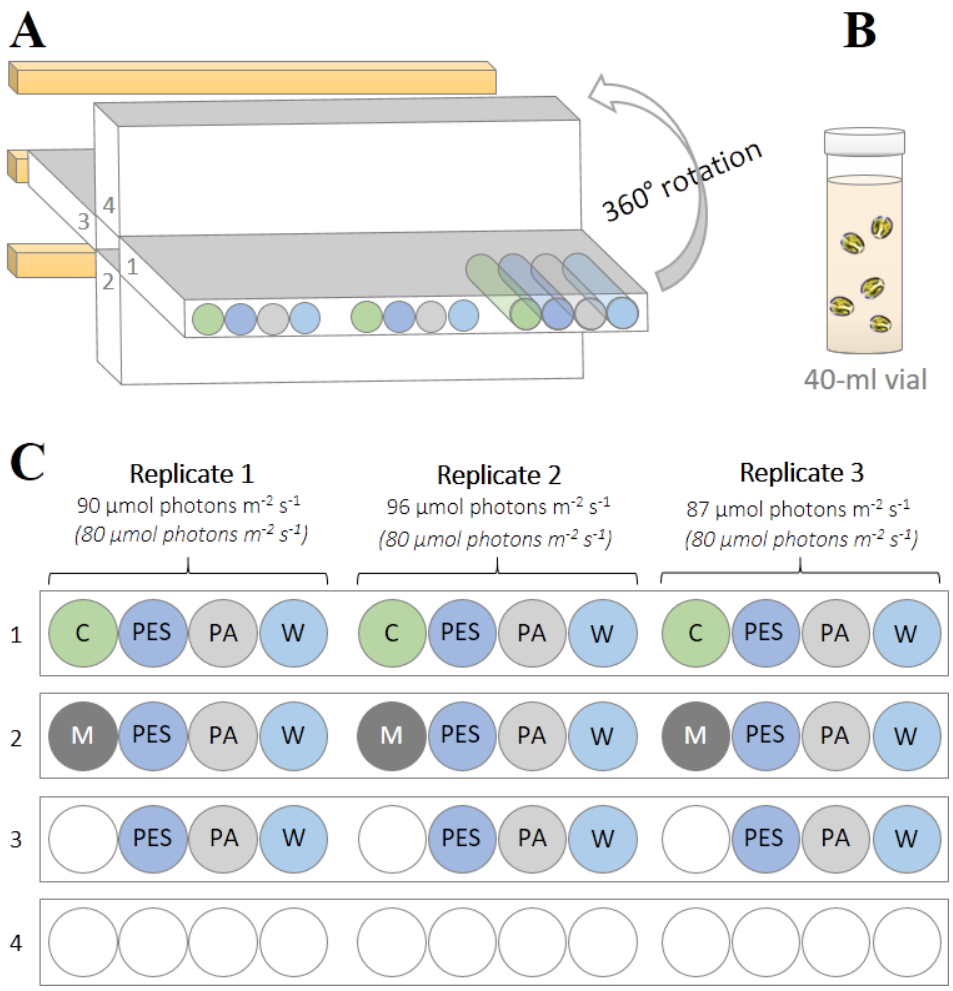

Figure A1: Plankton wheel (PW) exposure setup. A) 4-axes plankton wheel connected to a rotating mechanism, submerged in a water bath and with fluorescent light tubes behind. B) 40-ml glass vial to place on the PW. C) experimental setup with the 40-ml vials, where numbers 1, 2 and 3 represent low, medium and high MF concentration, respectively. Light irradiances are noted for samples in a vertical placement relative to the light source (*italic*) and horizontally (non-italic). C, algae control; M, cultivation medium control; PES, polyester, PA, polyamide; W, wool.

Exposure preparations: incubation shaker (MF leachates)

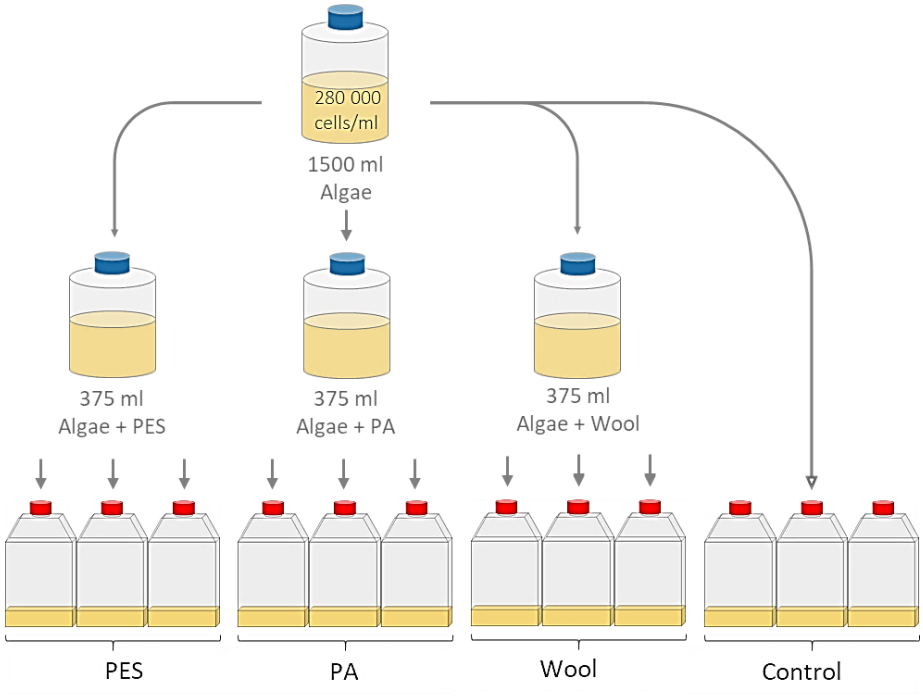

Figure A2: Incubation shaker preparation scheme and exposure setup. All culture flasks were prepared sterile into 3 replicates and placed on a rotating incubation shaker with led lights above.

Appendix B

Method development

Cultivation and subsampling

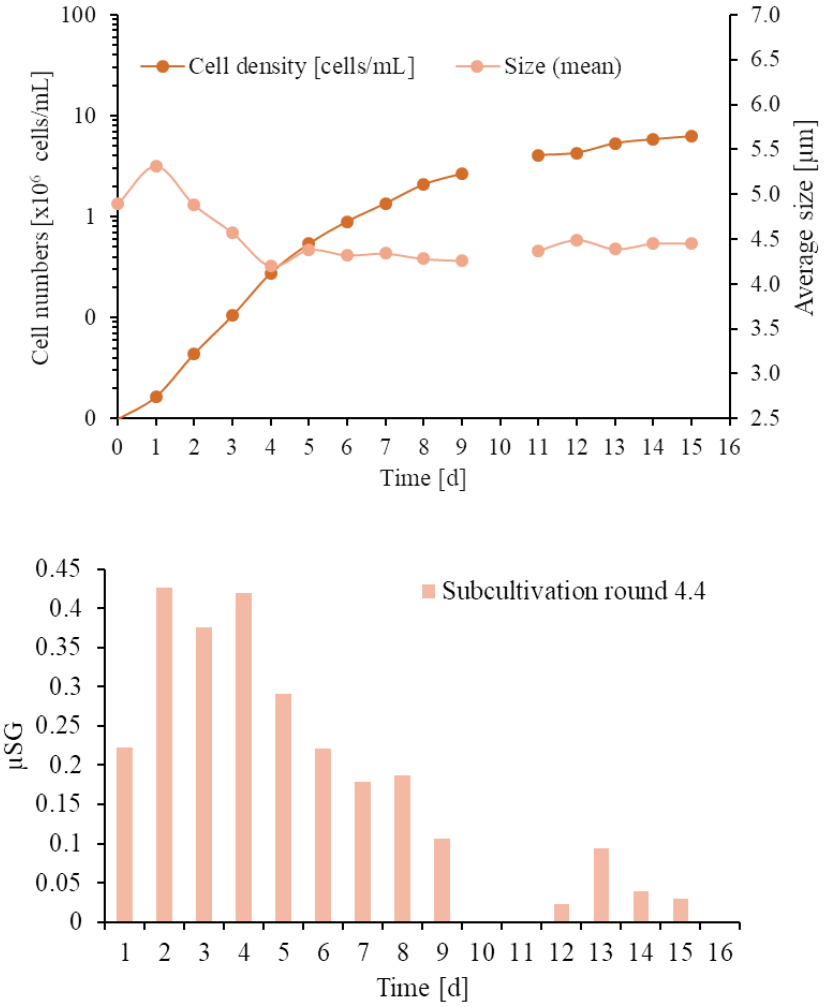

Figure B1: Growth curves, cell size and daily specific growth rates for non-exposed *I. galbana* in the parent culture in a 5-L borosilicate cultivation flask.

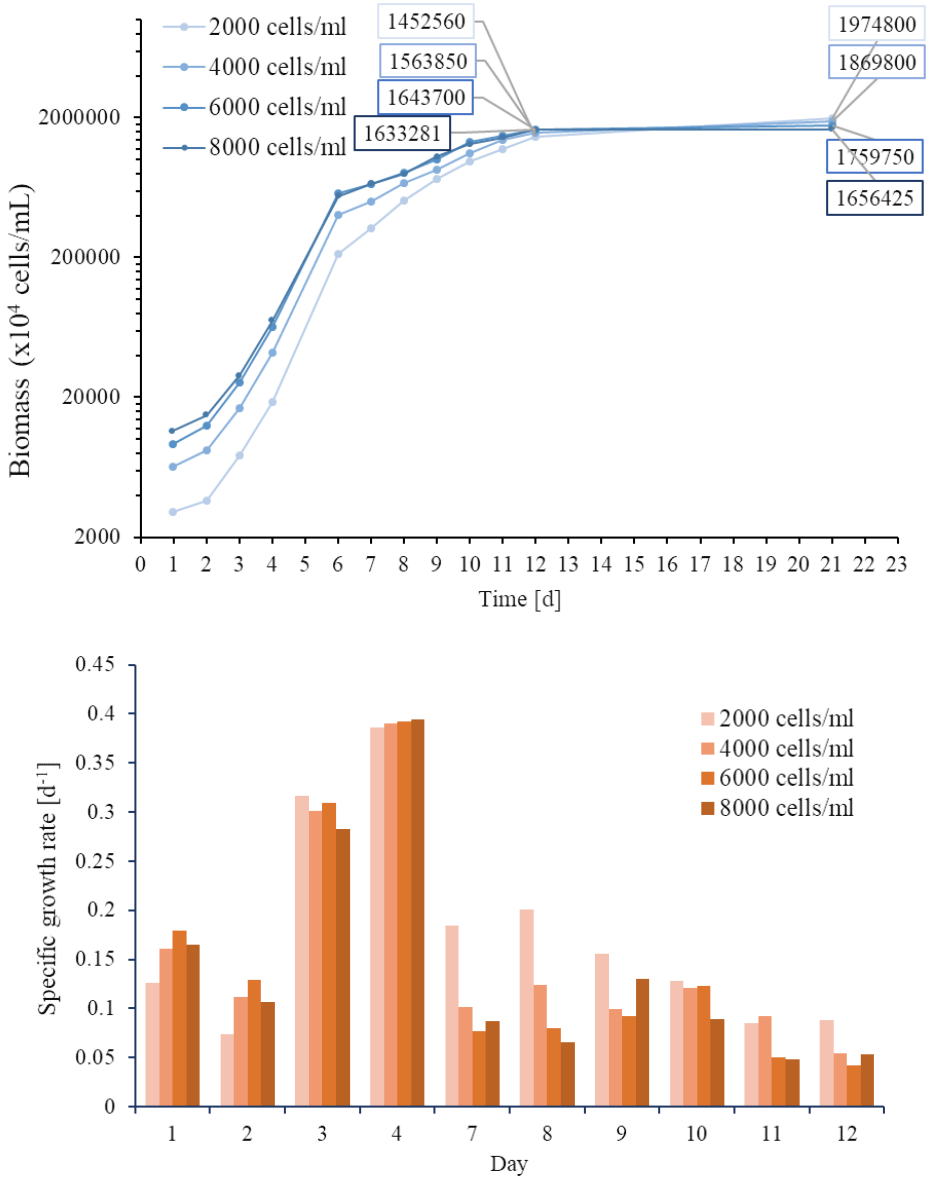

Figure B2: Growth curves and growth rates for non-exposed *I. galbana* in the pilot cultivation trial in the plankton wheel cultivation system. 2000-8000 cells/mL represent the initial cell density upon inoculation, and numbers in boxes represent time-specific population density [cells/mL].

Fluorescence measurements

Table B1: Instrument scan parameters for Chl-a and Nile Red fluorescence detection using Varian Eclipse fluorescence spectrophotometer. Em., emission; ex., excitation; CONW, Conwy-enriched medium.

Parameters	**Chl-*a* fluorescence**	**Nile Red (w/glycerol trioleate)**
Ex. wavelength [nm]	460	547
Em./ex. slit [nm]	5/5	5/2.5
Excitation filter [nm]	335-620, 550-1100	335-620, 550-1100
Scan control (speed)	Medium	Medium
PMT detector voltage	High	High
Zero/blank sample	CONW	CONW

Chl*a*F: determining excitation/emission wavelengths

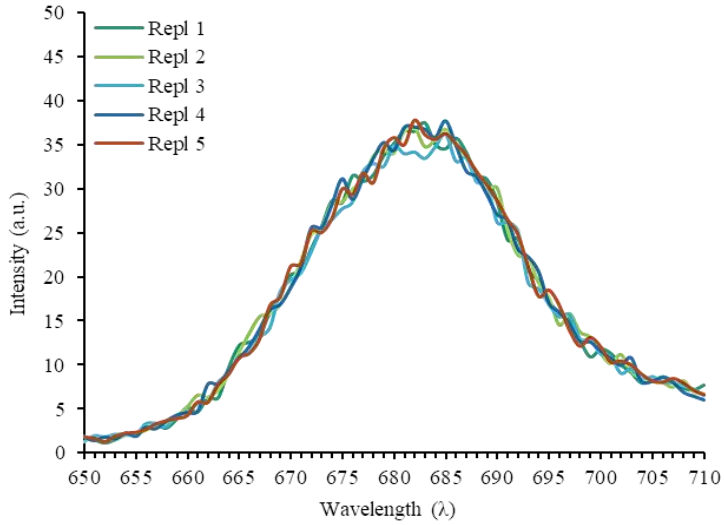

Figure B3: Chlorophyll-*a* fluorescence peak for five replicates of *I. galbana*, excited at 460 nm. The peak fluorescence intensity was found at 681-683 nm. The cell density of the excited culture was 500 000 cells/mL.

Nile red and triolein staining solutions

As a method of semi-quantifying the lipid content in *I. galbana* with or without exposure to MFs, a lipophilic chromophore staining protocol was tested. The neutral lipid triolein (glycerol trioleate, Sigma-Aldrich, Germany) was used as a proxy for neutral lipid bodies in the algae, and a concentration gradient of CONW-dissolved triolein stained with the lipophilic dye Nile Red (NR; Sigma-Aldrich, Germany) was made. The aim was to make a standard curve, by analysing the relative fluorescence intensity of NR at a wavelength specific to lipid-bound NR. Optimal NR staining parameters were chosen based on existing protocols (Bertozzini et al., 2011; Chen et al., 2009), with an aim of fitting instrument parameters specifically to *I. galbana*. An NR stock solution of 0.5 mg/mL was made in advance (1.0 mg NR per 2 mL acetone, Table B1), and 0.02 mL of the stock was diluted with CONW (1.98 mL) and triolein (0.2 mL) to a final concentration of 0.025 µg NR/mL sample. The triolein concentrations for the standard curve in the final samples were 0, 2.5, 5, 10, 15 and 20 µg/mL (Table B1). The samples were turned upside-down once, and incubated in darkness (10 min, 21°C) before analysis. Incubated samples were then scanned at ex. and em. wavelengths between 450-500 nm and 550-600 nm, respectively, to assess the optimal excitation and emission parameters for triolein-bound NR. Once the optimal parameters were identified, a standard curve of Nile red fluorescence intensity was made as a function of triolein concentration.

Table B2: Nile red stock solution and dilution gradient used to test the optimal dye ratio to algae and/or triolein samples. The final sample dilution represents the concentration in each 2 ml cuvette, before analysis. A concentration of 0.25 µg/mL was selected for further use.

NR stock	
NR powder [mg]	1
Acetone [mL]	2
Final conc. [mg/mL]	0.5

Dilutions per cuvette

NR solutions	**Concentration [mg/mL]**	**NR stock [µL]**	**Acetone [µL]**	**Final sample dilution [µg/mL]**
Stock	**0.5**			
1:5	0.100	2	18	1
1:10	0.050	1	19	0.5
1:20	0.025	0.5	19.5	0.25
1:50	0.010	0.2	19.8	0.1

Table B3: The triolein stock solution, and dilution gradients made to plot a fluorescence intensity standard curve, based on the lipid concentration (triolein). The final concentration in the sample cuvette was 2 mL

Triolein stock	
Glyceryl trioleate [mg]	15.11
Acetone [mL]	1.50
Final conc. [mg/mL]	10.07

Dilutions per cuvette

TO stock dilutions	**TO stock (fraction per 2 mL)**	**TO stock [µL]**	**TO in vial [µg]**	**Acetone [µL]**	**Final sample dilution**	
					[mg/mL]	**[µg/mL]**
0:20	0	0	0.00	20	0.000	0
0.5:19.5	0.025	0.5	5.04	19.5	0.0025	2.5
1:19	0.05	1	10.07	19	0.005	5
2:18	0.1	2	20.14	18	0.010	10
3:17	0.15	3	30.21	17	0.015	15
4:16	0.2	4	40.28	16	0.020	20

Nile red-staining: standard curve analyses

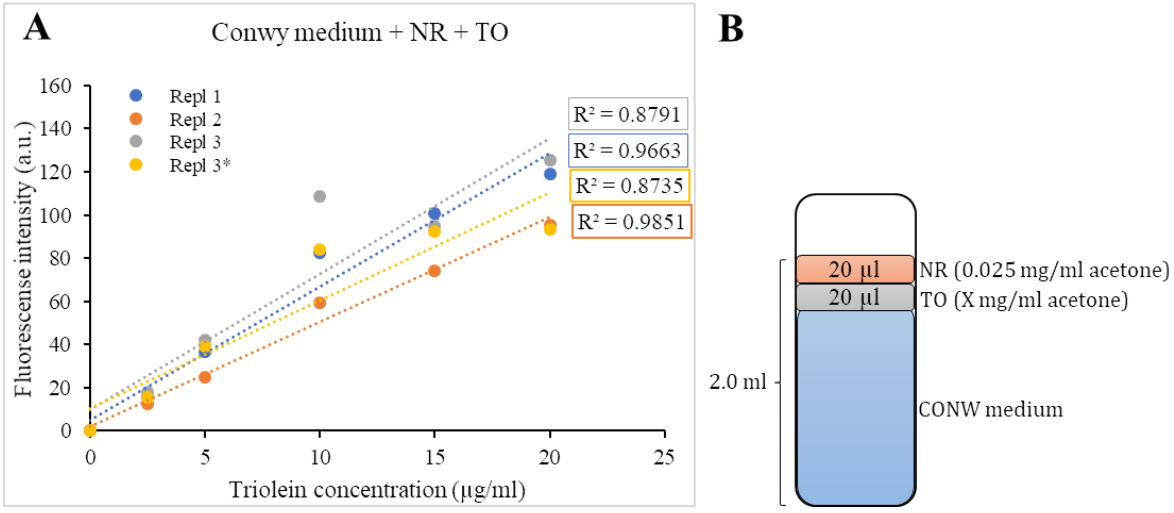

Figure B4: A) Nile red fluorescence intensity standard curves (*n*=3), as functions of triolein concentration. The Repl 3* was identical to Repl 3 but was vortexed before analysis. B) The samples were prepared as illustrated, with final NR concentrations of 0.25 µg/mL. NR, Nile Red; TO, triolein.

Sample filtration: removing MFs before analysis

As a method of removing MFs before analysis, all 10-ml subsamples were vacuum filtered through a nylon mesh cloth (NY7-HC, NYTAL®, Sefar Inc., Switzerland) with a pore size of 7.7 ± 1.8 µm. Firstly, pure algae cultures (5 replicates) were counted before and after filtration, to ensure that insignificant amounts of algae were retained on the filter. Secondly, algae cultures were diluted into vials containing MFs from each respective suspension stock, filtered and then counted. In this second test, cell densities were approximated from dilution factors, to not risk running and potentially blocking the Coulter® aperture with MFs.

To assess whether the presence of MFs impacted Chl*a*F measurements, algae cultures were filtrated with and without suspended MFs (PES 60 µm, 4.25×10^{-3} mg/mL), before spectrofluorometric Chl*a*F analysis (Section 2.2.2). Additionally, non-filtered algae cultures containing suspended MFs were also included, to test whether MFs influenced Chl*a*F measurements, and to evaluate the feasibility of Chl*a*F analysis without sampling filtration.

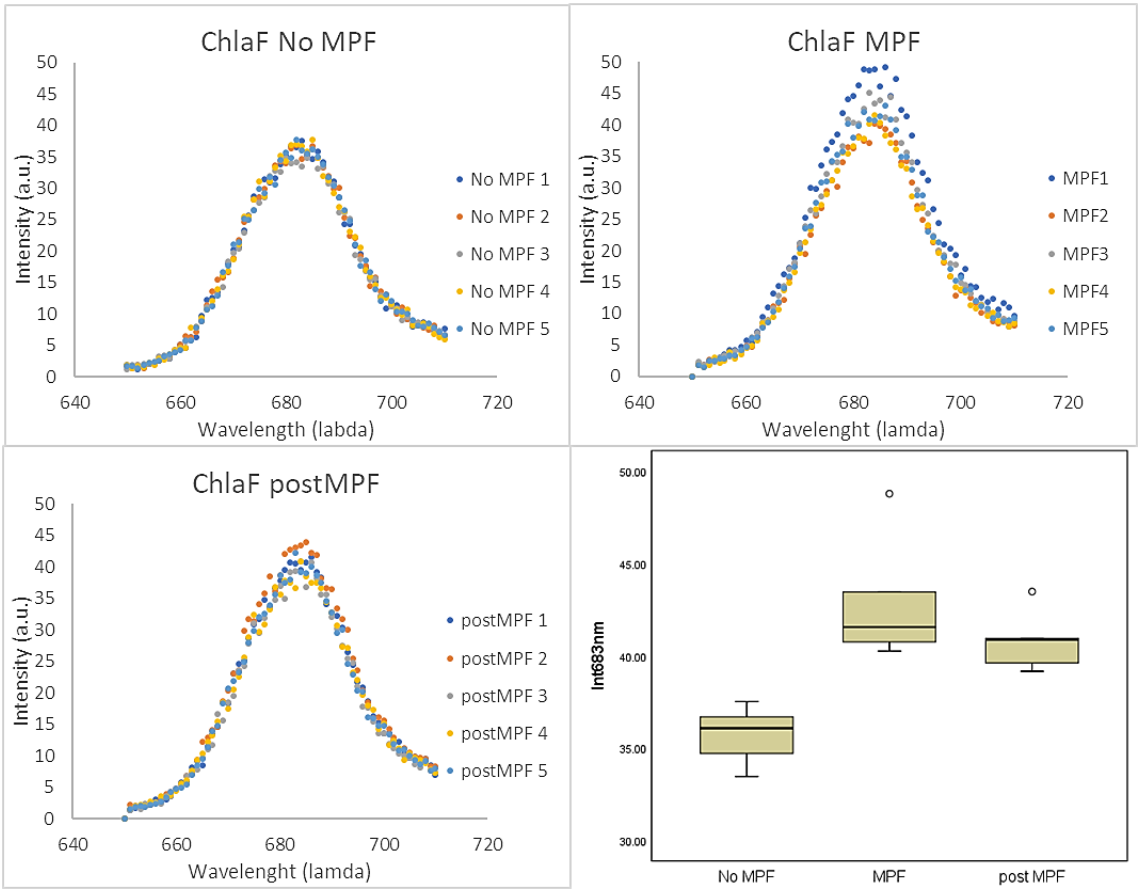

Figure B5: Fluorescence spectra of filtrated cultures of *I. galbana* without ("no MPF"), with ("MPF") and after 15 min of contact with MFs ("postMPF"); ex. at 460 nm. Box plots show difference in Chl*a*F at 683 nm. "no MPF", only *I. galbana*; "MPF", *I. galbana* and MFs; "postMPF", *I. galbana* after 15 min contact w/MFs.

72-h toxicity test

A 72h toxicity test was performed in a 96-well plate, using the setup illustrated in Figure B6. Five concentrations of MF leachates were used (1-5), each number representing concentrations from 0.0422-42.2 µg/mL, increasing with a factor of 10. The objective of the assess any concentration-response relationship of the MF leachates. All samples were made in triplicate, with one column representing leachate controls (4, 8 and 12) without algae. An initial cell density of 1 350 000 cells/mL were used in all wells with algae. All wells had a total volume of 200 µL, where all wells contained 100 µL of their respective sample and 100 µL of CONW, except for the "CONW" control, containing 200 µL CONW. "PES 1-5", "PA 1-5" and "Wool 1-5" were prepared with 100 µL algae inoculum (2 690 000 cells/mL) and 100 µL of the corresponding fibre leachate concentration. "Ctrl" contained 100 µL algae inoculum and 100 µL CONW. "Ctrl 1-5" (colour coded) contained 100 µL leachate and 100 µL CONW, whereas "CONW" contained 200 µL CONW, only.

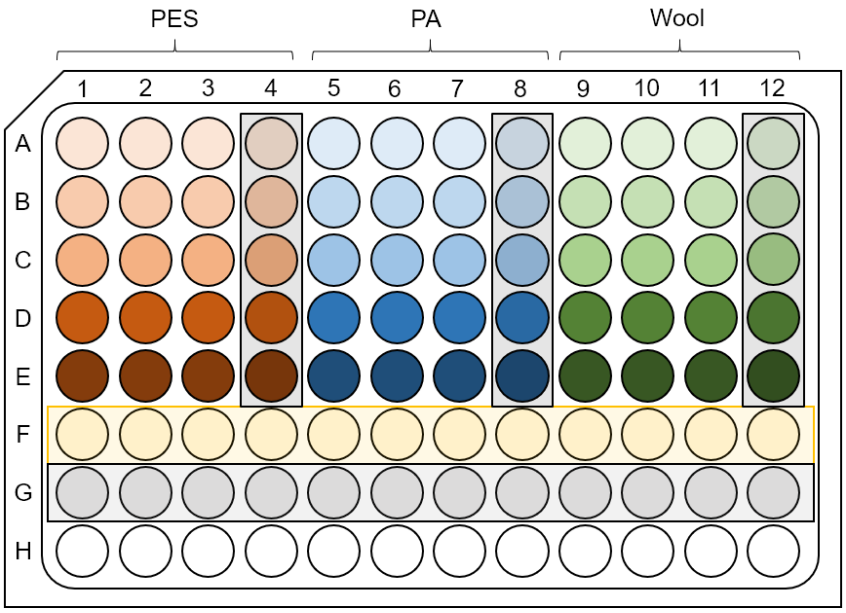

Plate layout	
Row	Content/MF leachate [mg/ml]
A	0.0000422
B	0.000422
C	0.00422
D	0.0422
E	0.422
F	Control (algae)
G	Control (CONW)
H	Empty
Boxes represent controls	

Figure B6: 96-wellplate setup for the 72-h toxicity test of MF leachates with *I. galbana*.

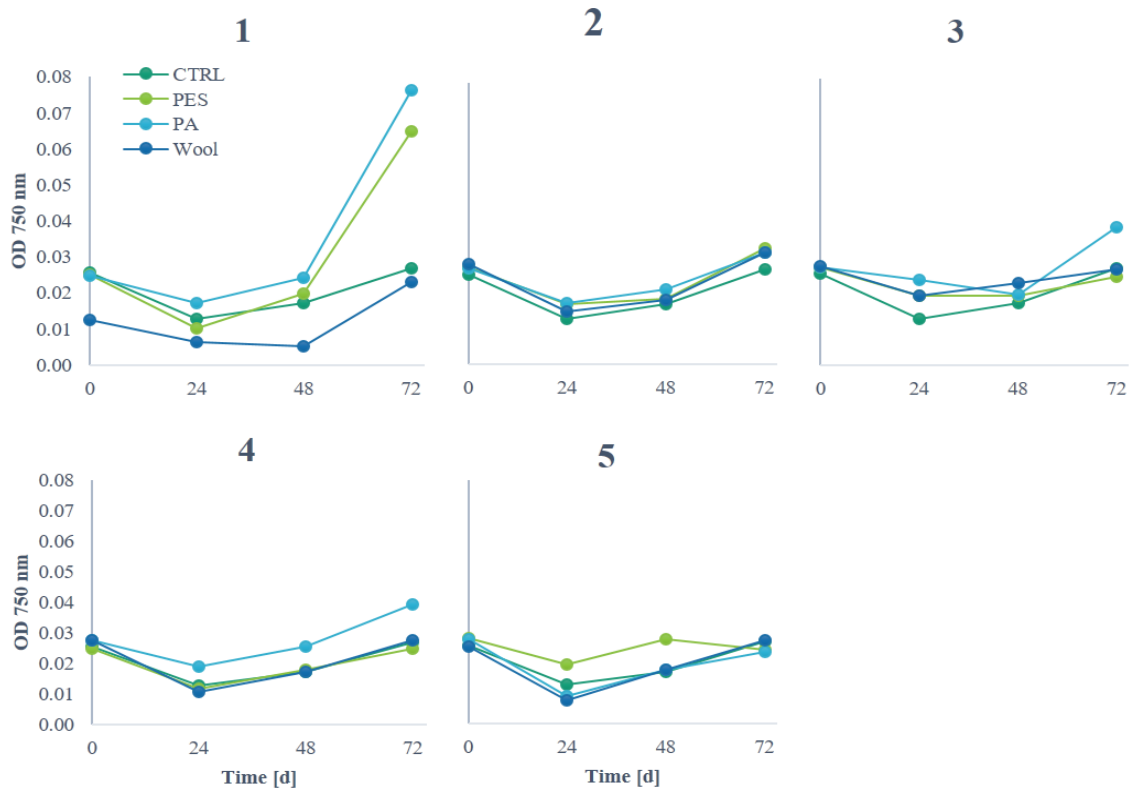

Figure B7: Results from the 72-h toxicity test with *I. galbana*, represented by optical density (OD) measured at 750 nm. Numbers 1-5 represents concentration from low (0.0422 µg/mL) to highest (42.2 µg/mL), respectively. Algae were non-exposed (Ctrl) and exposed to polyester (PES), polyamide (PA) or wool microfibre leachates in 96-wellplates.

Appendix C

Experimental results

Correlations between Chl*a*F and cell numbers (cells/mL)

Table C1: Spearman correlations for Chl*a*F vs. cell numbers, and cell numbers vs. pH.

Spearman's rho correlation							
		3000 µm			60 µm		
		Corr coeff	Sign.	N	Corr coeff	Sign.	N
	Algae	0.9505	<0.001	13	0.9821	<0.001	13
	PES (L)	0.9176	<0.001	13	0.9931	<0.001	13
	PES (M)	0.9286	<0.001	13	0.9341	<0.001	13
	PES (H)	0.9341	<0.001	13	0.9739	<0.001	13
	PA L	0.9021	<0.001	13	0.9835	<0.001	13
Cell vs ChlaF	PA M	0.9091	<0.001	13	0.9341	<0.001	13
	PA H	0.8811	<0.001	13	0.978	<0.001	13
	Wool L	0.9021	<0.001	13	0.9945	<0.001	13
	Wool M	0.9091	<0.001	13	0.9835	<0.001	13
	Wool H	0.9091	<0.001	13	0.9725	<0.001	13
	Algae	0.9491	<0.001	13	0.9011	<0.001	13
	PES (L)	0.9121	<0.001	13	0.9615	<0.001	13
	PES (M)	0.8956	<0.001	13	0.956	<0.001	13
	PES (H)	0.9176	<0.001	13	0.9176	<0.001	13
Cells vs pH	PA L	0.9371	<0.001	13	0.9066	<0.001	13
	PA M	0.9301	<0.001	13	0.9061	<0.001	13
	PA H	0.9371	<0.001	13	0.8462	<0.001	13
	Wool L	0.9371	<0.001	13	0.8681	<0.001	13
	Wool M	0.9371	<0.001	13	0.8956	<0.001	13
	Wool H	0.9371	<0.001	13	0.8352	<0.001	13

Table C2: Pearson correlation between growth and photosynthesis parameters. Growth (cell numbers) vs. Chl*a* (Chl*a*F); growth vs. pH.

Pearson correlation				
	Growth vs Chla		Growth vs. pH	
	3000 µm	60 µm	3000 µm	60 µm
Algae	0.995	0.998	0.990	0.985
PES L	0.991	0.996	0.982	0.990
PES M	0.990	0.996	0.984	0.988
PES H	0.991	0.998	0.983	0.980
PA L	0.992	0.996	0.986	0.990
PA M	0.990	0.998	0.984	0.989
PA H	0.996	0.994	0.983	0.985
Wool L	0.991	0.993	0.989	0.986
Wool M	0.992	0.997	0.985	0.990
Wool H	0.996	0.997	0.983	0.983

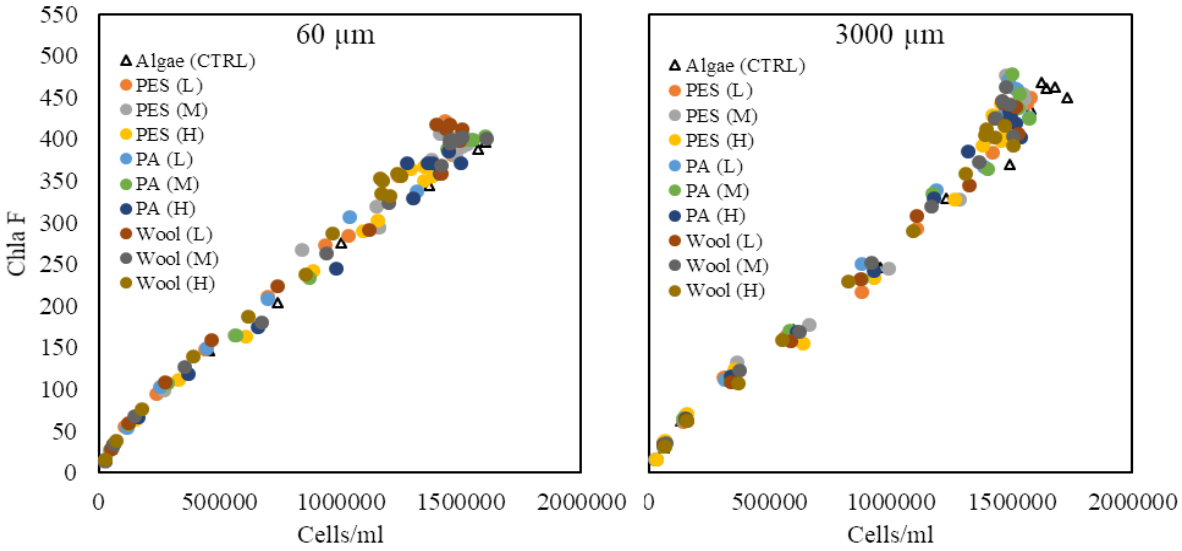

Figure C1: Correlation plots for Chl-*a* fluorescence (Chl*a*F) and cell density in *I. galbana* exposed to polyester (PES), polyamide (PA) and Wool MFs, and non-exposed (Ctrl). Concentrations: low (L), medium (M) and high (H).

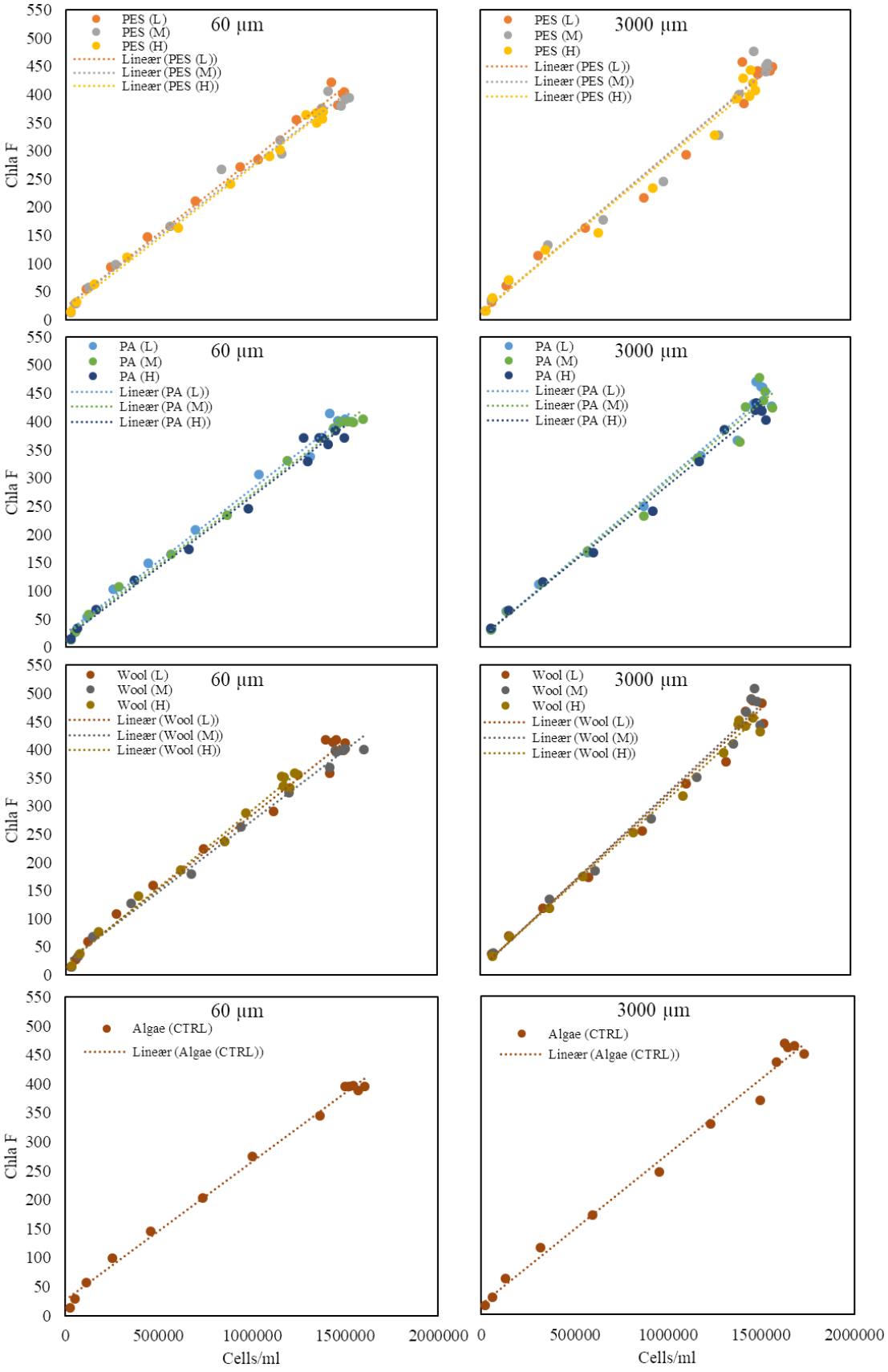

Figure C2: Correlation plots for chlorophyll-*a* fluorescence and cell density in *I. galbana;* non-exposed (Ctrl) and exposed to polyester (PES), polyamide (PA) and Wool MFs. Concentrations low (L), medium (M) and high (H) represent 4.22×10^{-5}, 4.22×10^{-4} and 4.22×10^{-3} mg MFs/mL growth medium, respectively.

Growth curves

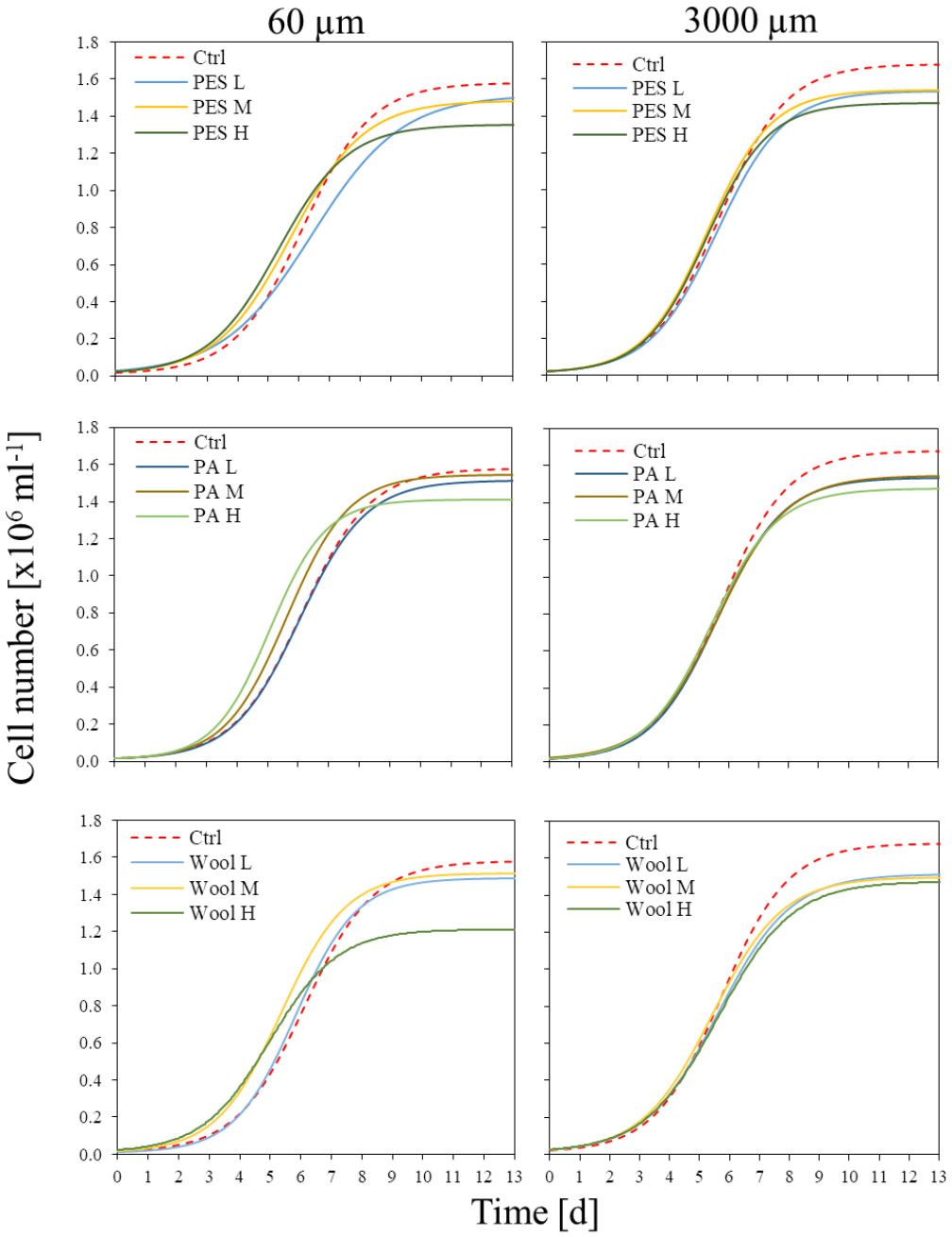

Figure C3: Growth curves for *I. galbana* exposed to 60 µm and 3000 µm MFs of polyester (PES), polyamide (PA) and wool, at low (L, 0.0422 µg/mL), medium (M, 0.422 µg/mL) and high (H, 4.22 µg/mL) concentrations. Global goodness of fit: R^2=0.99; $F_{30,361}$=4555, p<0.0001. Ctrl, non-exposed control (algae).

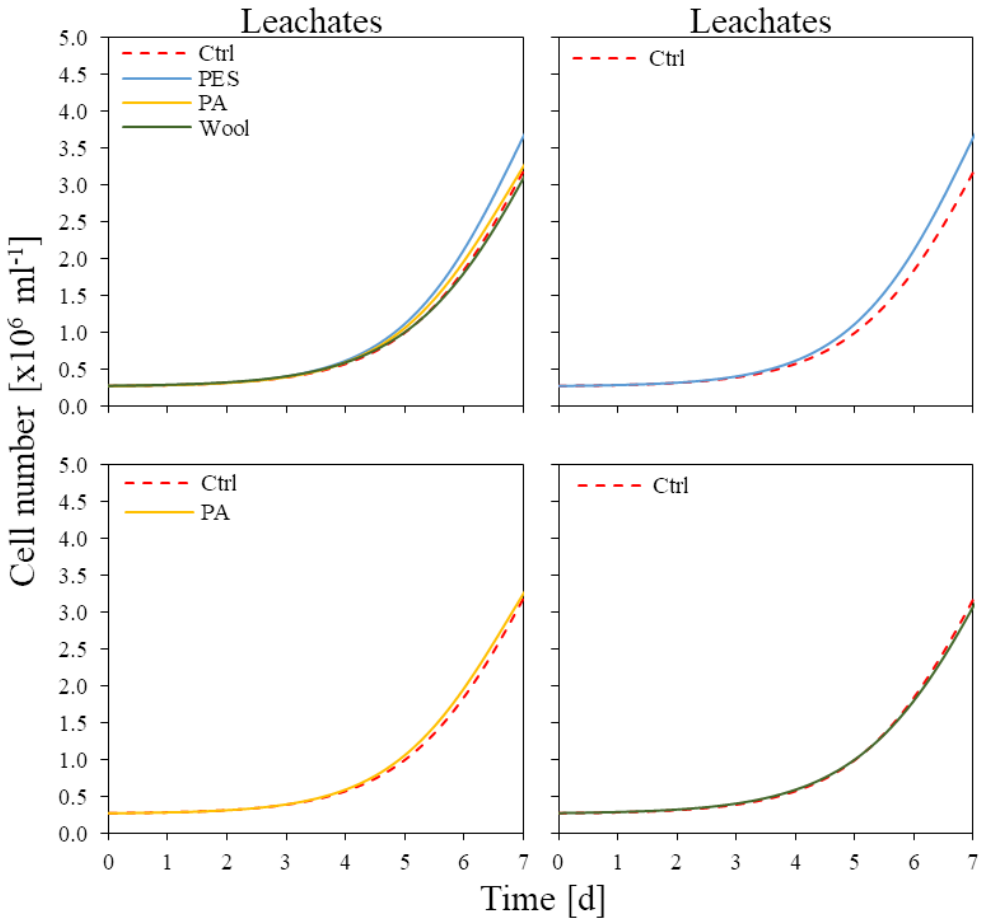

Figure C3: Continuation from the previous page. Growth curves for *I. galbana* exposed to MF leachates of polyester (PES), polyamide (PA) and wool at concentrations corresponding to 4.22 µg MFs/mL.

Cumulative biomass

Table C3: Cumulative biomass for *I. galbana* cultures exposed to 3000 µm PES, PA and wool at low, medium and high concentrations, with relative inhibition in percentages of non-exposed control (Ctrl). AUC, area under the (sigmoid regression) curves from Figure C3; SE, standard error of every regression estimate.

60 µm		13 d			7 d		
		AUC [Cells/mL]	Inhibition [%]	SE [%]	AUC [Cells/mL]	Inhibition [%]	SE [%]
Ctrl		11,654,602		0.6	2,164,625		3.5
PES	**L**	10,625,201	8.8	0.7	2,014,835	6.9	3.7
	M	11,456,603	1.7	0.7	2,472,003	-14.2	3.0
	H	11,007,004	5.6	0.7	2,631,998	-21.6	2.8
PA	**L**	11,265,861	3.3	0.7	2,125,829	1.8	3.5
	M	12,111,188	-3.9	0.6	2,583,272	-19.3	2.9
	H	11,861,359	-1.8	0.6	2,968,258	-37.1	2.5
Wool	**L**	11,399,792	2.2	0.7	2,270,519	-4.9	3.3
	M	12,264,190	-5.2	0.6	2,881,154	-33.1	2.6
	H	10,224,599	12.3	0.7	2,666,533	-23.2	2.8

Continuation of **Table C3**

3000 µm		13 d			7 d		
		AUC [Cells/mL]	Inhibition [%]	SE [%]	AUC [Cells/mL]	Inhibition [%]	SE [%]
Ctrl		12,304,514		0.5	2,830,891		2.1
PES	**L**	11,335,907	7.9	0.5	2,661,266	6.0	2.2
	M	11,887,091	3.4	0.5	3,031,891	-7.1	1.9
	H	11,404,633	7.3	0.5	2,923,558	-3.3	2.0
PA	**L**	11,435,871	7.1	0.5	2,720,848	3.9	2.1
	M	11,466,106	6.8	0.5	2,745,956	3.0	2.1
	H	11,276,992	8.4	0.5	2,837,480	-0.2	2.1
Wool	**L**	11,217,002	8.8	0.5	2,733,134	3.5	2.1
	M	11,414,988	7.2	0.5	2,907,614	-2.7	2.0
	H	10,937,746	11.1	0.5	2,683,061	5.2	2.2

Daily Chl*a*F per cell

Table C3: Chl*a*F per cell (± SD) for *I. galbana* exposed to 3000 µm MFs of polyester (PES), polyamide (PA) and wool at low (L, 0.0422 µg/mL), medium (M, 0.422 µg/mL) and high (H, 4.22 µg/mL) conc. n.d., no data.

Time [d]	Ctrl		PES L		PES M		PES H		PA L	
	Mean	SD	Mean	SD	Mean	SD	Mean	SD	Mean	SD
1	5.67E-04	6.0E-05	4.99E-04	4.0E-05	5.10E-04	7.0E-05	4.58E-04	1.3E-05	n.d.	n.d.
2	4.99E-04	2.8E-05	5.00E-04	4.3E-05	5.58E-04	4.0E-05	5.86E-04	1.3E-04	5.09E-04	2.8E-05
3	4.69E-04	1.5E-05	4.31E-04	7.5E-06	4.45E-04	2.4E-05	4.46E-04	1.2E-05	4.50E-04	4.3E-06
4	3.65E-04	1.6E-05	3.67E-04	3.9E-06	3.64E-04	2.4E-05	3.51E-04	1.9E-05	3.53E-04	2.9E-05
5	2.88E-04	1.0E-05	2.86E-04	1.5E-05	2.67E-04	3.5E-05	2.88E-04	1.3E-05	2.89E-04	3.5E-05
6	2.58E-04	1.1E-05	2.47E-04	8.5E-06	2.48E-04	2.3E-05	2.52E-04	1.5E-05	2.83E-04	5.3E-06
7	2.72E-04	3.1E-06	2.65E-04	2.8E-05	2.55E-04	2.2E-05	2.59E-04	6.6E-06	2.84E-04	1.3E-05
8	2.48E-04	1.1E-06	2.70E-04	7.3E-06	2.87E-04	1.2E-05	2.84E-04	1.1E-05	2.64E-04	8.4E-06
9	2.77E-04	2.2E-05	2.93E-04	1.8E-05	2.94E-04	9.5E-06	3.06E-04	2.8E-05	2.92E-04	1.3E-05
10	2.61E-04	1.2E-05	2.85E-04	9.0E-06	2.89E-04	1.3E-05	2.74E-04	7.3E-06	2.71E-04	9.2E-06
11	2.82E-04	2.6E-05	2.84E-04	1.3E-05	2.86E-04	1.4E-05	2.85E-04	3.2E-06	3.02E-04	7.5E-06
12	2.79E-04	2.3E-05	2.96E-04	1.6E-05	2.93E-04	1.3E-05	2.73E-04	6.3E-06	3.16E-04	4.4E-06
13	2.88E-04	1.5E-05	3.25E-04	2.3E-05	3.23E-04	1.4E-05	3.02E-04	3.1E-06	3.05E-04	1.2E-05

Time [d]	PA M		PA H		Wool L		Wool M		Wool H	
	Mean	SD	Mean	SD	Mean	SD	Mean	SD	Mean	SD
1	n.d.	n.d.	n.d.	n.d.	n.d.	n.d.	n.d.	n.d.	n.d.	n.d.
2	5.18E-04	6.1E-05	5.56E-04	1.2E-05	5.55E-04	7.9E-05	4.86E-04	2.5E-05	4.45E-04	1.7E-05
3	4.43E-04	1.6E-05	4.22E-04	1.4E-05	4.08E-04	2.0E-05	3.92E-04	4.2E-05	3.96E-04	5.5E-05
4	3.43E-04	1.1E-05	3.41E-04	2.5E-05	3.18E-04	1.4E-05	3.25E-04	4.4E-06	2.87E-04	8.4E-06
5	2.93E-04	1.6E-05	2.75E-04	7.2E-06	2.71E-04	1.3E-05	2.71E-04	3.8E-06	2.89E-04	3.9E-05
6	2.63E-04	8.6E-06	2.59E-04	1.4E-05	2.66E-04	7.3E-06	2.73E-04	1.9E-05	2.78E-04	1.6E-05
7	2.85E-04	1.1E-05	2.78E-04	1.2E-05	2.78E-04	1.2E-05	2.73E-04	1.7E-05	2.64E-04	1.2E-05
8	2.60E-04	7.1E-06	2.93E-04	8.6E-06	2.60E-04	1.2E-05	2.72E-04	8.8E-06	2.74E-04	9.1E-06
9	2.98E-04	2.0E-05	2.91E-04	2.1E-05	2.98E-04	3.0E-05	2.96E-04	7.0E-06	2.90E-04	1.7E-05
10	2.69E-04	1.3E-05	2.64E-04	2.0E-06	2.65E-04	7.6E-06	2.68E-04	1.1E-05	2.60E-04	6.2E-06
11	2.95E-04	1.3E-05	2.83E-04	1.4E-05	2.89E-04	1.2E-05	3.05E-04	1.5E-05	2.94E-04	9.3E-06
12	2.86E-04	1.3E-05	2.76E-04	1.2E-05	3.02E-04	1.4E-05	2.95E-04	2.3E-06	2.83E-04	3.5E-06
13	3.17E-04	6.2E-06	2.85E-04	9.1E-06	3.04E-04	6.7E-06	3.13E-04	1.0E-05	2.80E-04	1.3E-05

Table C4: Chl*a*F per cell (± SD) for *I. galbana* exposed to 60 µm MFs of polyester (PES), polyamide (PA) and wool at low (L, 0.0422 µg/mL), medium (M, 0.422 µg/mL) and high (H, 4.22 µg/mL) conc. n.d., no data.

Time [d]	Ctrl		PES L		PES M		PES H		PA L	
	Mean	SD	Mean	SD	Mean	SD	Mean	SD	Mean	SD
1	5.29E-04	8.0E-06	5.66E-04	3.1E-05	4.82E-04	3.9E-06	5.31E-04	3.0E-05	5.49E-04	1.5E-05
2	5.52E-04	9.5E-06	5.51E-04	1.2E-05	5.30E-04	3.7E-05	5.48E-04	9.2E-06	5.28E-04	5.4E-06
3	4.98E-04	4.4E-05	5.13E-04	2.3E-05	4.57E-04	2.0E-05	4.15E-04	1.9E-05	4.66E-04	1.4E-05
4	3.93E-04	1.8E-05	3.89E-04	8.6E-06	3.67E-04	1.0E-05	3.38E-04	2.1E-05	4.06E-04	4.8E-05
5	3.19E-04	1.7E-05	3.35E-04	6.2E-06	2.94E-04	1.6E-05	2.69E-04	1.1E-05	3.36E-04	3.8E-05
6	2.79E-04	1.7E-05	3.03E-04	3.0E-05	3.19E-04	2.3E-05	2.73E-04	1.5E-05	3.02E-04	4.4E-05
7	2.76E-04	1.8E-05	2.91E-04	1.9E-05	2.53E-04	1.1E-05	2.64E-04	1.4E-06	2.94E-04	1.0E-05
8	2.53E-04	1.5E-05	2.75E-04	1.6E-05	2.78E-04	1.4E-05	2.61E-04	1.5E-05	2.57E-04	1.4E-05
9	2.48E-04	1.2E-05	2.86E-04	9.5E-06	2.73E-04	2.0E-05	2.59E-04	5.9E-06	2.68E-04	2.3E-05
10	2.47E-04	9.5E-06	2.60E-04	4.3E-06	2.57E-04	1.2E-05	2.58E-04	9.3E-06	2.59E-04	1.1E-05
11	2.58E-04	1.2E-05	2.69E-04	2.6E-06	2.57E-04	4.0E-06	2.67E-04	1.1E-05	2.69E-04	1.2E-05
12	2.63E-04	9.5E-07	2.69E-04	5.9E-07	2.59E-04	3.9E-06	2.72E-04	1.2E-05	2.73E-04	1.1E-05
13	2.60E-04	5.7E-06	2.94E-04	2.1E-06	2.87E-04	3.4E-06	2.82E-04	1.6E-05	2.91E-04	3.0E-06

Time [d]	PA M		PA H		Wool L		Wool M		Wool H	
	Mean	SD	Mean	SD	Mean	SD	Mean	SD	Mean	SD
1	5.25E-04	8.6E-06	7.30E-06	5.0E-04	5.27E-04	1.7E-05	4.70E-04	2.8E-05	3.53E-05	5.3E-04
2	5.37E-04	4.5E-06	5.41E-04	1.5E-05	5.10E-04	9.3E-06	5.14E-04	2.5E-05	5.14E-04	2.3E-05
3	4.63E-04	1.6E-05	4.13E-04	2.5E-05	4.83E-04	1.6E-05	4.58E-04	1.6E-05	4.33E-04	2.9E-05
4	3.74E-04	4.8E-06	3.23E-04	2.4E-05	3.97E-04	3.9E-05	3.59E-04	1.5E-05	3.62E-04	3.4E-05
5	2.91E-04	1.9E-05	2.64E-04	1.3E-05	3.41E-04	2.2E-05	2.67E-04	4.3E-06	3.05E-04	2.3E-05
6	2.70E-04	7.4E-06	2.52E-04	1.6E-05	3.05E-04	1.8E-05	2.80E-04	9.8E-06	2.80E-04	2.5E-05
7	2.77E-04	1.5E-05	2.53E-04	1.1E-05	2.66E-04	3.1E-05	2.69E-04	4.1E-06	2.97E-04	1.4E-05
8	2.68E-04	8.3E-06	2.53E-04	5.6E-06	2.52E-04	2.9E-06	2.61E-04	1.8E-05	2.77E-04	1.7E-05
9	2.52E-04	3.5E-06	2.47E-04	3.1E-06	2.66E-04	3.0E-06	2.49E-04	8.1E-06	2.87E-04	1.9E-05
10	2.57E-04	3.8E-06	2.65E-04	4.4E-06	2.74E-04	5.7E-06	2.67E-04	1.0E-05	2.91E-04	1.0E-05
11	2.63E-04	5.6E-06	2.71E-04	2.9E-06	2.87E-04	1.2E-05	2.67E-04	4.8E-06	3.02E-04	4.5E-06
12	2.69E-04	1.3E-05	2.68E-04	4.6E-06	2.87E-04	4.6E-06	2.71E-04	3.5E-06	2.97E-04	1.1E-06
13	2.70E-04	2.5E-06	2.90E-04	2.6E-05	2.98E-04	1.4E-05	2.74E-04	7.5E-06	2.87E-04	1.1E-05

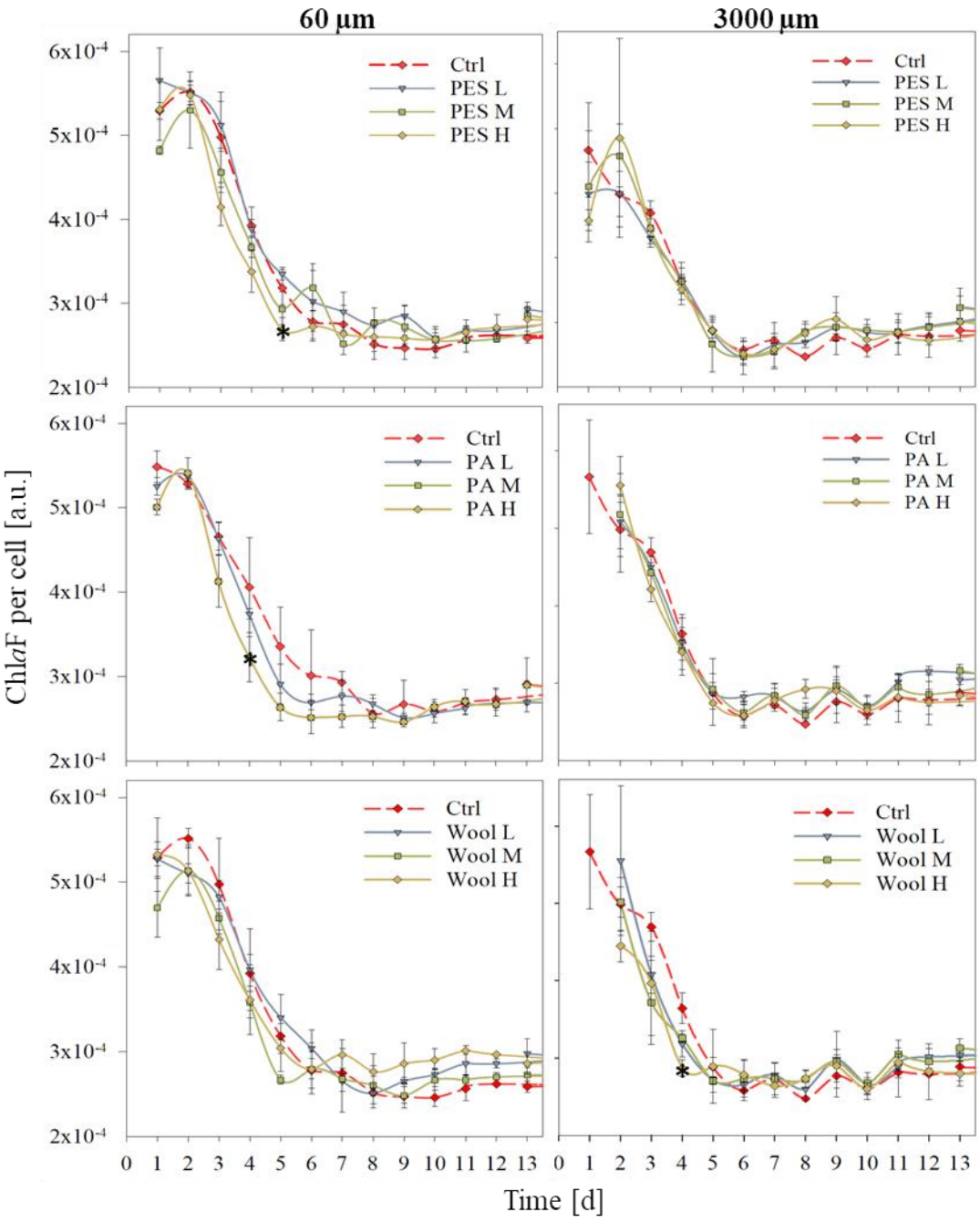

Figure C4: Daily relative Chl*a*F per *I. galbana* cell during chronic exposure to 60 µm and 3000 µm PES, PA and wool MFs at low (L, 0.0422 µg/mL), medium (M, 0.422 µg/mL) and high (H, 4.22 µg/mL) concentrations. Asterisk indicate statistically significant difference from the control (Ctrl) at $p<0.05$ for PES H and PA H (60 µm) and Wool H (3000 µm).

FTIR spectra: unadjusted absorbance intensities

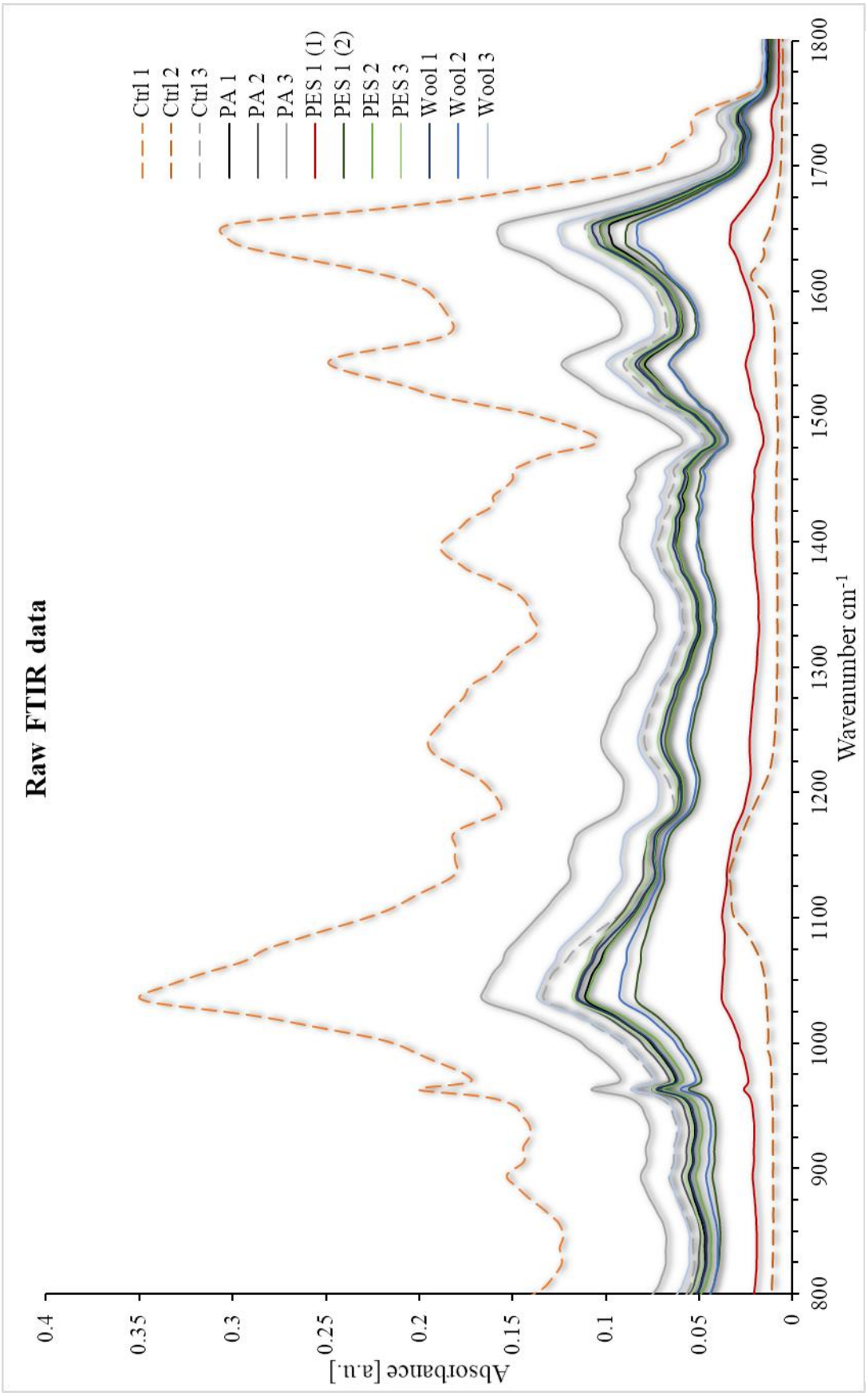

Figure C5: Raw FTIR data without processing and signal normalisation. Ctrl 2 and PES 1 (1) were excluded from the results, because of their odd spectra.

Single-peak intensities FTIR

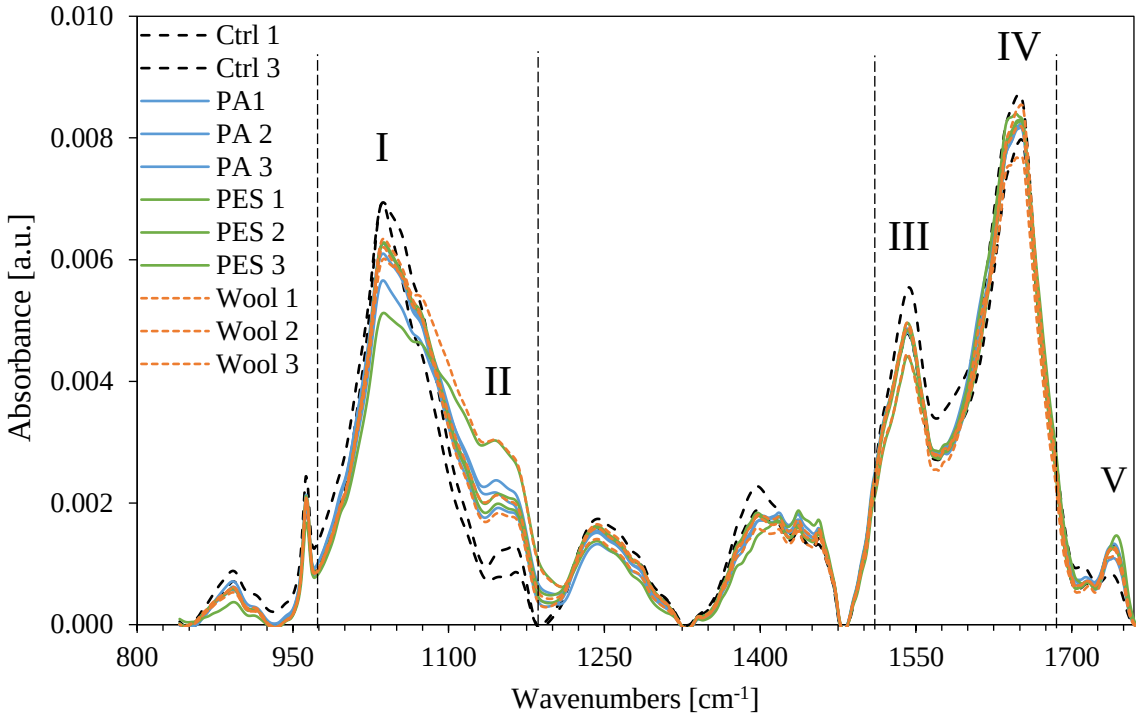

Figure C6: Individual ATR-FTIR absorbance spectra of *I. galbana* exposed for 7 d to MF leachates of polyester (PES), polyamide (PA) and wool (*n*=3; Ctrl *n*=2). Bands separated with dotted lines represent the dominating functional groups: carbohydrates (I & II), proteins (III) and (IV), and lipids (V). The roman number assignments are given in **Table 2.2.4**;

Table C3: Single-peak intensities for carbohydrates (C, 1035 cm^{-1} and CC, 1148 cm^{-1}), lipids (L, 1745 cm^{-1}) and protein (amide I, 1645 cm^{-1}) without normalisation to any peak.

		Ctrl	PES	PA	Wool
Carbo-hydrates (I)	**Mean**	6.93E-03	6.00E-03	5.87E-03	6.16E-03
	SD	*5.15E-07*	*3.58E-04*	*2.55E-04*	*1.39E-04*
	Range	0.0069-0.0069	0.0055-0.0063	0.0056-0.0063	0.0060-0.0063
Carbo-hydrates (II)	**Mean**	9.87E-04	2.38E-03	2.15E-03	2.33E-03
	SD	*2.04E-04*	*4.48E-04*	*1.83E-04*	*5.08E-04*
	Range	0.0008-0.0012	0.002-0.003	0.0019-0.0024	0.0018-0.003
Proteins	**Mean**	8.20E-03	7.90E-03	8.13E-03	8.04E-03
	SD	*4.18E-04*	*4.28E-04*	*3.40E-05*	*3.03E-04*
	Range	0.0078-0.0086	0.0073-0.0082	0.0081-0.0082	0.0076-0.0084
Lipids	**Mean**	9.13E-04	1.05E-03	1.05E-03	1.07E-03
	SD	*2.53E-04*	*1.12E-04*	*9.62E-05*	*5.75E-05*
	Range	0.000659-0.001166	0.000897-0.00114	0.00097-0.001199	0.000996-0.001134

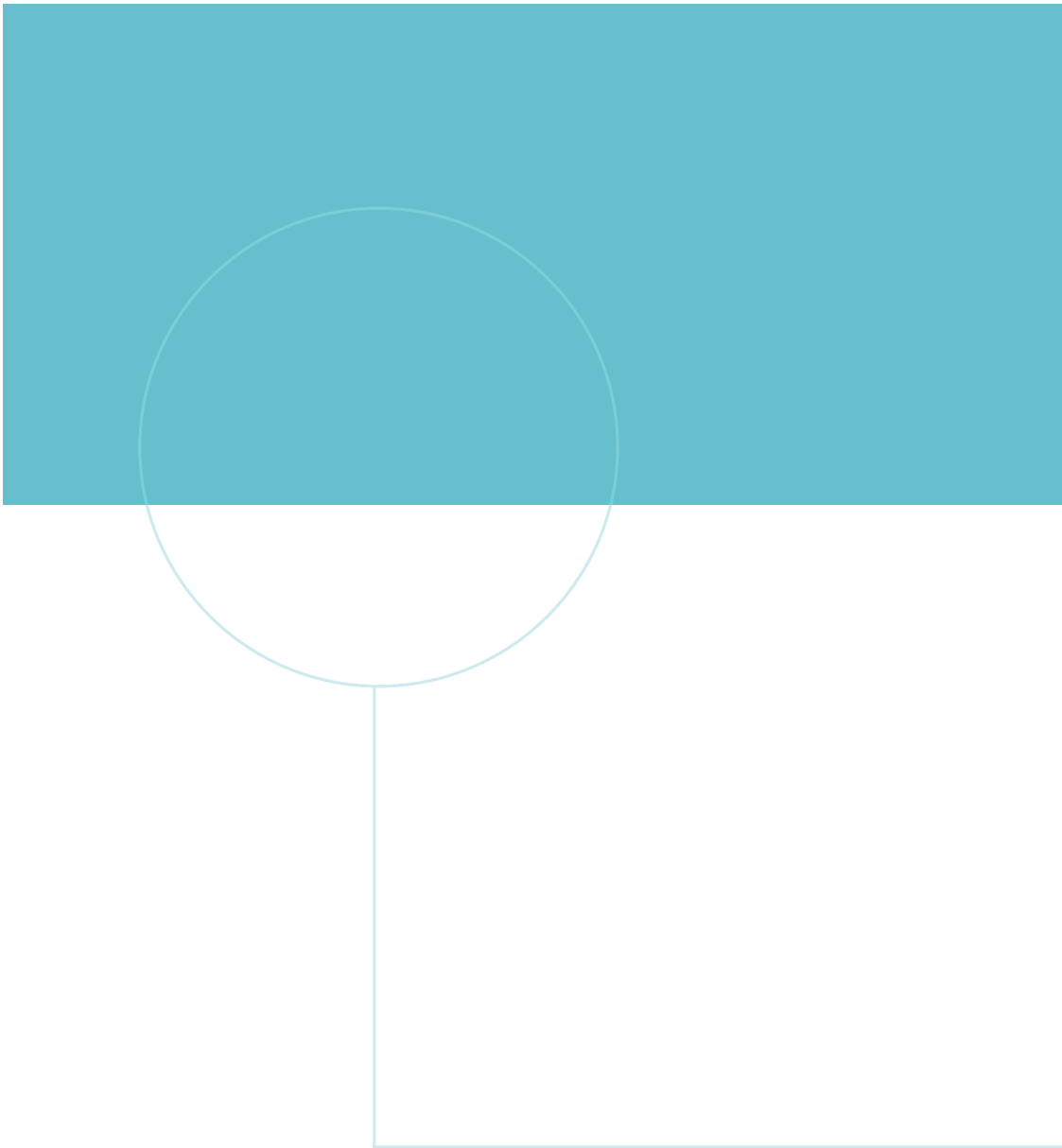

NTNU
Norwegian University of
Science and Technology